Micaela Brandão Lavender

Power-to-Methane In a Bioelectrochemical System

Propositions

1. Local hydrogen mediation in methane producing biocathodes is viable despite absence of hydrogen in the headspace and low cathode overpotentials.
   (this thesis)

2. Tackling the physical resistances in a bioelectrochemical system compromises biological performance.
   (this thesis)

3. A perfect technology is a flexible technology.

4. Scientific learning benefits from communicating failures.

5. Pessimists that find it difficult to do science are crucial for scientific progress.

6. The biggest challenge in a PhD trajectory is finding balance.

7. There is as much value as burden in the sense of responsibility.

Propositions belonging to the thesis, entitled

Power-to-Methane In a Bioelectrochemical System

Micaela Brandão Lavender
Wageningen, 27 September 2024

Power-to-Methane
In a Bioelectrochemical System

Micaela Brandão Lavender

Thesis committee

Promotor
Prof. Dr Annemiek ter Heijne
Professor of Biological Recovery and Re-use Technology
Wageningen University & Research

Co-promotor
Dr Sanne de Smit
Postdoctoral Researcher, Environmental Technology
Wageningen University & Research

Other members
Prof. Dr Maria J. Barbosa, Wageningen University & Research
Prof. Dr César I. Torres, Arizona State University, Tempe, USA
Prof. Dr Marianna Villano, Sapienza Università di Roma, Italy
Prof. Dr Lars T. Angenent, Universität Tübingen, Germany

This research was conducted under the auspices of the Graduate School for Socio-Economic and Natural Sciences of the Environment (SENSE)

Power-to-Methane
In a Bioelectrochemical System

Micaela Brandão Lavender

Thesis
submitted in fulfilment of the requirements for the degree of doctor
at Wageningen University
by the authority of the Rector Magnificus
Prof. Dr C. Kroeze,
in the presence of the
Thesis Committee appointed by the Academic Board
to be defended in public
on Friday 27 September, 2024
at 3.30 p.m. in the Omnia Auditorium

Micaela Brandão Lavender
Power-to-Methane In a Bioelectrochemical System
178 pages.

PhD thesis, Wageningen University, Wageningen, the Netherlands (2024)
With references, with summary in English and Portuguese.

DOI: https://doi.org/10.18174/670709

"To produce a mighty book, you must choose a mighty theme."

– Herman Melville

To my parents, whom I am in debt with my life and, whom many moments were stripped away from in the proceedings of this thesis.

Contents

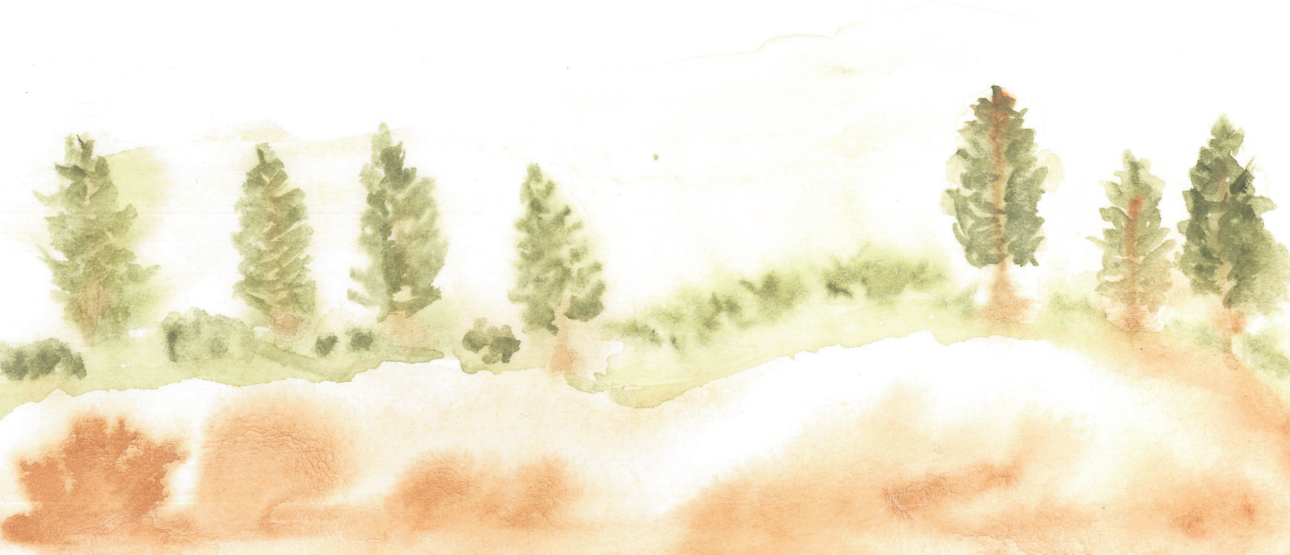

Chapter 1

General Introduction

1.1 *Motivum*: The energy transition and the need for energy storage in the form of methane

The climate crisis and the need to decarbonise the energy sector.

The use of the words "climate change" has increased exponentially since the 1980s with an even greater surge from the 2000s onward, as evidenced by Google's function "ngram viewer". However, as early as 1856, the influence of air properties, such as humidity, on the action of sun light, such as heating, has been investigated.[1] Many other ground breaking scientists, including Joseph Fourier, John Tyndall and Svante Arrehnius, have investigated the properties of the atmosphere and the gasses constituting it by comparing the atmosphere to a glass house, and describing how changes to its properties could lead to drastic changes in temperature on Earth.[2] In 1937, Guy Callendar estimated for the first time the rate of temperature increase, 0.003°C per year, as a result of the carbon dioxide concentrations in the atmosphere.[3] Back then, this corresponded to an estimated 150 gigatons of carbon dioxide released due to fuel consumption in the past half a century.[3] Nowadays, the emissions correspond to approximately 55 giagatons of CO_2 (equivalent) per year, and it has been predicted that a global temperature increase of 2°C can have a devastating impact on the world, as we currently know it.[4] Over 150 years of research has been conducted, including ground breaking science, however, there are still those whom deny climate change.

The acknowledgment of climate change, as a crisis, and efforts by the European Union (EU) to develop policies and targets regarding this crisis has dated back to the early 1990s.[5] However, this was never an easy task for the EU and its member states, since interests diverged immensely, especially between members with well founded carbon-based economies and members without such. It gets even more complex if the climate crisis is thought about on a global scale. Nevertheless, since 2014, the EU has committed to a set of targets to keep global warming from overshooting by 1.5°C, which had been suggested in the scientific evaluation made by the Intergovernmental Panel on Climate Change (IPCC).[6] The 2030 targets set by the EU are, 1) 40% reduction in overall green house gas (GHG) emissions (in comparison to those of 1990), 2) increasing the share of renewables by 27% in the overall energy consumption, and 3) improving energy efficiency by 27% in comparison to "business-as-usual".[6] The 2030 targets are set within the greater EU objective of net-zero GHG emissions by 2050. Additionally, in 2015 at the United Nations (UN) Climate Change Conference (COP21) the legally binding Paris Agreement was signed by 196 parties (on the global scale), all pledging efforts to minimise global warming and communicate about their actions.

However, the most recent report by the IPCC on climate change, states that there is currently a gap between what needs to be done on the global scale and what is being implemented.[4] Similarly, the International Renewable Energy Agency has reported that

the apparent trajectory of energy-related (GHG) emissions based on global agreements and efforts is still not enough in comparison to the trajectory that needs to be taken in order to keep up with the 1.5°C scenario.[7] Hence, decarbonising the energy sector needs to happen at a faster pace and on a larger scale.

The energy transition: decarbonising the energy sector and the important role of electricity storage.

The previous section argues that decarbonising the energy sector is needed in order to mitigate global warming and its consequences. According to the International Energy Agency incorporation of renewable electricity sources into electricity networks is crucial to decarbonise the electricity sector.[8] However, renewable electricity sources, such as solar and wind, are heavily dependent on varying climatic and weather conditions, therefore electricity produced from these site-specific renewable resources varies on an hourly, daily, monthly and yearly basis. For example, solar photovoltaic panels (PVs) will produce higher amounts of electricity in sunny hours during day time in comparison to low to no electricity during night time. In addition, not as much electricity will be produced during a cloudy day. Moreover and in general, in the winter months less radiation can be captured by PVs in comparison to summer months, therefore, less electricity is produced by PVs in winter seasons. With this said, incorporation of renewable energy into electricity networks introduces variability and uncertainty in relation to the amount of electricity which can be supplied at any given time.[9] Moreover, electricity demand also varies throughout the day, being higher when people are awake and on a monthly basis, being higher in winter months, because of the use of heating.

Mismatches between electricity supply and demand can result in unbalanced electricity grids which in turn can damage the overall electricity system (power grid). Electricity systems have, however, managed to cope to some extent with such uncertainty and variability using a variety of approaches. One example is the use of predictive weather and climate models to yield more precise predictions of the electricity supplied by renewable sources at a certain point in time. Another approach is to increase flexibility in the generation of other, mostly non-renewable, energy resources such as coal to quickly match the missing electricity to meet demand.

One other approach is to store the electricity. With the need to increase the share of renewable energy in electricity systems it is important to consider the possibility of storing electricity, so as to deal with mismatches between supply and demand. In this way, electricity can be stored, when supply exceeds demand and recovered, when demand exceeds supply. However, electricity can not be stored in its true form, thus it has to undergo, thermal, mechanical and/or chemical conversion.[10] In addition to conversion type, electricity storage technologies differ on their maximum capacity and their discharge rates. In general, the larger the capacity of a storage technology, the longer the discharge

rate. Pumped hydro storage, as an example, has a large capacity (100 MW-1 GW) and very long discharge rates, in the range of hours, whereas, flywheels have relatively low capacity (up to 1 MW) and fast discharge rates, in the order of seconds.[10, 11]

Taking into account that mismatches between power supply and electricity demand can happen on an hourly and up to a monthly basis both short-term and long-term electricity storage technologies with fast and slow discharge rates, respectively, are needed. As an example, hydro power is the largest incorporated electricity storage technology to date, and it is used for long-term electricity storage, for application in "bulk power management".[10] Chemical batteries are mostly used for short-term electricity storage and, as a result, are applied to make sure the power supply is "uninterrupted".[10] However, chemical batteries still have low power densities, as do other fast discharge technologies. Therefore, with the increasing mismatch between power supply and demand on an hourly basis, the need for electricity storage systems with large power densities and fast discharge rates is increasing.

The current difficulties in the energy transition and why power-to-methane can help overcome some of these issues.

Decarbonising the energy sector has not come without its hurdles. Currently, the main issues lie on three principles: institutional readjustments, policy and regulations, and infrastructure.[7] Job losses in the fossil fuel industry, and disparity between skills gained in the fossil fuel industry and the skills required in the renewable energy industry are examples of institutional readjustment related issues.[7] Regarding regulatory issues, there are still insufficient incentives, policies and frameworks around the use of renewables and their integration in the current energy market.[7] Last but not least, both lack of infrastructure to transport electricity to its end users, through grids, and few fully electrified end users (such as households) are preventing fully electrified energy systems.[7] Moreover, more electrified end users would worsen possible mismatches between electricity supply and demand, thus increasing the urgency for electricity (grid) balancing services, or in other terms, the need to make electrical systems more flexible with regards to surplus of electricity or surplus of demand. Overall, all infrastructure, including end users, electrical grids, and electricity storage systems should be carefully planned in order not to overload the electrical system at one end or the other. Therefore, the transition from a fossil fuel based energy system to an electrified energy system has to be paced and it can not be done "in a blink of an eye".

With regard to this, power-to-methane, as an electricity storage technology, can be advantageous in the current fossil fuel based dependant energy system. The conversion of electricity to methane gas (chemical energy) allows for transport and storage using currently existing infrastructure for (bio)gas transport and storage. In this way, power-to-methane is a technology, which can be readily implemented, since it can be easily integrated

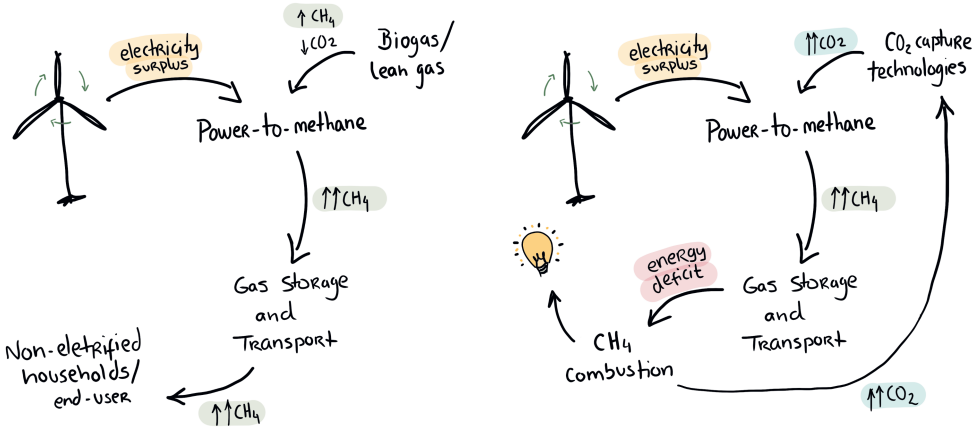

Figure 1.1: Flexible implementation of the power-to-methane technology.

within the currently existing energy transport and storage infrastructure, through gas pipelines. This readiness, and its importance in the current energy (and carbon) transition has been overlooked.[12] Moreover, integrating power-to-methane in the current fossil fuel based energy system would imply that the current gas flowing through the pipelines would be further energized (increasing the methane to CO_2 ratio) similar to a biogas upgrading technology. In comparison, H_2 as a chemical energy carrier, can not be so readily implemented, since H_2 easily escapes from the current gas pipeline infrastructure. In addition, methane is four times more energy dense than H_2, therefore, in theory, four times less storage volume is needed for the same amount of electricity.

With the current hurdles in energy transition there is the urgent need to create electricity storage systems that can function and be easily implemented in the current energy systems in order to decrease the stress on electrical grids and further grow the share of renewables. This is the case of power-to-methane storage, as discussed above. However, it is important to note that the ultimate goal is to phase out fossil-based energy systems, which entails that future energy systems do not rely (at least, so much) on gas as well. Hence, like other environmental related issues, there is the need to create flexible technologies to deal with the complex problem that is decarbonising the energy system and adapting to the changes that this transition entails. In this way, as shown in figure 1.1, in its early stage power-to-methane storage functions to energise and convert CO_2-rich streams to methane (upgrade gas) to be used by gas-dependent end-users. In a later stage power-to-methane storage can function, as part of an electricity-carbon cycle, where CO_2 is converted to methane when there is a surplus of electricity and where methane is converted back to CO_2, thereby generating electricity when there is a surplus in demand of electricity. The CO_2 released, if captured and not released to the atmosphere, can be used again, when

there is a surplus of electricity. This would most likely work in an industrial setting rather than a household setting.

1.2 *Fundamentum*: Power-to-methane in a bioelectrochemical system as an electricity storage technology.

In the previous section the relevance of power-to-methane storage technologies was addressed. This next section will dive into the fundamentals of bioelectrochemical systems and the application of bioelectrochemical systems as a power-to-methane technology.

Fundamentals of (bio)electrochemical systems and methane producing bioelectrochemical systems

(Bio)electrochemical systems

In an electrochemical system there is the physical separation of an overall chemical reaction into an oxidation reaction and a reduction reaction. At the anode electrode the the oxidation reaction occurs, releasing electrons to an external circuit, which travel to the cathode electrode, where the reduction reaction occurs with the consumption of these electrons. A daily example of an electrochemical system is a battery, where high energy reactants are converted to low energy products, hence releasing energy in the form of electrical energy. In rechargeable batteries, this process is reversible and with input of electricity (when charging the battery) the lower energy "products" are transformed back to higher energy "reactants". For these conversions to happen, electrochemical systems rely on chemical catalysts, and different catalysts can be used for the cathode and anode reactions.

Bioelectrochemical systems (BESs) rely on the same concept, as described previously, but, as the word "bio" implies either the oxidation or the reduction reaction or both are catalysed by microorganisms (or enzymes). Because microorganisms are diverse in nature and their metabolisms, in theory there are many possible applications for these systems. However, this is narrowed down because microorganisms need to be able to interact with solid electrodes or other kinds of mediators need to be present and this will be further discussed later on. Moreover, depending on the thermodynamics of the reaction, bioelectrochemical systems can either use up electricity to transform reactants into products, if the reaction is non spontaneous, or produce electricity with the conversion of reactants into products, if the reaction is spontaneous (recall the battery analogy above). These and many other aspects of bioelectrochemical systems have been recently summarised.[13]

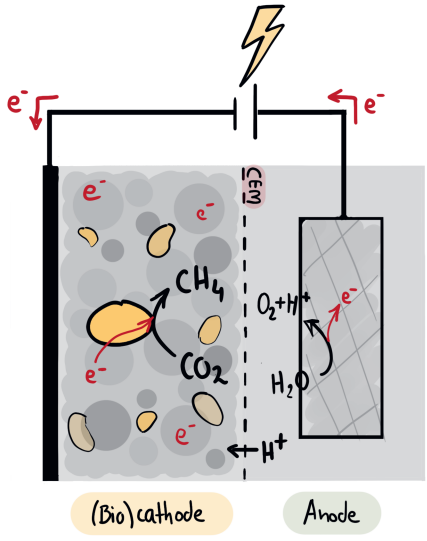

Figure 1.2: Schematic representation of a methane producing BES. On the left the (bio)cathode side, where the biological reduction of CO_2 to methane occurs. On the right the anode side, where water is oxidised. CEM-cation exchange membrane.

Methane producing bioelectrochemical systems

In a methane producing BES, CO_2 is biologically reduced to methane at the cathode side, as shown in the schematic representation in figure 1.2. The electrons needed for this reaction to happen are supplied by the oxidation of water at the anode side in the case of this thesis. The cathode and anode reactions are shown in table 1.1. The cathode and anode are separated by a cation exchange membrane (CEM) that allow protons, which are produced at the anode to travel to the cathode, where they are consumed. Because the conversion of CO_2 to methane, as a result of water oxidation, has a negative cell voltage (-1.06 V (-0.45 V - 0.61 V)) it is not thermodynamically favourable. Hence, input of electrical energy is needed to drive the reactions. The conversion of electrical energy into chemical energy, in the form of methane gas, classifies this system as a power-to-gas process. In contrast to conventional power-to-gas processes the methane producing BES allows the conversion to methane to happen in one chamber, whereas conventional processes rely on the electrochemical production of hydrogen gas (H_2) and subsequent conversion of CO_2 and H_2 into methane (either chemically or biologically).

Table 1.1: Chemical equations at the cathode and anode, and the respective electrode potential (E).

	Chemical equation	E (vs. Ag/AgCl)[1]	no.
Methanogenesis (Cathode)	$HCO_3^- + 9\,H^+ + 8\,e^- \longrightarrow CH_4 + 3\,H_2O$	-0.45 V	1
Water oxidation (Anode)	$2\,O_2 + 8\,H^+ + 8\,e^- \longrightarrow 4\,H_2O$	0.61 V	2

Methanogens and possible electron transfer mechanisms at methane producing biocathodes

Although the chemical equations at the cathode and anode have been described, the exact electron transfer mechanisms between the cathode electrode and methanogens are still not fully understood. The possibility that methanogens directly interact with the cathode electrode and take up electrons is widely discussed in literature.[14–19] The previous is referred to as direct electron transfer and evidence suggesting it occurs are few. The other possibility is that electron transfer happens through the existence of mediators, such as, H_2, acetate and formate, among others, also referred to as mediated electron transfer.[17] The theoretical electrode potentials resulting from the production of these mediators are shown in table 1.2, which shows that all potentials are below the potential for direct reduction of CO_2 to methane (more negative than -0.45 V, table 1.1), therefore, less energetically favourable in comparison. Nevertheless, it has been long proposed that the most likely routes in methane producing biocathodes, alike in anaerobic digestion, are via acetoclastic and hydrogenotrophic methanogenesis.[14, 17] In the case that CO_2 alone is fed into the biocathode without acetate or waste water (containing acetate), it is most likely that hydrogenotrophic methanogens become dominant. In fact, under these conditions, *Methanobacterium*, a genus of hydrogenotrophic methanogens, has been commonly found.[20, 21] The investigation into whether hydrogenotrophic methanogens can conduct direct electron transfer with solid electrodes is still scarce, nevertheless it remains a possibility.[14, 22]

Evaluating the performance of methane producing bioelectrochemical systems

Performance indicators

The performance of any bioelectrochemical system is typically evaluated on product formation rates and faradaic efficiency, which indicates the fraction of electrons that end up in the desired product. However, when considering BES for application as a

[1] at standard conditions and pH 7.

Table 1.2: Possible side reactions at methane producing biocathodes, and the respective electrode potential (E).

	Other possible equations at the cathode	E (vs. Ag/AgCl)[2]	no.
Hydrogen evolution	$2\,H^+ + 2\,e^- \longrightarrow H_2$	-0.62 V	3
Acetogenesis	$2\,HCO_3{}^- + 10\,H^+ + 8\,e^- \longrightarrow CH_3COOH + 4\,H_2O$	-0.51 V	4
Formate formation	$HCO_3{}^- + 3\,H^+ + 2\,e^- \longrightarrow HCOOH + H_2O$	-0.82 V	5

"power-to-X" technology it is important to also evaluate the fraction of your energy input ending up in the energy output, which is also known as energy efficiency. In order to calculate the energy efficiency, besides faradaic efficiency, one must also know something about the voltage efficiency of the BES. These four performance indicators are calculated as follows.

Methane production rates correspond to the amount of methane that can be produced in a specific amount of time and most commonly normalised by the surface area of the cathode current collector. See equation 1.1, where CH_{4gas} (in %) is the methane concentration in the produced/outlet gas; gas flow rate (in NL d^{-1}) is the rate of produced/outlet gas in normalised volume (NL) per day; and A_{CC} (in m^2) is the area of the current collector. In contrast, normalisation by volume of BES is more common in scale up attempts.

$$Methane\ production\ rate\ (NL\,m^{-2}\,d^{-1}) = \frac{CH_{4gas} \times gas\ flow\ rate}{100 \times A_{CC}} \tag{1.1}$$

Faradaic efficiency is also known as current-to-methane efficiency, defining the efficiency by which the electrons (at the cathode) are used for the reduction of CO_2 to methane. See equation 1.2, where P is the atmospheric pressure (101.33 kPa) since there is no pressure build up in the BES, R is the ideal gas constant (8.31 kPa L mol^{-1} K^{-1}), T is the temperature (in K), n is the fraction of electrons needed per molecule of CH_4 (equal to 8 mol_{e^-} $mol_{CH_4}{}^{-1}$), F is the faraday constant (96485 C $mol_{e^-}{}^{-1}$) and I (in C d^{-1}) is the amount of current applied in the BES (in A) in a day.

$$Faradaic\,efficiency\,(\%) = \frac{CH_{4gas} \times gas\ flow\ rate \times P}{100 \times R \times T} \times \frac{n \times F}{I} \tag{1.2}$$

Voltage efficiency is the ratio between the energy value of the product, in this case methane, which is the same as the heat released from the combustion of methane, and

[2] at standard conditions and pH 7.

the experimental cell voltage (over the entire BES). See equation 1.3, where ΔG_{CH_4} is the amount of heat released in the combustion of CH_4 (-890.4 x 10^3 J $mol_{CH_4}^{-1}$) and cell voltage (in V) is the observed cell voltage when running a methane producing BES.

$$Voltage\,efficiency\,(\%) = \frac{\Delta G_{CH_4}}{cell\ voltage \times n \times F} \tag{1.3}$$

Last, energy efficiency is the joint effect of the previous two efficiencies (see equation 1.4), and it describes the efficiency by which electrical energy is converted into chemical energy, the energy contained in methane.

$$Energy\,efficiency\,(\%) = \frac{CH_{4gas} \times gas\ flow\ rate \times P}{100 \times R \times T} \times \frac{\Delta G_{CH_4}}{I \times cell\ voltage} \tag{1.4}$$

Factors influencing the performance indicators

Many factors can influence the performance of a methane producing BES. In this section, an overview of these factors is given. The four, above mentioned, key performance indicators of methane producing BES are schematised in figure 1.3, along with some key parameters influencing them.

Methane production rates are dependant on the fixed electron transfer rates, also know as current density (under galvanostatic control). Moreover, the rates of methane production are highly dependant on the composition, density and activity of the microorganisms present at the cathode catalysing the conversion. If the threshold for methane production by microorganisms present is reached, further increasing the current density will not lead to an increase in methane production rates, and by-products will be formed, such as electrochemical formation of H_2. The activity of microorganisms, in turn, relies on the local conditions at the biocathode such as pH, the availability of growth factors such as nutrients and minerals, and the availability of substrates and products. These, in turn, can vary based on varying process conditions, such as the hydraulic retention time at the biocathode.

The larger the amount of electrons ending up in the desired product, in this case methane, the closer to 100% is faradaic efficiency. Hence, faradaic efficiency is heavily dependant on the composition, density and activity of the biological catalyst at the cathode, like methane production rates. Formation of by-products and/or growth of microorganisms are the most common reasons for faradaic efficiency below 100%. Nevertheless, growth is needed in order to operate BES in the long-term, hence this is a trade-off that can not be overcome.

Voltage efficiency is highly dependant on the resulting cell voltage, when operating a methane producing BES under fixed current. The resulting cell voltage is in turn

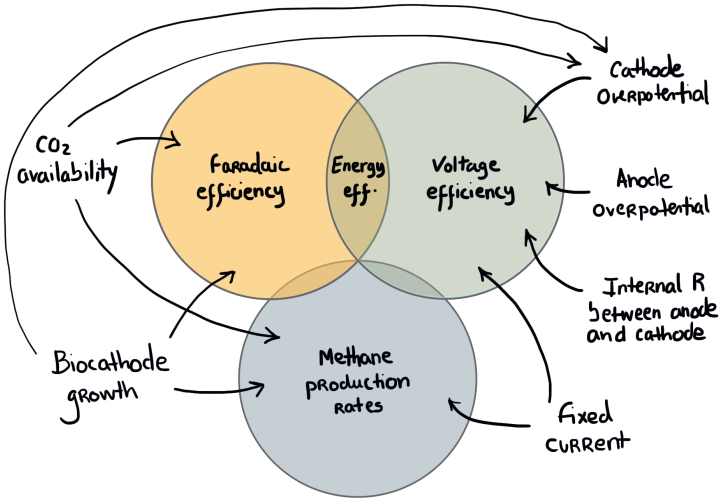

Figure 1.3: Schematic representation of the performance indicators and their main contributing factors.

influenced by existing resistances within the BES. These resistances can be associated with the cathode reaction, also know as the cathode overpotential (1), to the anode reaction (anode overpotential) (2), and to other internal resistances across the membrane (in this case CEM). The latter can be divided into pH associated resistances (3), ionic (electrolyte) associated resistances (4) and other transport associated resistances (5).[23] The bigger the contribution of these resistances/losses, the larger the resulting cell voltage, hence the lower the voltage efficiency. These resistances (1-5) are influenced by electrolyte composition, process conditions, and local conditions, such as substrate and product availability or gradients and so on.

State-of-the-art performance of methane producing bioelectrochemical systems

On the one hand, most efforts on methane producing BES, prior to this thesis, have focused on improving methane production rates and faradaic efficiency, and as discussed previously many parameters can influence these two, with special focus on the influence of these parameteres on the biological catalysts. Regarding this, experimenting with different inocula (either pure culture or mixed culture), testing different electrolyte, and or experimenting with different strategies to promote biological growth can have a positive impact on improving rates and faradaic efficiencies. Up to 2016, 30 L $m^{-2}_{\text{current collector}}$ day^{-1} had been reported as the largest methane production rates reached in methane producing BES.[17, 24] However, more recently, since 2018, the methane production rates in methane producing BES saw an increase up to 65 L $m^{-2}_{\text{current collector}}$ day^{-1},[21] and

133 L $m^{-2}_{current\ collector}$ day^{-1},[25] by using porous cathode materials such as graphite felt, graphite granules and granular activated carbon (GAC). Porous materials increase the surface area (per volume) available for interaction with microorganisms (and their growth), thus promoting increased reaction rates. The previous studies reported faradaic efficiencies between 66%,[21] and 84%.[25] However, since by-products were not detected, it was suggested that improving the reactor configuration and minimising gas losses could bring the faradaic efficiency of the former study closer to 100%.[21] Moreover, it is fairly common for methane producing BES to achieve faradaic efficiency above 80%,[17] hence this is not considered to be the limiting factor currently.

On the other hand, with the exception of a few studies,[20, 25–28] cell voltage and voltage efficiency (and resulting energy efficiency) are widely under reported in literature on methane producing BES. Therefore, these performance indicators are overlooked, although it seems that increasing rates comes at the expense of larger losses (and lower voltage efficiency).[17] From the two high-rate examples mentioned above, only the latter reported voltage efficiency with a value of 41%, being that the cell voltage was fixed at -2.8 V.[25] In this case, and with a resulting cathode potential of -0.90 V vs. Ag/AgCl methane producing BESs were operated at 35% energy efficiency.[25] In contrast, the other high rate work operated methane producing BES under fixed current and, although voltage efficiency was not reported, this resulted in the lowest cathode overpotential observed in literature with a cathode potential of -0.52 V vs. Ag/AgCl.[21] Nevertheless, the remaining of the loss contributors were not calculated in the previous work. It is important to note that additionally, the oxidation reaction at the anode highly influences the cell voltage. For example, oxidation of organics happens at lower potentials (less positive) than the oxidation of water. Up to now, the highest reported energy efficiency of methane producing BES with water oxidation at the anode is close to 40%.[25]

1.3 *In momento*: Setting the scene for this research, knowledge gaps and thesis overview

The overall aim in this thesis was to explore strategies to improve the performance of methane producing BES in terms of energy efficiency. With this is mind, the goal in Chapters 2 and 3 was to target voltage efficiency by decreasing losses associated to cathode overpotential, anode overpotential and resistances across the membrane. In Chapter 4 the methane producing BES was up scaled and the effect of scaling up on the distribution of voltage losses was assessed. Lastly, in Chapter 5 the local conditions at methane producing biocathodes were measured in the hope of better understanding what other limitations can be present at the biocathodes.

Decreasing cathode overpotential: GAC and operational parameters

Cathode overpotential is one of the main contributors to the overall losses in methane producing BES. Most studies on methane producing BES have operated at fixed cathode potentials between -0.60 V and -1.1 V vs Ag/AgCl,[15, 16, 29–31] since a larger (more negative) potential than theoretically expected, such as -0.44 V at standard conditions, should be applied in order for the conversion to take place. However, fixed low cathode overpotentials (e.g. cathode potential of -0.60 V) result in low methane production rates and, although larger methane production rates can be reached by fixing larger cathode overpotentials (e.g. cathode potential of -1.1 V), which leads to larger overall losses. More recently, methane producing BESs have been operated under galvanostatic control, which is under fixed current density.[15, 25, 32] Under galvanostatic control the electron transfer rates are fixed instead of the cathode potential.

The resulting cathode overpotential largely depends on the electrode materials used.[15, 21, 25, 33] Up to date, the best performing electrode material in methane producing BES is granular activated carbon (GAC), since it has reported the lowest cathode overpotentials with cathode potentials reaching -0.52 V vs Ag/AgCl, when controlled at a fixed current of -35 A m^{-2}.[21] In contrast, graphite granules operated under the same conditions reported a cathode potential of -0.90 V.[21] Although the reason for this low overpotential, when using GAC, has not been fully investigated, the use of GAC remains of special interest. In **Chapter 2** the operational strategies leading to low cathode overpotential, when using GAC as electrode material, are studied further.

Decreasing electrolyte associated losses by operating at haloalkaline conditions

Besides tackling cathode overpotential by using GAC as cathode material, proton, ion and other transport losses across the membrane are also usually large.[34] The operation of electrolysers for H_2 production under alkaline electrolytes, as a means to decrease transport losses, has been well established.[35] In **Chapter 3** the loss distribution and energy efficiency of methane producing BESs operated aunder haloalkaline conditions were investigated. A haloalkaline electrolyte is proposed to buffer both ion and proton movement across the membrane, hence decreasing its limitation due to the formation of large gradients. Avoiding gradients may also facilitate the long term operation of methane producing BES. Up to now, relatively short time scales have been investigated, up to 40 days,[21, 25] and up to 40% energy efficiency was reported.[25] In Chapter 3 the energy efficiency and the possibility of long term operation of methane producing BESs is assessed.

Exploring losses associated with scaling-up a methane producing BES

Scaling up bioelectrochemical systems currently faces a number of challenges; first, materials and designs that provide effective large surface areas and good microbe-material interactions

are needed in order to achieve high volumetric reaction rates; second, increasing size normally results in increasing distances between electrodes, hence increasing diffusion and mass transfer limitations; third, the design for scaling up is largely dependent on application, hence the design tends to be function-oriented.[36–40] Taking into account these challenges, in **Chapter 4**, a scaled up methane producing BES is designed with focus on: 1) the use of GAC, due to its large surface area normalised by volume; 2) the possibility to be further up scaled in modules, thus minimising the increased losses associated with increasing distances; and 3) a reactor set up that allows for CO_2 absorption, from gas to liquid and its conversion. Once designed, the BES was constructed and operated and its performance was investigated both in terms of methane production rates and voltage losses.

Exploring local conditions in methane producing biocathodes

Tackling the overall voltage losses and the resulting energy efficiency of methane producing BES without knowing the local conditions at the biocathode is not always obvious. Moreover, the local conditions present in GAC beds have not been investigated. Therefore, the goal in **Chapter 5** was to report the local conditions in methane producing GAC-based biocathodes and to investigate possible existing limitations. Knowing these limitations can better steer the research direction into optimising the desired process. Although this has not been done for methane producing biocathodes, research on chain elongation biocathodes has tried to answer similar research questions in the field.[41, 42] Inspired by these, H_2, pH and ORP (oxidation reduction potential) local measurements in the GAC bed were conducted in Chapter 5. H_2 is a possible intermediate at methane producing biocathodes (see previous sections), pH is an indicator of the availability of protons, which are needed for the conversion of CO_2 to methane, and ORP can give an indication of the presence of oxidative and reductive chemical species in the GAC bed. The combination of these measurements could enhance the understanding of the proportion of the surface area of the GAC that is truly active.

General Discussion

The final chapter of this thesis, **Chapter 6**, provides an overview of what has been achieved, specifically in terms of the performance of methane producing BESs and how this performance compares with other competing biological processes. Moreover, the remaining scientific challenges are reviewed and future research directions are proposed. Finally, the potential use of bioelectrochemical systems in future efforts towards decarbonisation is discussed.

References

[1] E. Foote. “Circumstances affecting the heat of the sun’s rays”. *Am. J. Sci. Arts* 22.66 (1856), 383–384.

[2] J. R. Fleming. “John Tyndall, Svante Arrhenius, and Early Research on Carbon Dioxide and Climate”. In: *Historical Perspectives on Climate Change*. Oxford University Press, 1998. DOI: 10.1093/oso/9780195078701.003.0011. eprint: https://academic.oup.com/book/0/chapter/353936947/chapter-pdf/43672757/isbn-9780195078701-book-part-11.pdf.

[3] G. S. Callendar. “The artificial production of carbon dioxide and its influence on temperature”. *Quarterly Journal of the Royal Meteorological Society* 64.275 (1938), 223–240.

[4] IPCC. *Sections. In: Climate Change 2023: Synthesis Report. Contribution of Working Groups I, II and III to the Sixth Assessment Report of the Intergovernmental Panel on Climate Change*. Tech. rep. IPCC, Geneva, Switzerland, 2023, 35–115.

[5] T. Rayner and A. Jordan. “Climate change policy in the European Union”. In: *Oxford research encyclopedia of climate science*. 2016.

[6] E. Commission. *A Policy Framework for Climate and Energy in the Period from 2020 to 2030*. 2014.

[7] IRENA. *World Energy Transitions Outlook 2023: 1.5°C Pathway*. Tech. rep. IRENA, Abu Dhabi, United Arab Emirates, 2023, 36–63.

[8] I. E. Agency. *System integration of renewables decarbonising while meeting growing demand*. 2020. (Visited on 2020).

[9] J. Cochran, M. Miller, O. Zinaman, M. Milligan, D. Arent, B. Palmintier, M. O’Malley, S. Mueller, E. Lannoye, A. Tuohy, et al. *Flexibility in 21st century power systems*. Tech. rep. National Renewable Energy Lab.(NREL), Golden, CO (United States), 2014.

[10] P. Ralon, M. Taylor, A. Ilas, H. Diaz-Bone, and K. Kairies. *Electricity Storage and Renewables: Costs and Markets to 2030*. Tech. rep. IRENA, Abu Dhabi, United Arab Emirates, 2017.

[11] T. Schaaf, J. Grünig, M. R. Schuster, T. Rothenfluh, and A. Orth. “Methanation of CO2-storage of renewable energy in a gas distribution system”. *Energy, Sustainability and Society* 4.1 (2014), 2.

[12] I. S. Balderas. “A carbon transition as a pre-requisite for a smooth and rapid energy transition”. PhD thesis. Wageningen University and Research, 2024. Chap. 3.

[13] F. Harnisch, T. Sleutels, and A. Ter Heijne. *Basic Electrochemistry for Biotechnology*. John Wiley & Sons, 2023.

[14] S. Cheng, D. Xing, D. F. Call, and B. E. Logan. "Direct biological conversion of electrical current into methane by electromethanogenesis". *Environmental science & technology* 43.10 (2009), 3953–3958.

[15] M. C. van Eerten-Jansen, N. C. Jansen, C. M. Plugge, V. de Wilde, C. J. Buisman, and A. ter Heijne. "Analysis of the mechanisms of bioelectrochemical methane production by mixed cultures". *Journal of Chemical Technology & Biotechnology* 90.5 (2015), 963–970.

[16] M. Villano, F. Aulenta, C. Ciucci, T. Ferri, A. Giuliano, and M. Majone. "Bioelectrochemical reduction of CO2 to CH4 via direct and indirect extracellular electron transfer by a hydrogenophilic methanogenic culture". *Bioresource technology* 101.9 (2010), 3085–3090.

[17] F. Geppert, D. Liu, M. van Eerten-Jansen, E. Weidner, C. Buisman, and A. Ter Heijne. "Bioelectrochemical power-to-gas: state of the art and future perspectives". *Trends in biotechnology* 34.11 (2016), 879–894.

[18] Y. Bai, L. Zhou, M. Irfan, T.-T. Liang, L. Cheng, Y.-F. Liu, J.-F. Liu, S.-Z. Yang, W. Sand, J.-D. Gu, et al. "Bioelectrochemical methane production from CO2 by Methanosarcina barkeri via direct and H2-mediated indirect electron transfer". *Energy* 210 (2020), 118445.

[19] H. Kobayashi, R. Toyoda, H. Miyamoto, Y. Nakasugi, Y. Momoi, K. Nakamura, Q. Fu, H. Maeda, T. Goda, and K. Sato. "Analysis of a methanogen and an actinobacterium dominating the thermophilic microbial community of an electromethanogenic biocathode". *Archaea* 2021 (2021), 1–13.

[20] M. C. Van Eerten-Jansen, A. T. Heijne, C. J. Buisman, and H. V. Hamelers. "Microbial electrolysis cells for production of methane from CO2: long-term performance and perspectives". *International Journal of Energy Research* 36.6 (2012), 809–819.

[21] D. Liu, M. Roca-Puigros, F. Geppert, L. Caizán-Juanarena, S. P. Na Ayudthaya, C. Buisman, and A. Ter Heijne. "Granular carbon-based electrodes as cathodes in methane-producing bioelectrochemical systems". *Frontiers in bioengineering and biotechnology* 6 (2018), 78.

[22] P. F. Beese-Vasbender, J.-P. Grote, J. Garrelfs, M. Stratmann, and K. J. Mayrhofer. "Selective microbial electrosynthesis of methane by a pure culture of a marine lithoautotrophic archaeon". *Bioelectrochemistry* 102 (2015), 50–55.

[23] T. H. Sleutels, A. Ter Heijne, C. J. Buisman, and H. V. Hamelers. "Bioelectrochemical systems: an outlook for practical applications". *ChemSusChem* 5.6 (2012), 1012–1019.

[24] P. Clauwaert and W. Verstraete. "Methanogenesis in membraneless microbial electrolysis cells". *Applied microbiology and biotechnology* 82 (2009), 829–836.

[25] A. G. Vidales, S. Omanovic, and B. Tartakovsky. "Combined energy storage and methane bioelectrosynthesis from carbon dioxide in a microbial electrosynthesis system". *Bioresource Technology Reports* 8 (2019), 100302.

[26] M. Villano, G. Monaco, F. Aulenta, and M. Majone. "Electrochemically assisted methane production in a biofilm reactor". *Journal of Power Sources* 196.22 (2011), 9467–9472.

[27] G. K. Rader and B. E. Logan. "Multi-electrode continuous flow microbial electrolysis cell for biogas production from acetate". *International Journal of Hydrogen Energy* 35.17 (2010), 8848–8854.

[28] F. Geppert, D. Liu, E. Weidner, and A. ter Heijne. "Redox-flow battery design for a methane-producing bioelectrochemical system". *International Journal of Hydrogen Energy* 44.39 (2019), 21464–21469.

[29] P. Batlle-Vilanova, S. Puig, R. Gonzalez-Olmos, A. Vilajeliu-Pons, M. D. Balaguer, and J. Colprim. "Deciphering the electron transfer mechanisms for biogas upgrading to biomethane within a mixed culture biocathode". *RSC advances* 5.64 (2015), 52243–52251.

[30] Z. Mao, S. Cheng, Y. Sun, Z. Lin, L. Li, and Z. Yu. "Enhancing stability and resilience of electromethanogenesis system by acclimating biocathode with intermittent step-up voltage". *Bioresource Technology* 337 (2021), 125376.

[31] G. Zhen, T. Kobayashi, X. Lu, and K. Xu. "Understanding methane bioelectrosynthesis from carbon dioxide in a two-chamber microbial electrolysis cells (MECs) containing a carbon biocathode". *Bioresource technology* 186 (2015), 141–148.

[32] D. Liu. "Strategies for Improving Methane Production from CO 2 and Electricity in Bioelectrochemical Systems". PhD thesis. Wageningen University and Research, 2018.

[33] G. Baek, J. Kim, S. Lee, and C. Lee. "Development of biocathode during repeated cycles of bioelectrochemical conversion of carbon dioxide to methane". *Bioresource technology* 241 (2017), 1201–1207.

[34] T. H. Sleutels, H. V. Hamelers, R. A. Rozendal, and C. J. Buisman. "Ion transport resistance in microbial electrolysis cells with anion and cation exchange membranes". *International Journal of Hydrogen Energy* 34.9 (2009), 3612–3620.

[35] F. Jensen and F. Schubert. "Hydrogen generation through static feed water electrolysis". In: *Hydrogen Energy: Part A*. Springer, 1975, 425–439.

[36] R. M. Alonso, M. I. San-Martín, R. Mateos, A. Morán, and A. Escapa. "Scale-up of bioelectrochemical systems for energy valorization of waste streams". In: *Microbial Electrochemical Technologies*. CRC Press, 2020, 447–459.

[37] A. Janicek, Y. Fan, and H. Liu. "Design of microbial fuel cells for practical application: a review and analysis of scale-up studies". *Biofuels* 5.1 (2014), 79–92.

[38] D. A. Jadhav, S.-G. Park, S. Pandit, E. Yang, M. A. Abdelkareem, J.-K. Jang, and K.-J. Chae. "Scalability of microbial electrochemical technologies: Applications and challenges". *Bioresource Technology* 345 (2022), 126498.

[39] F. Enzmann, M. Stöckl, A.-P. Zeng, and D. Holtmann. "Same but different–Scale up and numbering up in electrobiotechnology and photobiotechnology". *Engineering in life sciences* 19.2 (2019), 121–132.

[40] A.-J. Wang, H.-C. Wang, H.-Y. Cheng, B. Liang, W.-Z. Liu, J.-L. Han, B. Zhang, and S.-S. Wang. "Electrochemistry-stimulated environmental bioremediation: Development of applicable modular electrode and system scale-up". *Environmental Science and Ecotechnology* 3 (2020), 100050.

[41] S. M. de Smit, J. J. Langedijk, L. C. van Haalen, S. H. Lin, J. H. Bitter, and D. P. Strik. "Methodology for in situ microsensor profiling of hydrogen, pH, oxidation–reduction potential, and electric potential throughout three-dimensional porous cathodes of (bio) electrochemical systems". *Analytical Chemistry* 95.5 (2023), 2680–2689.

[42] S. M. de Smit, J. J. Langedijk, J. H. Bitter, and D. P. Strik. "Alternating direction of catholyte forced flow-through 3D-electrodes improves start-up time in microbial electrosynthesis at applied high current density". *Chemical Engineering Journal* 464 (2023), 142599.

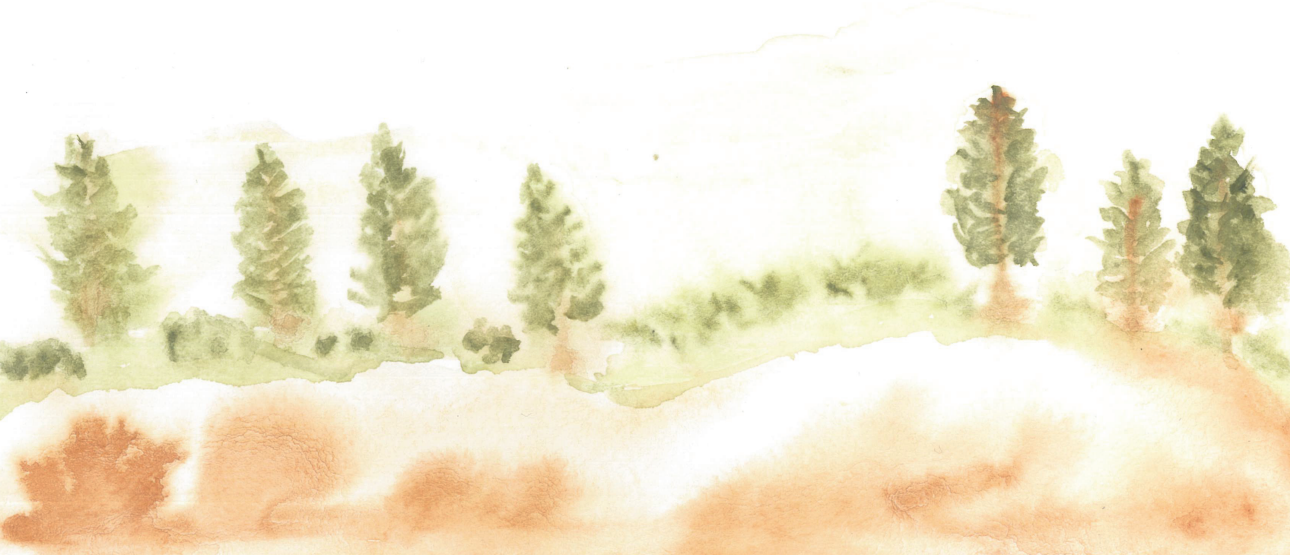

Chapter 2

Reduced overpotential in methane producing biocathodes by using GAC as electrode material

This chapter is published as:

M. B. Lavender, S. Pang, D. Liu, L. Jourdin, and A. Ter Heijne. "Reduced overpotential of methane-producing biocathodes: Effect of current and electrode storage capacity". *Bioresource Technology* 347 (2022), 126650

Abstract

Cathode overpotential is a key factor in the energy efficiency of bioelectrochemical systems. In this study the aim is to demonstrate the role of applied current density and electrode storage capacity on cathode overpotential. To do so, eight reactors using capacitive granular activated carbon as cathode material were operated. Four reactors were controlled at -5 A m^{-2} and four at -10 A m^{-2}. Additionally, to evaluate the electrode storage capacity, weekly charge/discharge tests were conducted for half of the reactors at each applied current density. Results show that cathode potential as high as -0.50 V vs. Ag/AgCl can be reached. Furthermore, the resulting low cathode overpotential is both dependent on applied current density and employment (or not) of charge/discharge tests: reactors at -10 A m^{-2} without charge/discharge regimes did not result in increasing cathode potential whereas reactors at -5 A m^{-2} and at -10 A m^{-2} with charge/discharge regimes did.

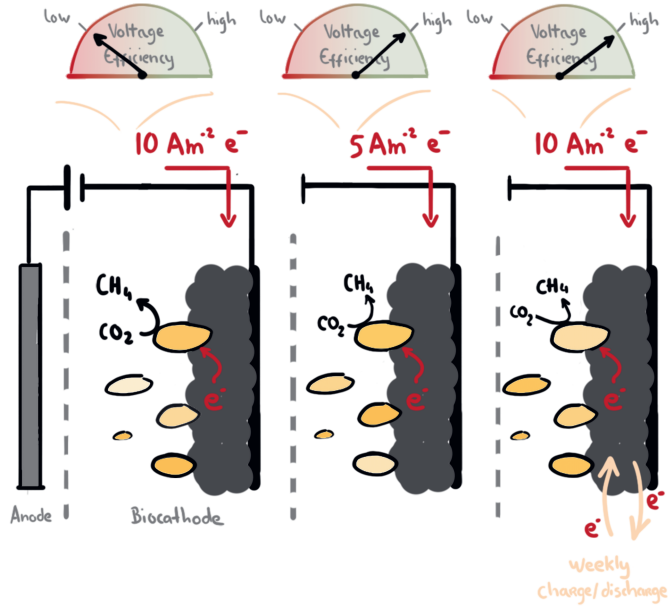

2.1 Introduction

In order to decarbonize the energy market it is crucial to incorporate renewable energy sources.[2] Because renewable energy sources are climate dependent, there is a growing demand for efficient and long-term storage technologies, allowing electricity storage when supply is larger than demand.[2, 3] Power-to-gas technologies have gained increased interest as alternative electricity conversion and storage technologies.[4] Power-to-methane in a bioelectrochemical system (BES) is one of those technologies.[5–10] In bioelectrochemical power-to-methane, CO_2 is biologically reduced to methane at the cathode, while the electrons needed for this reaction are obtained from water oxidation at the anode. Input of electrical energy is required to drive these reactions.[6] Two possible electron transfer mechanisms for methane production have been proposed: direct electron transfer (DET) and mediated electron transfer (MET).[5, 6, 11] In DET, known as electromethanogenesis, the electrons at the biocathode are directly used by the microorganisms to reduce CO_2 to methane.[5] In MET, electrons are used to electrochemically or biologically produce intermediates like hydrogen, acetate, or formate, which are then used to reduce CO_2 to methane.[6]

The performance of methane producing biocathodes has been investigated with diverse sources of inocula sludge,[12, 13] cathode materials,[9, 14, 15] and operational conditions.[7, 9, 10, 16] Regarding the latter, most research focused on controlling methane producing biocathodes at a fixed potential between -0.60 V and -1.1 V vs Ag/AgCl.[10, 11, 17–19] Alternatively, biocathodes can also be controlled under galvanostatic conditions. In a previous study, it was shown that galvanostatic control at -35 A m^{-2} resulted in high methane production rates of 65 L CH4 m^{-2} d^{-1}.[9] Interestingly, in the same study, it was found that using activated carbon granules (GAC) as cathode material resulted in a cathode potential of -0.52 V vs Ag/AgCl while the use of graphite granules (GG) resulted in a cathode potential of -0.9 V vs Ag/AgCl. The low overpotential resulting from the use of GAC is of special interest once this results in high voltage efficiency. Since energy efficiency is the product between voltage efficiency and faradaic efficiency towards methane,[6] high voltage efficiency in turn leads to highly (energy) efficient biocathodes. However, the reason for this low overpotential was not further investigated.

In this study strategies to obtain highly efficient methane producing biocathodes were explored. The goal was to do so by focusing on increasing voltage efficiency as a result of lower cathode overpotential. For this, GAC was used as electrode material and two different operational conditions were tested. Therefore, eight reactors were controlled galvanostatically, half of which at constant -5 A m^{-2} and the other four at constant -10 A m^{-2}. Moreover, charge-discharge tests were conducted on half of the reactors in order to evaluate the electron storage capacity of GAC. Performance of the biocathodes was analysed from the perspective of product formation, cathode potential and resulting efficiency.

2.2 Results and discussion

Cathode potential of -0.5 V was reached depending on the applied current density and the employment or not of charge/discharge tests.

After inoculation, at day 0, all reactors showed cathode potentials in the range of -0.85 V to -0.95 V (Figure 2.1). Out of the four reactors which were controlled at -5 A m^{-2} (Figure 2.1 (left)), all showed a gradual increase in cathode potential with time. Although, the time at which this change in potential happened was slightly different between the reactors. While three reactors showed a slow change in cathode potential, R.5(1) showed a distinct profile of suddenly changing cathode potential around day 15. Out of the four reactors which were controlled at -10 A m^{-2} (Figure 2.1 (right)) only those two reactors that underwent charge-discharge regimes showed similar patterns of gradual increase in cathode potential with time. Moreover, the latter showed the earliest shift in potential between day 6 and 11, and together with R.5(2) (-5 A m^{-2} without charge-discharge regime) reached a biocathode potential close to -0.5 V at day 30. Such high cathode potential (equivalent to -0.29 V vs SHE) has been previously and uniquely reported for methane producing biocathodes also composed of GAC as electrode material and controlled up to -35 A m^{-2}.[9] GAC is a porous material with high specific surface area and as a result, it can store charge in the form of an electric double layer. This has been demonstrated for bioanodes.[20, 21] In a previous study, by applying on-off regimes of current supply of 4min-2min, 3min-3min and 2min-4min, it has been demonstrated that GAC biocathodes result in smaller fluctuations in potential (between -0.5 V and -0.55 V) in comparison to graphite granules (between -0.65 V and -0.9 V),[8] although both assume identical methane production rates. Thus, it is shown the capacitive property of GAC allows a slower change in potential during charging and discharging (at open circuit conditions) in comparison to materials with low specific surface area, like GG. However, the role that capacitive materials can have on achieving lower overpotentials is still unclear. Nevertheless, the present results suggest that both can be linked.

Polarization curves done before inoculation and at the end of the runs supported the trends observed above (Figure 2.2). Just before inoculation, polarization curves of seven reactors (left plot in figure 2.2) showed similar potentials ranging between approximately -1.1 V to -0.9 V when the applied current ranged between 0 and -60 A m^{-2}. The exception was R.10(2), that showed a slightly less negative potential range. At the end of the run, the polarization curves for all the reactors controlled at -5 A m^{-2} (R.5(1), R.5(2), R.5CD(1), R.5CD(2)) and for those reactors controlled at -10 A m^{-2} and with charge-discharge regimes (R.10CD(1) and R.10CD(2)) (right plot in figure 2.2) shifted to less negative potential ranges (ranging between approximately -0.9 V to -0.5 V). Thus, these polarization curves are in line with the developed potential throughout the continuous run of these reactors (Figure 2.1). In contrast, the polarization curves for R,10(1) and R.10(2) at the end of the runs show even lower ranges in potential than before inoculation.

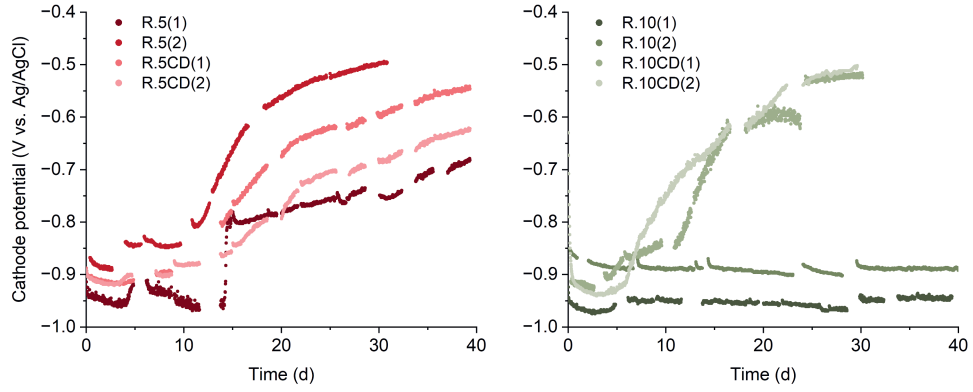

Figure 2.1: Overview of the cathode potential for all eight reactors (R.) after inoculation (day 0), four of which were galvanostatic controlled at -5 A m^{-2} (pink, left) and the other four underwent galvanostatic control at -10 A m^{-2} (green, right). Thus, 5 and 10 correspond to the applied current density (A m^{-2}). CD represents reactors which underwent charge/discharge experiments. Each condition was performed in duplicate, denoted by (1) and (2). Gaps in data represent periods when reactors were sampled, when polarization curves were conducted and for those represented by CD when charge-discharge regimes were applied as well (these measurements had a total duration of 1 to 2 days).

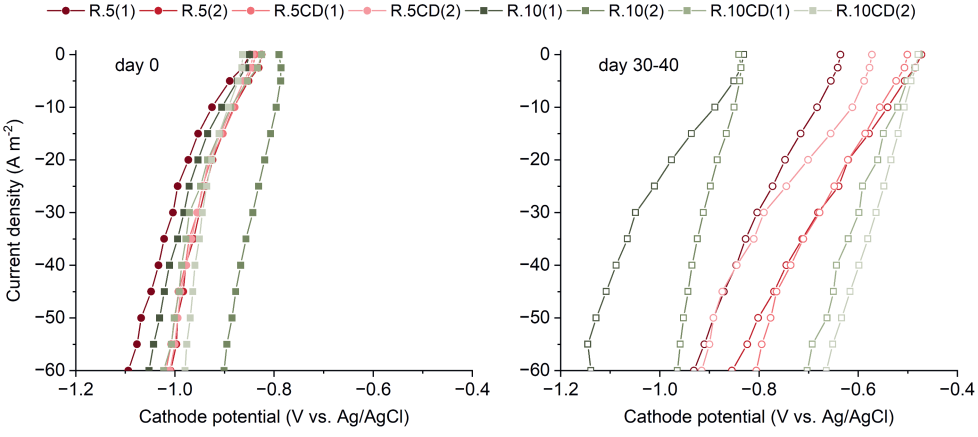

Figure 2.2: Polarization curves on inoculation day (day 0, left, full) and at the end of the run (right, empty) of the eight bioelectrochemical reactors controlled at either -5 A m^{-2} (pink circles) or -10 A m^{-2} (green squares) and that underwent or not charge/discharge experiments.

Overall, out of the eight reactors, six showed some kind of development in cathodic potential, although patterns of changing potential are not completely identical between replicates. Unexpectedly, R.10(1) and R.10(2) showed constant cathode potential between -0.89 V and -0.95 V throughout the 40 days of operation. Although it is unclear why cathode potential did not increase to more positive values in these two reactors, this work shows first evidences of the influence of different current densities in BES's performance. Because in literature the extent of galvanostatic controlled BES's is limited, further investigation is needed in order to raise hypothesis concerning the previous observation. More strikingly, comparatively, potential development did occur for those that underwent charge/discharge regimes (R10CD). Additionally, all reactors underwent polarization curves (including R.10(1) and R.10(2)), thus excluding an effect of this electrochemical technique on (positively) changing cathode potential. Whereas, suggesting that charge/discharge regimes somehow lead to the adaptation of the biocathode to other ranges in cathode potential. Electrochemical methods, and specifically, cyclic voltammetry (CV) have recently been shown to affect microbial electrosynthesis.[22] It was hypothesized that metals (from trace elements/micro nutrients) and/or biofilm release and re-deposition during CV cycles increased performance of these bioelectrochemical systems. In particular, discharge cycles might allow/facilitate the attachment of negatively charged microbial cells that would otherwise be repulsed by a negatively charged electrode/cathode.[23] Furthermore, it has been observed that microbial communities in bioelectrochemical systems are distinct in composition when operating under open circuit conditions in comparison to closed circuit conditions.[24, 25] Similarly, operation of a microbial electrolysis cell under intermittent open and closed circuit conditions has shown a more diverse microbial composition at the anode in comparison to operation under constant closed circuit.[26] Thus, it is hypothesized that applying charge/discharge cycles (in a comparatively short amount of time) mimics the changes in electron donating and non-donating properties of the biocathodes which, in turn, might lead to the selection of a different and/or more diverse microbial community at the biocathode. For future reference, analysis of the microbial community can help further understand the underlying reasoning for observing low overpotential.

Methane production and energy efficiency are crucial in order to evaluate and compare the performance of the eight biocathodes.

Two important parameters when analysing the performance of a methane producing biocathode are methane production rate and energy efficiency. The higher the supply of electrons/electron donors the higher methane production rates are expected. In this sense, the biocathodes can be either operated at high current densities or at higher cathode overpotentials, which in turn lead to higher current densities.[6] Nevertheless, high overpotentials do not come without the consequence of larger voltage losses, in turn impacting energy efficiency. Therefore, in order to optimize the performance of a methane

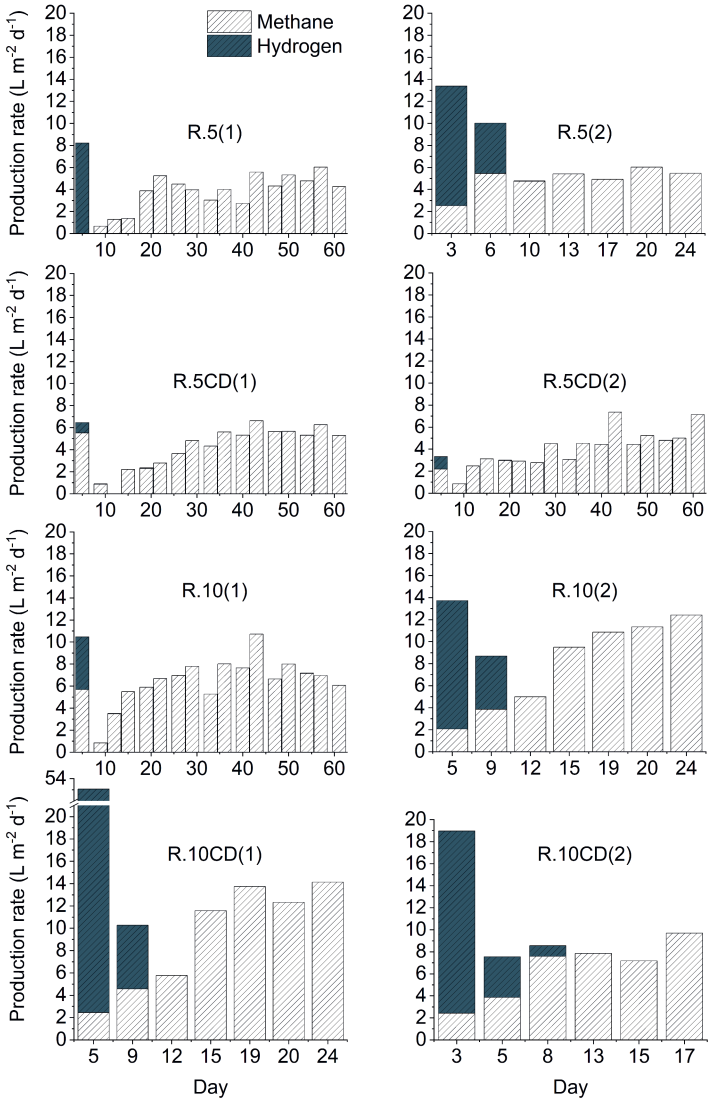

Figure 2.3: Bar graphs of methane (light stripes) and hydrogen (dark blue) production rate (L m^{-2} d^{-1}) for reactors R.5(1), R.5(2), R.5CD(1), R.5CD(2), R.10(1), R.10(2), R.10CD(1), and R.10CD(2), throughout the sampling days of the experimental runs. Inset figures show the full extent of bar graphs (with the same axis titles) for those reactors which could not be clearly represented (R.5(2), R.10CD(1) and R.10CD(2)).

Table 2.1: Methane production rate, faradaic efficiency towards methane, voltage efficiency and energy efficiency for the eight reactors.

Reactor (R.)	5(1)	5(2)	5CD(1)	5CD(2)	10(1)	10(2)	10CD(1)	10CD(2)
Sampling days	33-40	17-24	33-40	33-40	33-40	19-24	19-24	13-17
Methane prod. rate (NL $m^{-2}_{proj.\ cat.}$ d^{-1})	3.3±0.7	5.±0.6	5.1±0.7	4.0±0.8	7.0±1.5	11.5±0.8	13.4±1.0	8.2±1.3
Faradaic eff. to methane (%)	28	46	43	34	30	49	57	35
Voltage eff. (%)	44	44	46	44	33	33	37	38
Energy eff. (%)	12	20	20	15	10	16	21	13

producing biocathode, one must attempt to balance high production rates with low voltage losses.[6, 27]

Methane and hydrogen were quantified in the gas bag, hence their production rate was analysed. In figure 2.3 the production rate for both hydrogen and methane is shown for different sampling days of the eight reactors. It is shown that hydrogen was only detected during the first few days of the experimental run of all eight reactors. Moreover, it is shown that overall methane production rate increased throughout the first few days of the experimental runs. For some reactors (R.5CD(1), R.5CD(2) and R10(1)), methane production rate was comparatively large in the first sampling day (day 5), which is attributed to methane production from the inocula (anaerobic sludge). Large hydrogen production rates on the first sampling day are associated to initially high overpotential.

For further analysis, at the end of the experimental run, methane production rate was averaged out over three consecutive sampling days (Table 2.1). Methane production rate, faradaic efficiency towards methane, voltage efficiency and energy efficiency were calculated and are summarized in table 2.1. During this time no or negligible (below 0.2% faradaic efficiency) hydrogen and acetate was found.

Methane production ranged between 3.3 and 13.4 L m^{-2} d^{-1} at the end of the experimental run of the eight biocathodes, being higher for those reactors that were subjected to higher current density (-10 A m^{-2}), as expected. The resulting faradaic efficiency towards methane ranged between 28% and 57%. These values are relatively low in comparison to recent literature.[7, 9, 27, 28] Specially, biocathodes R.5(1), R.5CD(2) and R.10CD(2) show comparatively lower faradaic efficiency when compared to their duplicates. Interestingly, as shown in figure 2.1, these biocathodes also show more negative cathode potentials in comparison to their duplicates during the corresponding sampling periods. Therefore, the development/increase in cathode potential for those reactors seems to be related to developing/increasing methane production rates. Hence, the low cathode overpotential cannot explain the low faradaic efficiency. Nevertheless, methane losses when flushing the catholyte recirculation bottle to open air with CO_2 have not been excluded. Other possible electron sinks leading to lower faradaic efficiency towards methane are by-products, besides hydrogen and acetate, as can be the case of formate ([10, 29]). Additionally, biomass growth was not quantified and this can be an important electron sink. In respect, reactor optimization and further analysis are important factors for future consideration.

In this study the biocathodes were operated under galvanostatic control at two different current densities. Voltage efficiency ranged between 33% and 46%, being slightly lower for all reactors controlled at -10 A m^{-2} when compared to those controlled at -5 A m^{-2}. This translates in increased losses in the former, as expected, since losses increase when the reaction rate increases. Additionally, the most relevant observation is the lower voltage efficiency seen for the reactors controlled at -10 A m^{-2} without employment of charge/discharge regimes in comparison to all others, including those controlled at -10 A m^{-2} with employment of charge/discharge regimes. This lower voltage efficiency is, therefore, a direct consequence of the higher cathode overpotential. With this said, 1) it is important to further investigate the effect of charge/discharge regimes and possibly other electrochemical techniques on optimizing voltage efficiency and 2) operation under galvanostatic control can be seen as a strategy to increase voltage efficiency as it allows the cathode potential to increase over time. Although understudied, one other reported strategy to decrease cathode overpotential in methane producing biocathodes has relied on galvanostatic control of electrodes, in this case with the aim to reduce the overpotential for hydrogen evolution through use of catalysts.[14, 27] At ten times the current density (-100 A $m^{-2}_{\text{membrane area}}$) and higher methane production rates (at 98% faradaic efficiency) a potential of -0.86 V vs Ag/AgCl (-0.65 V vs SHE) was observed,[27] which is more negative compared to the cathode potential reported in this study.

The energy efficiency of the set-ups ranged between 10% to 21%, slightly lower than recently reported,[7] although few studies on methane producing biocathodes have reported energy efficiency at all.[7, 8] Additionally, energy efficiency differs between duplicates as a result of different values of faradaic efficiency towards methane. As discussed above, this can be explained by comparatively lower faradaic efficiency towards methane when sampling

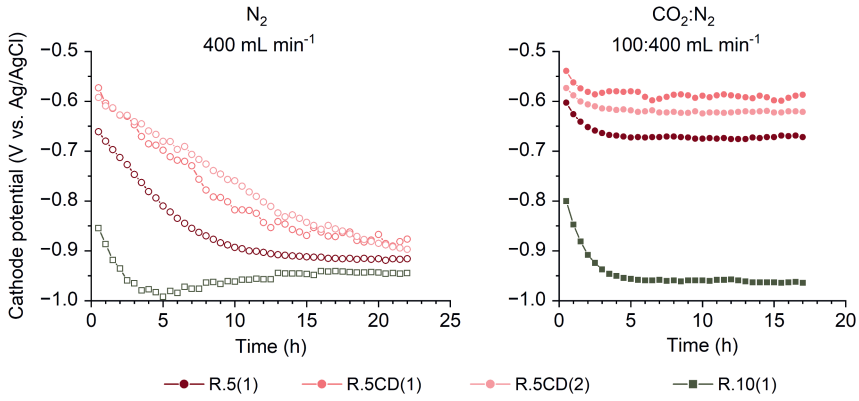

Figure 2.4: Observed cathode potential over time for R.5(1), R.5CD(1), R.5CD(2) and R.10(1) in the absence and presence of CO_2.

during earlier "development stage" in comparison to the replicates (see also potential development in Figure 2.1).

Cathode potential correlated with biological CO_2 reduction.

To further investigate the correlation between CO_2 reduction and the resulting cathode potential of the methane producing biocathodes, the cathode potential of four biocathodes under conditions with and without CO_2 was measured. For this experiment three reactors in which increase of cathode potential was observed during the continuous experiment (R.5(1), R.5CD(1) and R.5CD(2)) and one reactor which showed no potential development (R.10(1)) were selected. Results are shown in figure 2.4.

When the catholyte was flushed with N_2 alone, cathode potentials of R.5(1), R.5CD(1) and R.5CD(2) gradually decreased to around -0.9 V (figure 2.4). Moreover, the cathode potential for R.10(1) rapidly decreased to values below -0.9 V reaching an equilibrium after 12 hours. Comparatively, when CO_2 was replenished in the catholyte the cathode potential for R.5(1), R.5CD(1) and R.5CD(2) increased close to the previously measured values between approximately -0.55 V and -0.65 V. In contrast, the biocathode potential for R.10(1) remained below -0.9 V in the presence of CO_2, similarly to when CO_2 was absent. These results suggest that 1) The resulting low overpotential for R.5(1), R.5CD(1) and R.5CD(2) is related to the presence of CO_2 and most likely its reduction to methane; 2) In the absence of CO2 R.5(1), R.5CD(1) and R.5CD(2) reach potentials close to -0.9 V vs Ag/AgCl, indicating a similar reduction process as R10(1) in the presence and absence of CO_2, most likely hydrogen formation, although this was not confirmed via measurements. Potentials in the range of -0.9 V have been associated in recent studies to hydrogen-mediated electromethanogenesis.[27]

Additionally, the theoretical thermodynamic equilibrium potential for CO_2 reduction to methane is -0.46 V vs Ag/AgCl (3M KCl) and for hydrogen evolution is -0.63 V vs Ag/AgCl (3M KCl) under experimental conditions (T=30°C, pH=7) and assuming P=1bar.[12] Only at extremely low hydrogen partial pressures (100 μbar) is the thermodynamic potential for hydrogen evolution close to -0.51 V, thus comparable to the cathodic potential achieved by R.5(1), R.10CD(1) and R.10CD(2) after 30 days of operation. However, methanogenic activity was similar in R.10(1) in comparison to the other reactors. Therefore, R.10(1) may have experienced similar hydrogen partial pressure, which in turn would not explain the lower cathode potential recorded in that reactor. Nevertheless, it has been recently reported that the microorganisms in methane producing biocathodes develops differently depending on the applied voltage.[30] Studying the microorganisms could help to further understand the differences in cathodic potentials. With this said, elucidating the exact electron transfer mechanisms and its relation to cathode potential in methane producing biocathodes requires further investigation. This can bring further insights on how to increase energy efficiency of methane producing biocathodes.

2.3 Conclusions

In this research it is shown that a cathode potential of -0.50 V vs Ag/AgCl can be reached in methane producing biocathodes. Moreover, it is observed that increasing cathode potential in methane producing biocathodes is dependent on applied current density and on employment or not of charge/discharge tests. Furthermore, it was observed that in absence of CO2 the cathode potential of the set-ups, that had shown increased cathode potential, approximately decreased from -0.5 V to -0.9 V. Low cathode overpotential allows higher voltage efficiency, hence leading to higher energy efficiency in biocathodes with similar methanogenic activity.

2.4 Experimental methods

Experimental set-up

Eight two-chamber Bioelectrochemical Systems (BESs) were used in this experiment, so that each condition was tested in duplicate. The same set-up as detailed in the supplementary information by Liu et al. [9] was used.

Every cell had an anodic chamber and a cathodic chamber with flow channels of 33 cm3 each (11 cm × 2 cm × 1.5 cm). The anodic chamber and cathodic chamber were separated by a cation exchange membrane (FumaTech GmbH, Ingbert, Germany) with a projected surface area of 22 cm^2 (11 cm × 2 cm). Granular Activated Carbon, with a specific surface area of 764 m^2 g-1 (Cabot Norit Nederland B.V., Zaandam, the Netherlands; 1–3 mm diameter), was tightly packed in each cathodic chamber with a total weight of 9.54 g,

8.06 g, 9.32 g, 8.81 g, 9.17 g, 8.25 g, 8.64 g and 8.62 g for R.5(1), R.5(2), R.5CD(1), R.5CD(2), R.10(1), R.10(2), R.10CD(1) and R.10CD(2), respectively. A plain graphite plate with the same working area as the membrane (22 cm^2) was used as a current collector. Platinum-iridium coated titanium plates also with the same working area as the membrane were used as anode material (Magneto Special Anodes BV, Schiedam, The Netherlands). The anode chambers were filled up with glass beads (7 mm diameter) (Hecht-Assistent, Sondheim v. d. Rhön, Germany) to keep similar pressure on both sides of the membrane, and to ensure that the GAC granules made good contact with the graphite plate current collector on the other side of the membrane. A plastic spacer (Sefar Nitex 06-3300/59, Buffalo, NY, USA) was added between compartments of the cell (including around the membrane) to ensure distributed pressure and an airtight system. A reference electrode (3M KCl Ag/AgCl, QM710X, ProSense Qis, Oosterhout, The Netherlands; +0.210 V vs. NHE) was connected to the catholyte solution just outside each cathode chamber. All cathode potentials in this paper are therefore reported against (3M KCl) Ag/AgCl. The ohmic losses were evaluated previously for two abiotic set-ups (with GAC) that were equivalent to the ones used in this work. These ohmic losses (0.5 Ohm) were concluded to result in a potential drop of approximately -6mV and -12mV for those set-ups controlled at -5 A m^{-2} and -10 A m^{-2}, respectively. Thus, this potential drop is considered to be negligible.

Every cathodic chamber was connected to a gas-liquid separation bottle (60 mL) with a 2 L gas bag (Cali-5-BondTM). The solution was recirculated from the cathode, via the gas-liquid separation bottle, to a recirculation bottle (500 mL) continuously flushed with CO_2, and back to the cathode. The anolyte of four reactors shared a 5 L recirculation bottle in which N_2 was continuously sparged to remove any produced oxygen. Anolyte and catholyte recirculation rates were both controlled at 7 mL min^{-1} with inflow at the bottom of the cell and outflow at the top.

Electrolyte and inocula

All cathode chambers were inoculated with 10 mL of a mixed anaerobic sludge (volatile suspended solid = 2.28 g L^{-1}) with 50% v/v anaerobic granular sludge from the paper industry wastewater treatment facility in Eerbeek (The Netherlands) and 50% v/v anaerobic sludge from the municipal wastewater treatment facility in Ede (The Netherlands). All cathodic chambers contained a medium composed of 50 mM phosphate buffer (2.77 g L^{-1} $NaH_2PO_4.2\,H_2O$ and 4.58 g L^{-1} Na_2HPO_4), 0.2 g L^{-1} NH_4Cl, 0.13 g L^{-1} KCl, 1 mL L^{-1} vitamin and 1 mL L^{-1} mineral solution.[31] The anode chambers contained a solution only with 50 mM phosphate buffer. Conductivity and pH for both mediums was approximately 0.5 S m^{-1} and 7.1±0.2, respectively.

Experimental operation and analysis

The reactors were galvanostatically controlled (constant current) using a potentiostat (Ivium n-Stat with IviumSoft v2.462, Eindhoven, The Netherlands). Four reactors (R.5(1), R.5(2), R.5CD(1) and R.5CD(2)) were controlled at a constant current of -5 A m^{-2} (normalized by membrane surface area), while the other four reactors (R.10(1), R.10(2), R.10CD(1) and R.10CD(2)) were controlled at a constant current of -10 A m^{-2}. CD stands for Charge/Discharge (see below). Cathode potentials were measured every minute.

Polarization curves were acquired once for each reactor before inoculation and once per week for each reactor after inoculation. The current density was controlled and increased from 0 A m^{-2} to -60 A m^{-2} with steps of 5 A m^{-2}. Each step lasted 1200 seconds to reach a steady cathode potential.

After inoculation, four reactors (R.5CD(1), R.5CD(2), R.10DC(1) and R.10CD(2)) were subjected to a charge/discharge regime once per week after the polarization curve measurement. This charge/discharge regime consisted of alternately applying a current of +23 A m^{-2} and -32 A m^{-2} within a cathode potential range from -0.5 V to -0.7 V. Each charge or discharge step stopped when cathode potential reached the set boundary, or when the duration of a step was more than 15000 seconds. When one of these two conditions was met, the current was reversed to start the next (charge or discharge) step. Each charge/discharge test consisted of 5 cycles of charge and discharge processes.

Throughout the operation, reactors were at 30°C in a temperature controlled cabinet. Ammonium concentration and pH of the catholyte were measured three times per week. Moreover, liquid and gas samples from each reactor were taken twice per week, before and after measuring polarization curves. Gas composition and acetate concentration were measured by Gas Chromatography as described previously.[8] The gas volume was quantified by emptying gas bags manually with a syringe when sampling. With this, methane production rate was calculated and normalized by membrane surface area (which is the same as cathodic (graphite plate) and anodic projected surface area). Additionally, faradaic efficiency towards methane, voltage efficiency and energy efficiency were calculated according to standard procedure.[6]

To study the effect of (absence of) CO_2 on biocathode potential, four matured methane producing biocathodes, i.e. R.5(1), R.5CD(1), R.5CD(2) and R.10(1), were flushed with pure N2 at high flow rate of 400 mL/min for approximately 24h to remove the dissolved CO_2 in the catholyte. During this period, cathode potentials of these four biocathodes were monitored while they were continuously applied with corresponding current densities of -5 A m^{-2} and -10 A m^{-2}. After this test, the catholyte was flushed with a mixture of CO_2:N_2 to reintroduce CO_2. This was done at the same constant current as applied before. Again, cathode potentials of these four biocathodes were monitored during this operation.

Acknowledgments

This work was financially supported by the MIB Innovation Grant at Wageningen University & Research. Additionally, we would like to thank Diana Machado de Sousa for the fruitful discussions.

References

[1] M. B. Lavender, S. Pang, D. Liu, L. Jourdin, and A. Ter Heijne. “Reduced overpotential of methane-producing biocathodes: Effect of current and electrode storage capacity”. *Bioresource Technology* 347 (2022), 126650.

[2] P. Ralon, M. Taylor, A. Ilas, H. Diaz-Bone, and K. Kairies. *Electricity Storage and Renewables: Costs and Markets to 2030*. Tech. rep. IRENA, Abu Dhabi, United Arab Emirates, 2017.

[3] A. Chauhan and R. Saini. “A review on Integrated Renewable Energy System based power generation for stand-alone applications: Configurations, storage options, sizing methodologies and control”. *Renewable and Sustainable Energy Reviews* 38 (2014), 99–120.

[4] M. Götz, J. Lefebvre, F. Mörs, A. M. Koch, F. Graf, S. Bajohr, R. Reimert, and T. Kolb. “Renewable Power-to-Gas: A technological and economic review”. *Renewable energy* 85 (2016), 1371–1390.

[5] S. Cheng, D. Xing, D. F. Call, and B. E. Logan. “Direct biological conversion of electrical current into methane by electromethanogenesis”. *Environmental science & technology* 43.10 (2009), 3953–3958.

[6] F. Geppert, D. Liu, M. van Eerten-Jansen, E. Weidner, C. Buisman, and A. Ter Heijne. “Bioelectrochemical power-to-gas: state of the art and future perspectives”. *Trends in biotechnology* 34.11 (2016), 879–894.

[7] A. G. Vidales, S. Omanovic, and B. Tartakovsky. “Combined energy storage and methane bioelectrosynthesis from carbon dioxide in a microbial electrosynthesis system”. *Bioresource Technology Reports* 8 (2019), 100302.

[8] D. Liu. “Strategies for Improving Methane Production from CO 2 and Electricity in Bioelectrochemical Systems”. PhD thesis. Wageningen University and Research, 2018.

[9] D. Liu, M. Roca-Puigros, F. Geppert, L. Caizán-Juanarena, S. P. Na Ayudthaya, C. Buisman, and A. Ter Heijne. “Granular carbon-based electrodes as cathodes in methane-producing bioelectrochemical systems”. *Frontiers in bioengineering and biotechnology* 6 (2018), 78.

[10] M. C. van Eerten-Jansen, N. C. Jansen, C. M. Plugge, V. de Wilde, C. J. Buisman, and A. ter Heijne. “Analysis of the mechanisms of bioelectrochemical methane production by mixed cultures”. *Journal of Chemical Technology & Biotechnology* 90.5 (2015), 963–970.

[11] M. Villano, F. Aulenta, C. Ciucci, T. Ferri, A. Giuliano, and M. Majone. “Bioelectrochemical reduction of CO2 to CH4 via direct and indirect extracellular electron

transfer by a hydrogenophilic methanogenic culture". *Bioresource technology* 101.9 (2010), 3085–3090.

[12] P. F. Beese-Vasbender, J.-P. Grote, J. Garrelfs, M. Stratmann, and K. J. Mayrhofer. "Selective microbial electrosynthesis of methane by a pure culture of a marine lithoautotrophic archaeon". *Bioelectrochemistry* 102 (2015), 50–55.

[13] M. Siegert, X.-F. Li, M. D. Yates, and B. E. Logan. "The presence of hydrogenotrophic methanogens in the inoculum improves methane gas production in microbial electrolysis cells". *Frontiers in microbiology* 5 (2015), 778.

[14] F. Kracke, A. B. Wong, K. Maegaard, J. S. Deutzmann, M. A. Hubert, C. Hahn, T. F. Jaramillo, and A. M. Spormann. "Robust and biocompatible catalysts for efficient hydrogen-driven microbial electrosynthesis". *Communications Chemistry* 2.1 (2019), 45.

[15] M. Siegert, M. D. Yates, D. F. Call, X. Zhu, A. Spormann, and B. E. Logan. "Comparison of nonprecious metal cathode materials for methane production by electromethanogenesis". *ACS sustainable chemistry & engineering* 2.4 (2014), 910–917.

[16] G. Baek, J. Kim, S. Lee, and C. Lee. "Development of biocathode during repeated cycles of bioelectrochemical conversion of carbon dioxide to methane". *Bioresource technology* 241 (2017), 1201–1207.

[17] P. Batlle-Vilanova, S. Puig, R. Gonzalez-Olmos, A. Vilajeliu-Pons, M. D. Balaguer, and J. Colprim. "Deciphering the electron transfer mechanisms for biogas upgrading to biomethane within a mixed culture biocathode". *RSC advances* 5.64 (2015), 52243–52251.

[18] Z. Mao, S. Cheng, Y. Sun, Z. Lin, L. Li, and Z. Yu. "Enhancing stability and resilience of electromethanogenesis system by acclimating biocathode with intermittent step-up voltage". *Bioresource Technology* 337 (2021), 125376.

[19] G. Zhen, T. Kobayashi, X. Lu, and K. Xu. "Understanding methane bioelectrosynthesis from carbon dioxide in a two-chamber microbial electrolysis cells (MECs) containing a carbon biocathode". *Bioresource technology* 186 (2015), 141–148.

[20] C. Borsje, D. Liu, T. H. Sleutels, C. J. Buisman, and A. ter Heijne. "Performance of single carbon granules as perspective for larger scale capacitive bioanodes". *Journal of Power Sources* 325 (2016), 690–696.

[21] L. C. Juanarena. "Granular activated carbon in capacitive microbial fuel cells". PhD thesis. Wageningen University and Research, 2019.

[22] S. M. de Smit, C. J. Buisman, J. H. Bitter, and D. P. Strik. "Cyclic voltammetry is invasive on microbial electrosynthesis". *ChemElectroChem* 8.17 (2021), 3384–3396.

[23] D. Massazza, A. J. Robledo, C. N. R. Simón, J. P. Busalmen, and S. Bonanni. "Energetics, electron uptake mechanisms and limitations of electroautotrophs growing on biocathodes–A review". *Bioresource Technology* 342 (2021), 125893.

[24] J. Huang, Z. Wang, C. Zhu, J. Ma, X. Zhang, and Z. Wu. "Identification of microbial communities in open and closed circuit bioelectrochemical MBRs by high-throughput 454 pyrosequencing". *PloS one* 9.4 (2014), e93842.

[25] N. Shehab, D. Li, G. L. Amy, B. E. Logan, and P. E. Saikaly. "Characterization of bacterial and archaeal communities in air-cathode microbial fuel cells, open circuit and sealed-off reactors". *Applied microbiology and biotechnology* 97 (2013), 9885–9895.

[26] B. S. Zakaria and B. R. Dhar. "An intermittent power supply scheme to minimize electrical energy input in a microbial electrolysis cell assisted anaerobic digester". *Bioresource Technology* 319 (2021), 124109.

[27] F. Kracke, J. S. Deutzmann, W. Gu, and A. M. Spormann. "In situ electrochemical H 2 production for efficient and stable power-to-gas electromethanogenesis". *Green Chemistry* 22.18 (2020), 6194–6203.

[28] H. Zhou, D. Xing, M. Xu, Y. Su, J. Ma, I. Angelidaki, and Y. Zhang. "Optimization of a newly developed electromethanogenesis for the highest record of methane production". *Journal of Hazardous Materials* 407 (2021), 124363.

[29] T. Reda, C. M. Plugge, N. J. Abram, and J. Hirst. "Reversible interconversion of carbon dioxide and formate by an electroactive enzyme". *Proceedings of the National Academy of Sciences* 105.31 (2008), 10654–10658.

[30] C. Flores-Rodriguez and B. Min. "Enrichment of specific microbial communities by optimum applied voltages for enhanced methane production by microbial electrosynthesis in anaerobic digestion". *Bioresource technology* 300 (2020), 122624.

[31] E. Wolin, M. Wolin, and R. Wolfe. "Formation of methane by bacterial extracts". *Journal of Biological Chemistry* 238.8 (1963), 2882–2886.

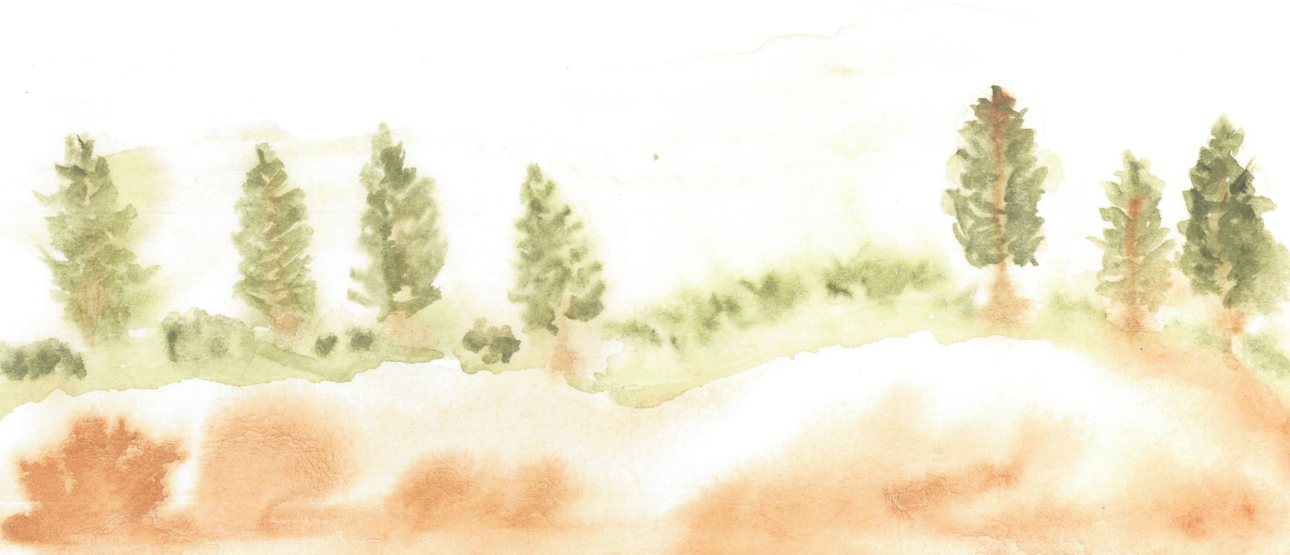

Chapter 3

High energy efficiency and long-term operation of methane producing BES at haloalkaline conditions

Manuscript in preparation by Micaela Brandão Lavender, Dandan Liu & Annemiek ter Heijne.

Abstract

A methane producing bioelectrochemical system (BES) is an alternative power-to-gas technology which converts electrical energy and CO_2 into CH_4. The main indicators to assess its performance are methane production rate, faradaic efficiency and energy efficiency. Energy efficiency is one of the main limitations since reported values remain low (20-40%). In previous work, it was demonstrated that Granular Activated Carbon (GAC) as cathode material resulted in low cathode overpotentials. Here, we aim to increase the energy efficiency of methane producing BES, by combining GAC with operation at haloalkaline conditions. With haloalkaline electrolyte, an energy efficiency of up to 70% is observed at -4.5 A m^{-2}, compared to 50% with standard electrolyte. High energy efficiency resulted from lower electrolyte-associated resistances, leading to a cell voltage of -1.4 V. Stable performance of two BES, with energy efficiency above 40% and up to 70%, was observed for the majority of the operational time (380 and 590 days).

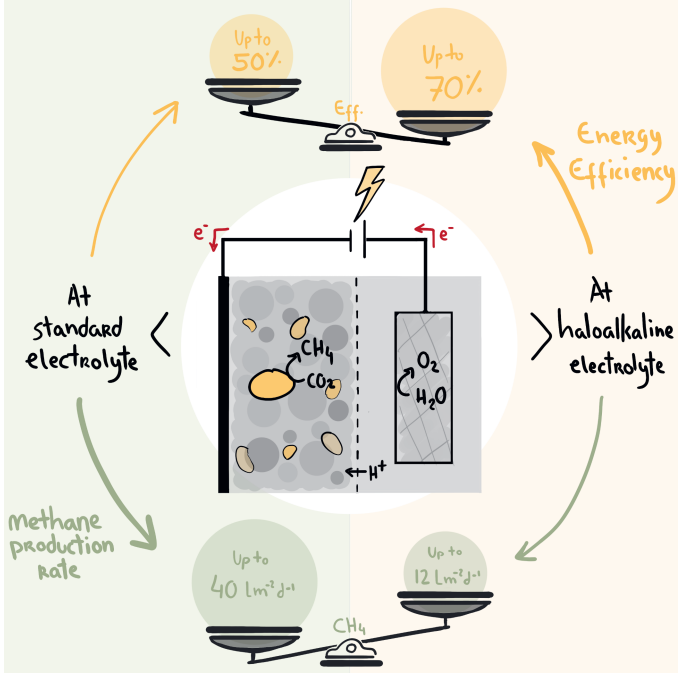

3.1 Introduction

In order to stay within the IPCC pathways leading to a limiting increase in global temperatures of 1.5°C by 2050, it is crucial to develop the renewable energy sector.[1] In line with this, in 2020, over 80% of the total installed capacity of new electricity generating technologies was attributed to renewable energy technologies alone.[2] However, growing shares of renewable energy inevitably lead to fluctuations in electricity generation and in turn lead to mismatches between electricity supply and demand. Therefore, both long- and short-term electricity storage technologies are pivotal to deal with these variations and mismatches.[2]

Using electrical energy to convert chemical compounds into energy carriers can allow for long-term and stable energy storage in the form of chemical energy. In this sense, the concept of power-to-methane dates all the way back to 1994, when CO_2 conversion to CH_4 with the consumption of electrolysis-produced H_2 has been suggested as a strategy for CO_2 recycling.[3] However, as is the case in the thermochemical Sabatier process or other electrochemical processes, the complete reduction of CO_2 is highly dependent on metal catalysts, reasonably high temperatures and most of the times high pressures.[4–7] With this said, biological processes (and their bio-catalysts) are often alternatives to these expenditures.[8] As a result, in an effort to tackle both the "energy crisis" and the "CO_2 crisis", methane producing bioelectrochemical technologies have been under study.[9–12]

In a methane producing bioelectrochemical system (BES), CO_2 is sparged through the electrolyte which is then circulated to the cathode side of a bioelectrochemical cell. There, the CO_2 is biologically reduced to CH_4, consuming electrons and protons. The electrons needed for this reduction reaction are provided by an oxidation reaction at the anode, in this case H_2O oxidation to O_2 and protons. The protons produced at the anode can travel to the cathode side by crossing the cation exchange membrane separating both chambers. Input of electricity is needed to drive the electron movement (current) from the anode to the cathode since the overall reaction is not thermodynamically spontaneous. The energy efficiency expresses which part of the energy input, in the form of electricity, ends up in energy in the form of methane[1]. Thus, energy efficiency is an important performance indicator when considering the potential of methane producing BES as a power-to-gas technology.[13] Energy efficiency can also be understood as the product between faradaic and voltage efficiency.

On the one hand, faradaic efficiency, also known in this case as current-to-methane efficiency, is an indicator of the fraction of the electrons (provided to the cathode) ending up in the desired product. Hence, it is highly dependent on the current, and the resulting methane

[1]The energy density of methane for combustion is 890.4 kJ mol^{-1} and the energy input is the product between the applied current (C) and the resulting cell voltage (V).

production rates. Methane production is highly dependent on biological composition, density and activity, which in turn relies on process conditions such as pH, electrolyte composition, availability of nutrients and minerals, availability of substrates and products, hydraulic retention times, and interactions with the electrode material. So far, the performance of any bio(electrochemical) system is typically evaluated on faradaic efficiency and (desired) product formation rates. Thus, up to now, most efforts have focused on improving methane production rates and faradaic efficiency. Taking this into account, the best performing lab scale methane producing bioelectrochemical systems report methane production rates ranging between 133 and 202 L m^{-2} day^{-1}, whilst reporting faradaic efficiencies above 80%.[14–16]

On the other hand, voltage efficiency expresses the difference between the measured cell voltage and the theoretical cell voltage based on process conditions. The difference between measured and theoretical cell voltage results from the existence of several resistances in a (bio)electrochemical system associated to (1) pH, (2) electrolyte composition (including ions), (3) other transport losses, (4) anodic overpotentials and (5) cathodic overpotentials.[17] The bigger the contribution of these resistances/losses, the larger the difference between measured and theoretical cell voltage, hence lower the voltage efficiency. In the examples mentioned above, although high rates of methane production and high faradaic efficiencies are achieved, these come at the expense of large (applied) cell voltages, such as -2.8 V,[15, 18] and -5.5 V,[16] whereas the theoretical cell voltage would be around -1.2 V, depending on process conditions. Hence, voltage efficiencies are fairly low. With the exception of the previous mentioned studies and a few additional,[14–16, 19–21] voltage efficiency is both widely overlooked and under reported.

The combination of faradaic and voltage efficiency expresses the energy efficiency. Up to now, 40% energy efficiency is the maximum reported in literature on methane producing BESs with continuous flow designs (with anodic water oxidation),[14, 15] and only one batch study showed higher efficiency of 54%.[18] In all cases voltage efficiency is the limiting factor. With the aim of increasing voltage efficiency (hence, energy efficiency) by reducing cathode overpotential (5), methane producing biocathodes were operated with granular activated carbon as cathode material. This resulted in the lowest cathode overpotential reported up to date, with a cathode potential of -0.50 V vs Ag/AgCl.[21, 22] Nevertheless, the resulting energy efficiency ranged around 20%.[21] Furthermore, all these previous experiments are conducted on relatively small time scales (up to 40 days) and it is unclear what would be the trend in both faradaic and voltage efficiency if operation extended for longer periods of time.[14–16, 21, 22] Therefore, the need remains to further explore strategies that lead to high voltage efficiency, hence high energy efficiency, and that simultaneously allow for long-term and stable operation of methane producing BES.

The use of alkaline electrolytes as a means to achieve high voltage (and energy) efficiency in electrolysers for H_2 production has been well established.[23] In a similar way, we

hypothesize that operation of methane producing bioelectrochemical systems under a haloalkaline electrolyte might lead to high energy efficiency in comparison to previous studies. The highly conductive and highly buffered environment is expected to lead to lower internal (/electrolyte) resistances and lessen pH changes, allowing for longer operational times and lower voltage losses. To the best of our knowledge haloalkaline conditions have not been investigated before. With this said, the goal of the current study is to assess if the strategy of operation under a haloalkaline electrolyte can lead to long-term operation at high energy efficiency of methane producing bioelectrochemical systems.

In this work, two methane producing BES (B1 and B2) were first started-up and operated under 50mM phosphate electrolyte and neutral pH, as done in previous work.[21, 24] During the remaining of the paper we refer to this as standard electrolyte. After reaching stable performance under operation with standard electrolyte the electrolyte was changed to a haloalkaline buffer (0.6M to 1M bicarbonate, pH 8.5), which for simplicity reasons we refer to haloalkaline electrolyte from now on. During the entirety of the operational run, 590 days for B1 and 380 days for B2, methane production rates, faradaic efficiency and energy efficiency are measured/calculated in order to evaluate and compare the performance under both electrolytes. Additionally, cathode potential, anode potential, pH, conductivity, temperature and substrate concentrations are measured on the regular basis in order to analyse the contribution of the previously mentioned losses (1 to 5) during operation under both electrolytes. In addition, scanning electron microscopic (SEM) pictures are taken of the (bio-)cathode in order to visualise the microorganisms responsible for the conversion. With this comprehensive analysis the outlook of this technology is further discussed and main focus points for future research are proposed.

3.2 Results

General performance: High energy efficiency and distribution of losses

In this research two methane producing BESs, B1 and B2, were first started up and operated with standard electrolyte and after achieving stable operation (see following section) the electrolyte was changed to a haloalkaline electrolyte and operation continued. In this section, the focus is solely on the results during operation at applied current density of -4.5 A m^{-2} (-333 A m$^{-3}_{\text{Cathode Volume}}$), since this is the control strategy held in common for operation with both electrolytes, allowing for comparison. The detailed performance throughout the whole operation will be discussed in the following section (2.2). In figure 3.1, faradaic, voltage and energy efficiency of both methane producing BES, B1 (top) and B2 (bottom), are shown for operation with standard electrolyte (left) and haloalkaline electrolyte (right).

During operation with standard electrolyte an average faradaic efficiency of 66% for B1 and 81% for B2 was achieved. During the same time period, the voltage efficiency was

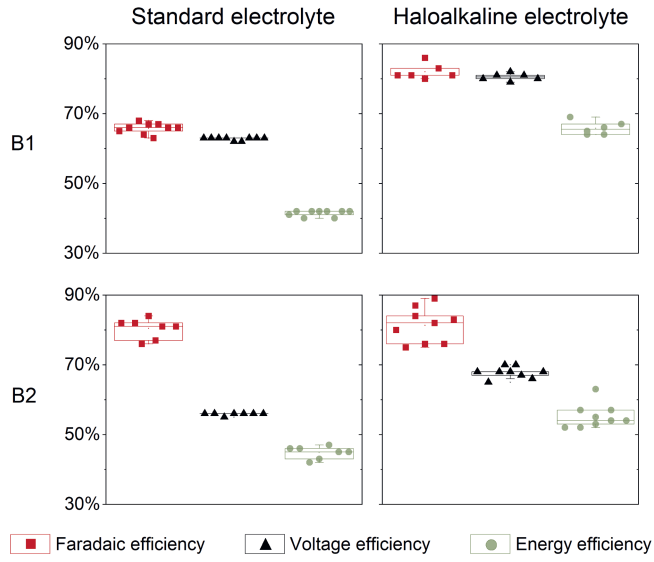

Figure 3.1: Box plot of the faradaic (red squares), voltage (black triangles) and energy efficiency (green circles), for set-ups B1 (top) and B2 (bottom) when operated with standard (left) and haloalkaline electrolyte (right) at a fixed current of -4.5 A m^{-2}. Used data points are: for B1-standard days 104-132; for B1-haloalkaline days 231-248; for B2-standard days 163-186; and for B2-haloalkaline days 276-299 and 317-320.

around 63% for B1, with the cell voltage averaging -1.8 V, and 56% for B2, with the cell voltage averaging -2.1 V. The measured cell voltage can be found in the supplementary information chapter, figures 1 and 4. As a result, the average energy efficiency, which can also be calculated as the product between the previous two, was 41% for B1 and 45% for B2. Here, operation under standard electrolyte yielded higher energy efficiency in comparison to previous work also under standard electrolyte, 21%[21] and 22%[24]. The main changes that might be responsible for this are the 1) improved anode material and increased surface area (see section 4.2.1), possibly leading to lower losses associated to the water oxidation reaction and the 2) improved gas collection design of the overall set-up (see section 4.2.1), possibly improving the collection of methane and decreasing leakages.

When operating with haloalkaline electrolyte, the average voltage efficiency increased, compared to standard electrolyte, to values averaging 80% for B1, with the cell voltage averaging -1.4 V, and 68% for B2, with the cell voltage averaging -1.7 V. The average faradaic efficiency of the former, B1, increased to 82%, resulting in an increase in energy efficiency to 66%, in comparison to when it was operated with standard electrolyte. The

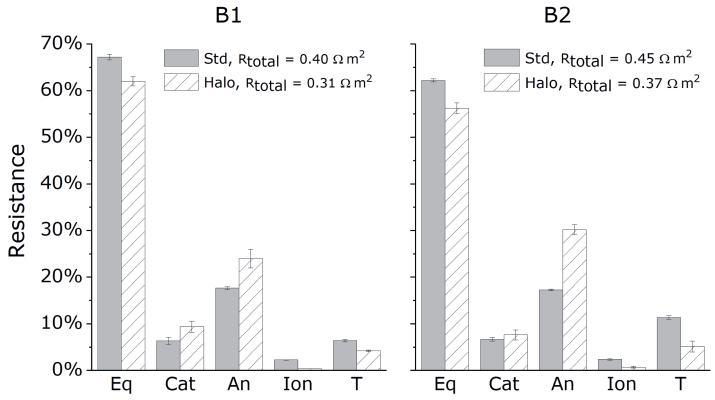

Figure 3.2: Bar plot showing the distribution of resistances, equilibrium voltage (eq), cathode overpotential (cat), anode overpotential (an), ionic (ion) and transport related (t), normalised by total resistance (whose value is indicated in legend), in %. Values are averaged for the operation of B1 (left) and B2 (right) at both standard (grey, full) and haloalkaline electrolyte (white, stripped) and at applied -4.5 A m^{-2}. Same data points as figure 3.1 are used.

average faradaic efficiency of the latter, B2, remained around 81%, leading to an increase in average energy efficiency to 55%. The increased energy efficiency, 55% and 66%, is the highest reported up to date, whether comparing to similar designs (26%-40%),[15, 16] or to designs involving hydrogen mediated methanogenesis (30%).[14]

The above mentioned results show that operating with haloalkaline electrolyte results in higher voltage efficiency in comparison to operation under standard electrolyte (at same current density), in turn leading to unprecedented energy efficiency. In order to further understand this, the different resistances were quantified. In figure 3.2, the total resistance and its distribution over the different losses is shown. The total resistance can be distributed in the following losses: the equilibrium voltage (Eq), the cathode overpotential (Cat), the anode overpotential (An), the electrolyte resistance (Ion) and other transport losses(T) (see section 4.3.1).[25] The total resistance when operating with haloalkaline electrolyte (0.31 and 0.37 Ω m^2, for B1 and B2 respectively) is at least 18% lower than with standard electrolyte (0.40 and 0.45 Ω m^2, for B1 and B2 respectively), which is in line with the higher voltage efficiency with haloalkaline electrolyte (see figure 3.1).

Besides observing lower total losses with haloalkaline electrolyte, the contribution of the different losses differs in comparison to standard electrolyte. The total voltage required for the overall reaction to occur,[25] in this case reduction of CO_2 to CH_4 (at the cathode) with water oxidation at the anode, assumed values between 56% to 67%. This was calculated at real process conditions, including measured pH. Although not shown, pH accounted for 0.06 Ω m^2 when operating with standard electrolyte and -0.02 to -0.01 Ω m^2 when operating

at haloalkaline electrolyte. These differences are the result the anolyte pH being slightly higher than the catholyte pH during operation with haloalkaline electrolyte, whereas anolyte pH was lower than catholyte pH during operation with standard electrolyte (see supplementary information chapter, figures 3 and 6).

The second largest loss is attributed to the anode overpotential (17% to 30%) and it is larger during operation at haloalkaline conditions compared to standard conditions. The anode electrode was state-of-the-art for water oxidation (see section 4.2.1) and these losses are hard to overcome in line with current knowledge. Nevertheless, increasing the anode surface area might be a strategy to further reduce the anode losses. In contrast, the contribution of the cathode overpotential to the overall resistance is for all cases below 10%. Low cathode overpotential is inline with that observed for methane producing biocathodes under galvanostatic control when using GAC as electrode material.[21, 22] Moreover, for all cases the resistance associated to cathode overpotential is the same, 0.03 Ω m^2. The cathode overpotential accounts for mass transfer limitations, charge transfer limitations and the energy required for biological growth at the cathode.[25] Apparently, the sum contribution of these three limitations does not change with the change in electrolyte from standard to haloalkaline. 0.03 Ω m^2 is in line with what has been reported for other microbial electrosynthesis systems, in which CO_2 is converted into acetate or other fatty acids (0.004 to 0.09 Ω m^2).[17]

The contribution of electrolyte losses and transport losses to the overall resistance also decreased for both B1 and B2 when switched from standard to haloalkaline conditions. Switching to a haloalkaline electrolyte at the anode and cathode results in a higher concentration of ions on both sides of the membrane, on the one hand, leading to lower electrolyte resistances on either side and, on the other hand, leading to lower losses associated to ion transport across the membrane.

Long-term operation of methane producing biocathodes: performance and challenges

The two methane producing BESs were first operated with standard electrolyte and subsequently with haloalkaline electrolyte. B1 was operated for a total of 590 days, the first 270 days with standard electrolyte and the remaining 320 days with haloalkaline electrolyte. B2 was operated for a total of 380 days, 220 days with standard electrolyte and 100 days with haloalkaline electrolyte. For the majority of the operational time both B1 and B2 were operated at constant current density, with the exception of a few days (maximum of 20 days in the whole run) where cathode potential was controlled. In figure 3.3, the applied current density (in A m^{-2}) and the resulting methane production rate (in normalised L m^{-2} d^{-1}) and cathode potential (in V vs. Ag/AgCl) are shown throughout the operation of B1 and B2, respectively. Both the current density and the methane production rate are normalised by the area of the current collector (m^2 of graphite plate).

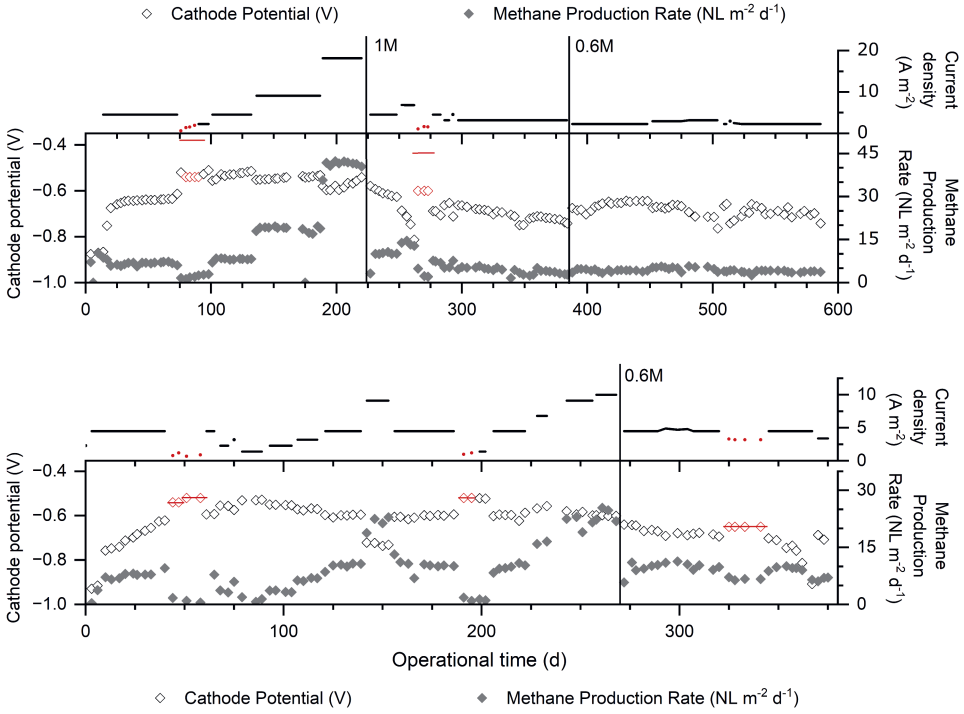

Figure 3.3: Current normalised to surface area of the current collector, in A m^{-2} (top), and resulting methane production rate also normalised by surface area of the current collector, in NL m^{-2} d^{-1}, and cathode potential, in V vs. Ag/AgCl, (bottom) throughout operation of B1 (A) and B2 (B). Vertical lines represent the change from operation with standard electrolyte to either 1M bicarbonate electrolyte (B1) or to 0.6M bicarbonate electrolyte (B1 and B2). Red dots and diamonds represent operation at controlled cathode potential.

In the following sections, these and other performance indicators are discussed in more detail.

Galvanostatic control start-up and resulting low cathode overpotential

Both B1 and B2 were start up at similar conditions (inoculate, standard electrolyte and current density) to previous work.[21, 24] As shown in figure 3.3, when starting up the two reactors at -4.5 A m^{-2} the cathode potential increased throughout the first 30 to 40 days of operation, reaching a value of approximately -0.62V vs Ag/AgCl. However, the rate by which this increase occurred was different for both B1 and B2. In order to reach a less negative cathode potential, thus a lower cathode overpotential, the potential was then controlled at around -0.52V vs Ag/AgCl. Methane formation has been reported at such low cathode overpotential in the previous work on galvanostatic controlled BESs.[21] The

galvanostatic control of -4.5 A m^{-2} was re-established after two weeks of cathode potential control. For B1, once current control was re-established around day 90, the potential increased to -0.52V, showing that the biocathode adapted after a few days of potential control. In contrast, for B2 the cathode potential only slightly increased (to approximately -0.60V) after going back to current control around day 60. The main difference between both reactors is that B1 was switched to potential control after a long time of stable performance, both in terms of cathode potential and methane production, whereas for B2 the potential control was immediately applied once the cathode potential reached -0.62V. This might indicate that a stable performance, both in terms of cathode potential and methane production rate, is important to successfully reduce cathode overpotential by applying this strategy of "potential control followed by galvanostatic control". In general, low cathode overpotential is observed, when using GAC as electrode material, as previously suggested.[21]

The operational challenge of haloalkaline electrolyte: increasing methane production rates

During the first 100 days, approximately, the methane production rate ranged around 8 NL m^{-2} d^{-1} for B1 and B2 when operated under galvanostatic control. Around day 150, still with standard electrolyte, the current density was increased to -9 A m^{-2} for both reactors, and accordingly the methane production rate increased to 20 to 23 NL m^{-2} d^{-1}. Moreover, the cathode potential for B1 remained around -0.55V, whereas the cathode potential for B2 decreased abruptly to -0.75V, although reaching similar methane production rates as B1. Thus, for B2, current control of -4.5 A m^{-2} was re-established and, later on, a step wise increase in current density was followed reaching up to -10 A m^{-2} (at day 256) with a resulting cathode potential of -0.60V (in contrast to -0.75V previously) and a methane production rate of up to 25 NL m^{-2} d^{-1}. For B1, the current density was further increased at day 190 to -18 A m^{-2} and the resulting methane production rate reached around and above 40 nL m^{-2} d^{-1} while the cathode potential, after a small decrease, developed back to -0.55V. These results, with standard electrolyte, are close to those observed in previous experiments with similar reactor design (65 L_{CH_4} m^{-2} d^{-1} and a cathode potential of -0.52V vs Ag/AgCl).[22] In contrast, five times higher methane production rates have been reported (up to 202 L_{CH_4} m^{-2} d^{-1}) at the expense of larger cathode overpotentials (cathode potential of -1.84V vs Ag/AgCl).[16]

When switching to the haloalkaline electrolyte (1M bicarbonate for B1 and 0.6M bicarbonate for B2) the current density was decreased back to the initial value, -4.5 A m^{-2}. At this point, similar methane production rates, in comparison to standard electrolyte, were reached (around 8 NL m^{-2} d^{-1}). However, the cathode potential decreased for both reactors, stabilising at around -0.63V for B1 and around -0.69V for B2. For B1, the current density was slightly increased at day 250 but this lead to a sharp drop in cathode potential, thus the cathode potential was controlled at -0.60V. For B2, the cathode potential was

also controlled at −0.60 V at day 320. When the current density was again controlled at -4.5 A m^{-2}, a decrease in cathode potential was observed for both reactors. As a result, with haloalkaline electrolyte lower rates had to be set for both B1 and B2 in order to minimize losses associated to cathode overpotential. Throughout the operation with haloalkaline electrolyte the current density was controlled between -2 and -4.5 A m^{-2}, resulting in methane production rates ranging between 4 and 11 NL m^{-2} d^{-1}, at least two-fold lower in comparison to the reasonable rates observed with standard electrolyte (40 for B1 and 25 NL m^{-2} d^{-1} for B2).

Effects of haloalkaline electrolyte and long-term operation on efficiency

In figure 3.4 the faradaic, voltage and energy efficiency are shown throughout the operational run of B1 and B2. After the start-up period, the faradaic efficiency towards methane averaged close to 80% for both reactors under standard electrolyte, reaching values around 85% for B1 and 93% for B2. During the same period for both reactors, the voltage efficiency stabilized at around 50% or 60% depending on the applied current density. The higher the applied current density, the lower the voltage efficiency as a result of increased voltage losses. For the same time period, while operating with standard electrolyte, the resulting energy efficiency remained around 40% and above (up to 50%) in both reactors.

Switching to 1M bicarbonate haloalkaline electrolyte, in B1, initially led to a significant increase in voltage efficiency up to 80% and consequentially an unprecedented increase in energy efficiency up to 70%. However, with time, an unstable performance was observed, in terms of faradaic efficiency towards methane and voltage efficiency. Between days 250 and 265 the unstable faradaic efficiency was accompanied with a sharp increase in anode potential (see supplementary information chapter, figure 1), a decrease in voltage efficiency, an increase in oxygen concentration in the gas bag (supplementary information chapter, figure 2) probably due to oxygen cross over from the anode to the cathode, and lower rates of changing conductivity (see supplementary information chapter, figure 3), all consistent with the membrane leakage found on day 265. After substituting the membrane, a relatively stable faradaic efficiency, around 60%, was observed up to day 325. After day 325, hydrogen was detected in the gas phase reaching up to 18% faradaic efficiency towards hydrogen. This unstable performance is possibly a consequence of higher osmotic stress on the microorganisms at the cathode under 1M bicarbonate electrolyte, in contrast to 0.6M bicarbonate used for B2 (described below). Therefore, the electrolyte in B1 was switched to 0.6M bicarbonate at day 380, after which, a stable operation and performance in terms of faradaic and voltage efficiency was resumed. For the remaining of the run of B1, approximately 200 days, the energy efficiency remained around and above 40%.

In B2, when switched to 0.6M bicarbonate haloalkaline electrolyte, the faradaic efficiency was stable at around 70% to 75% and the voltage efficiency increased to around 70%. As a result, the energy efficiency remained stable around 50% to 55% throughout the

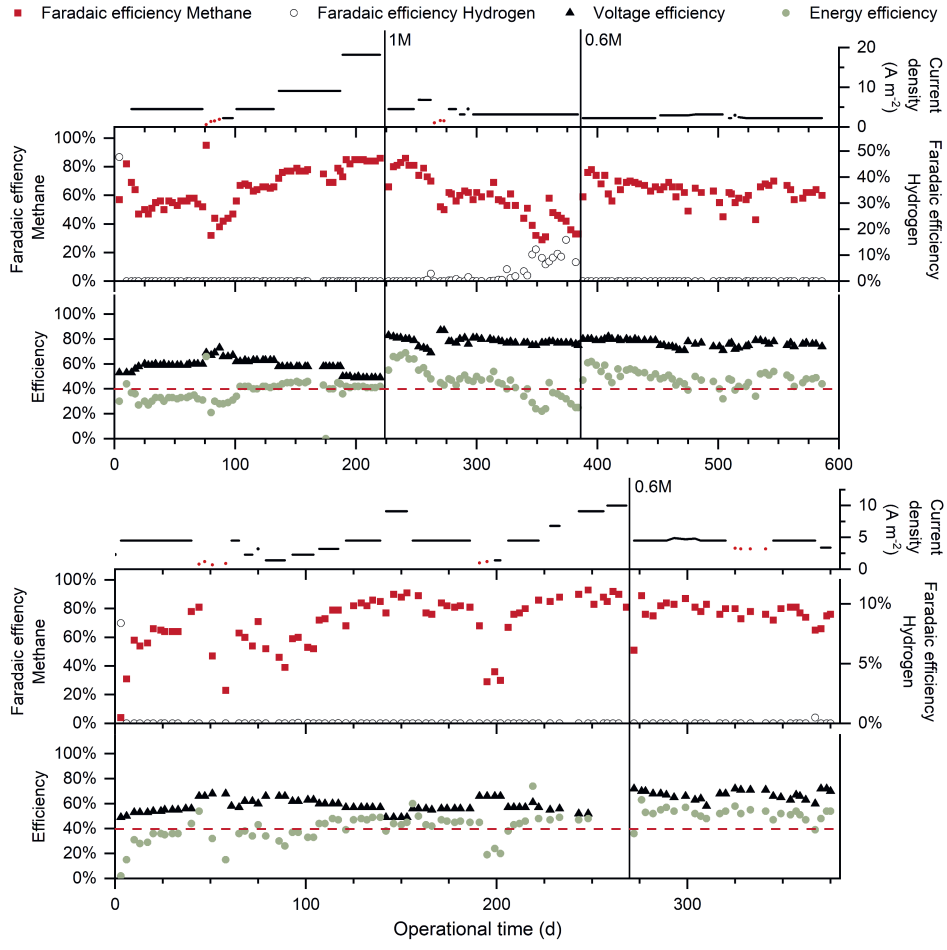

Figure 3.4: Faradaic efficiency towards methane and hydrogen (by-product) (middle), voltage efficiency (bottom) and energy efficiency (bottom) throughout the operational time of B1 (A) and B2 (B). The control strategy, the applied current density, is shown on top. Regarding this, note that the red dots represent the resulting current when operation is at controlled cathode potential. Dashed horizontal red line represents the 40% literature limit. Vertical lines represent the change from operation with standard (0.05M phosphate) electrolyte to either 1M bicarbonate electrolyte (B1) or to 0.6M bicarbonate electrolyte (B1 and B2).

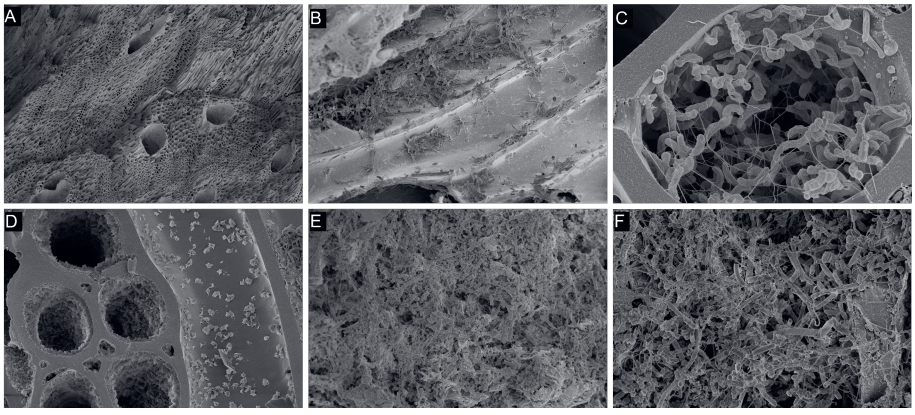

Figure 3.5: Scanning electron microscopy (SEM) pictures of granular activated carbon collected from B2 (A, B, C and D) and B1 (E and F). For details and scale see supplementary information chapter, figures 7-12.

operation under haloalkaline electrolyte (100 days). In general, a stable operation with 0.6M bicarbonate electrolyte was observed in both B1 and B2.

Visualizing the biocathodes

At the end of the operation of both B1 and B2, scanning electron microscopy (SEM) pictures were taken of samples of the granular activated carbon, in order to visualize the microorganisms attached to the electrode. Figure 3.5 shows a compilation of several pictures taken of B1 and B2. Figure A, clearly shows the porous structure of granular activated carbon, with a mix of smaller sized and bigger sized pores, up to around 200 μm in diameter. Figure B, shows agglomerates of biofilm formation in GAC collected from B2 as well as less dense biofilm sections of the electrode material, suggesting that not all the electrode surface area was covered. Figure C, zooms in into a pore of approximately 20 μm diameter with clear signs of biofilm growth and attachment. Mainly, rod-shaped microorganisms are identified in this pore. Interestingly, pili-like structures are observed as well. Pili-like structures have been observed, between many other places, at biocathodes, *e.g.* under sulfate reducing conditions.[26, 27] In contrast, figure D shows precipitates at the surface of the electrode material and its pores. These can be bicarbonate precipitates and/or caused by accumulation of metals from the trace metal solution added for biological growth and/or trace metals present in the inoculate sludge. It is important to note that such precipitation can lead to fouling of the electrode material, in turn impacting the performance of the BES. Both figures E and F show a complex composition of the microbial community attached to the electrode material of B1, varying from spherical shaped microorganisms to rod-shaped ones. Also, pili-like structures can be observed.

Although these SEM pictures can give us first evidences of biological activity, shape and interactions with electrode, it would be relevant to go one step further and execute analysis regarding the microbiological composition, such as next generation sequencing of the biocathodes.

3.3 Discussion

This paper shows the performance of two methane producing bioelectrochemical systems operated under haloalkaline conditions and for long operational times of 590 (B1) and 380 (B2) days. Moreover, a stable performance is observed with energy efficiency of 40% and above for the majority of the run time (with standard electrolyte and with 0.6M bicarbonate haloalkaline electrolyte). The long-term and stable operation support the applicability of this technology as an alternative power-to-gas technology for electricity storage, with little evidence of deterioration within this time span. Additionally, a maximum energy efficiency of 70% is reported when operating with a haloalkaline electrolyte, 40% being the upper limit found in literature on methane producing BES.[15] The high energy efficiency is a direct consequence of decreased electrolyte-associated voltage losses, in comparison to standard electrolyte. In fact, only recently have few studies elaborated on the use of high salt electrolytes (alone), up to 70 mS cm^{-1}, as means to achieve lower voltage losses in CO_2 reducing bioelectrochemical systems for the production of acetate,[28, 29] and formate.[29] Although the reported energy efficiency reached 46% (cell voltage of -2.3 V), accounting for joint production of organics and hydrogen,[29] the rates are comparatively low (-0.2 A m^{-2}) and the longevity of the processes is not studied.[28, 29]

Additionally to the observed low voltage losses, the use of a haloalkaline electrolyte is relevant 1) due to increased substrate availability (in concentration) in the liquid phase, in comparison to standard electrolyte, and 2) for easing the prospects of integration with other processes involving CO_2 absorption and desorption, such as CO_2 direct air capture.[30]

Nevertheless, there are three main focus points we consider important in regards to future research: dealing with conductivity changes of the electrolyte, exploring other start-up strategies, and increasing rates of methane production. These three points are discussed in more detail below.

The need for (novel) designs that deal with changing conductivity

When operating under standard electrolyte, the electroneutrality of the system is kept mainly due to proton movement from the anode to the cathode, since the concentration gradient of protons is higher than the concentration gradient of other cations. These protons are taken up by the cathodic reaction, hence being consumed, thus not accumulating. In contrast, under haloalkaline electrolyte the conductivity changes gradually in both

the anolyte and the catholyte (see supplementary information chapter, figures 3 and 6) as cations, such as Na^+ and K^+, travel from the anode to the cathode in order to keep electroneutrality.[31] Further insights into these transport processes would be relevant. Changes in conductivity were handled by replacing part of or the entire content of the catholyte and the anolyte on the regular basis. This is not a strategy that can be executed in a full-scale system. Hence, it is important to develop new strategies and/or designs to deal with this changing conductivity. One option, often recurred to, is a one-chamber electrochemical cell (with no separator). However, due to the anaerobic nature of the cathodic biological reaction and the oxygen production at the anode, removing the separator between the cathode and the anode will most certainly lead to problems regarding biological activity due to oxygen toxicity. This is important to take into account if a design using this one-chamber concept is developed for this purpose. Another option is to add an interchange vessel to the reactor set-up. Once the oxygen is stripped from the anolyte and the CH_4 is stripped from the catholyte these two electrolytes can be mixed in order to stabilize conductivity. However, in this kind of strategy microorganisms will be present in both the anode and cathode chamber, thus the selective pressures on the microorganisms will be various, including both reductive and oxidative environments. Moreover, in the presence of possible reversible redox reactions the faradaic efficiency towards methane can be hampered. Hence, additional considerations are needed, such as filtering out the microorganisms at the anode inlet, and/or opting for applying this interchange strategy intermittently rater than continuously, and/or opting for applying the interchange after a period where the biofilm is established upfront.

The need to investigate other start-up strategies

In this work we opted to start up the reactors at standard conditions to have a comparison situation for haloalkaline conditions. However, this is time consuming (around 100 days) and it is not known if this is the best start-up strategy for operation of methane producing biocathodes at haloalkaline conditions. Hence, we suggest that new start-up strategies are investigated in order to, at an earlier stage, start selecting for microorganisms that can thrive at haloalkaline (high salts and high pH) conditions. An option might be starting up directly at haloalkaline conditions with inoculates adapted to high saline environments, for example from marine sediments,[32] or soda lakes. Another possible strategy would be the pre-acclimation of methanogens-rich inocula to haloalkaline conditions.

The trade-off between methane production rates and energy efficiency

Although operation at haloalkaline conditions (0.6M) was stable in terms of energy efficiency, lower current densities had to be set in order to minimize losses associated to cathode overpotential, resulting in a maximum production around 11 NL^{CH_4} m^{-2} d^{-1}. The increased cathode overpotential, when attempting to set higher rates, can potentially be a consequence of by-product formation and/or low microbial growth rates.

Potential by-products are hydrogen, acetate, formate, other volatile fatty acids (VFAs), and/or extracellular polymeric substances (EPS). Throughout the operational time, hydrogen was not detected with exception of the unstable operation of B1 at 1M (see section 2.2.3). The presence of the remaining potential by-products could not be investigated due to the challenging high salt matrix. Hence, for future reference it is important to develop tools and methods to evaluate the presence and quantify these compounds (both organics and polysaccharides) within the matrix of the haloalkaline electrolyte.

Low microbial growth rates can be a consequence of high osmotic stress when the microorganisms do not find strategies to deal with the increasing presence of cations. It has been shown for example that methanogenic activity in anaerobic digestion decreases with increasing concentration of salts, and furthermore is highly dependent on the nature of the cations (rather than the anions).[33] Moreover, increased EPS production correlated to increasing concentration of cations (salinity) has been reported for anaerobic communities,[34] possibly as a strategy to "fight" the osmotic stress. This might also be an explanation for the unstable performance and lower methanogenic activity in B1 at 1M bicarbonate buffer in comparison to 0.6M (see section 2.2.3). Therefore, further experiments are needed to test the effect of different electrolyte compositions in terms of concentrations, and cations and their ratios on the methanogenic activity of methane producing biocathodes.

In summary, there is a trade-off between production rates and energy efficiency. Only when it is clear which one of these parameters is more relevant for the implementation of this technology can research be steered in the desired direction. In this work high energy efficiency is reached and we propose that future research focuses on 1) improving reactor design, 2) developing effective start-up strategies, and 3) understanding the effect of high concentration of cations (and anions) on microbial activity and toxicity, in order to improve the overall performance of haloalkaline methane producing biocathodes.

3.4 Experimental methods

Experimental set-up

Two set-ups, B1 and B2, were built for this experimental work with similar design to previous works,[21, 24] but with key differences in 1) anode electrode and 2) gas collection strategy. A schematic representation of the experimental set-up is shown in figure 3.6.

Bioelectrochemical cell and reactor set-up

The core of each set-up consists of an up-flow electrochemical cell (at the centre of figure 3.6) composed of two chambers, the anode and the cathode chamber, which are separated by a cation exchange membrane (FumaTech GmbH, Ingbert, Germany). In the cathode

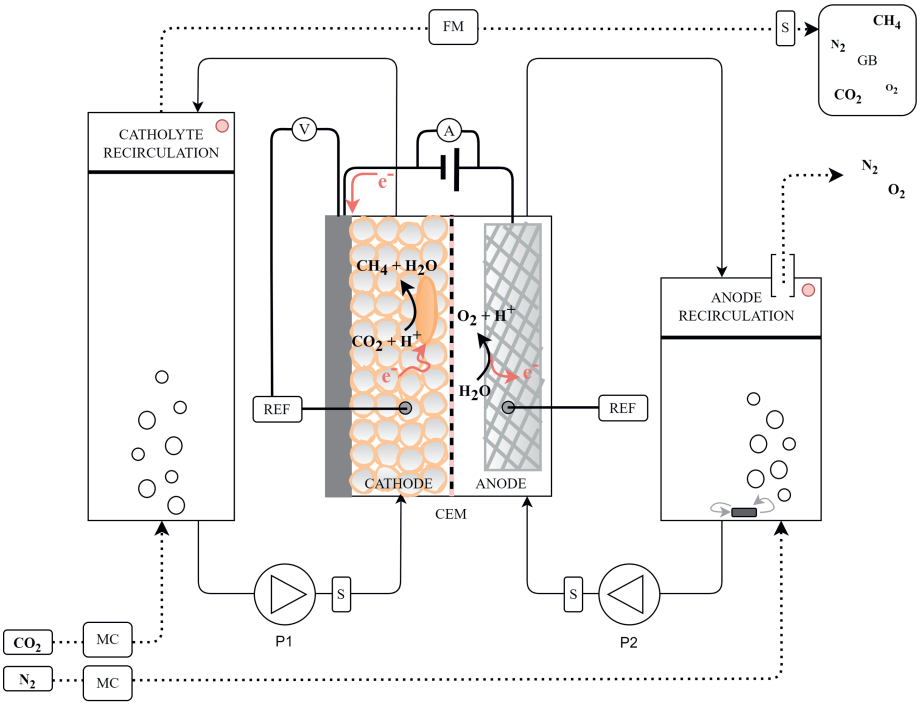

Figure 3.6: Schematic representation of the experimental set-up. Full lines represent liquid flows, dashed lines represent gas flows and full bold lines represent the electrochemical circuit. Note the following abbreviations: REF-Reference electrode, CEM-Cation Exchange Membrane, S-Sampling port (either liquid or gas), MC-Mass flow Controllers, FM-(gas) Flow Meter, GB-Gas Bag, P1-Pump for catolyte re-circulation and P2-Pump for anolyte re-circulation. Pink circles represent the existence of oxygen sensors.

side (V = 30 cm^3) a graphite plate (0.002 m^2) is used as current collector and the chamber is tightly packed with granular activated carbon (GAC) (NORIT ACTIVATED CARBON PK13 M, CABOT NORIT, The Netherlands) ensuring maximum contact between the (working) electrode materials. Approximately 10 g of GAC were added to both set-ups B1 and B2. In the anode chamber (V = 60 cm^3) an Iridium-Ruthenium coated Titanium electrode (Baoji Zhufeng Metal Processing Co., Ltd., China) with 100 cm^2 meshed area is fitted. This electrode is commercial available for water splitting at low losses. 3M KCl Ag/AgCl QM710X reference electrodes (ProSense Qis, Oosterhout, The Netherlands) are connected to both the cathode and anode chambers. Thus, all potentials recorded in this work are reported against (3M KCl) Ag/AgCl (+0.210 V vs. NHE). The electron flow between the anode and the cathode was controlled by using a potentiostat (Ivium n-Stat with IviumSoft v2.462, Eindhoven, The Netherlands). A leak-free set-up and a

good pressure distribution is ensured by using a plastic spacer (Sefar Nitex 06–3300/59, Buffalo, NY, USA) between all compartments of the cell.

The catholyte and anolyte were recirculated upwards through the respective cathode and anode chamber, and recirculated back to the catholyte recirculation column (12 mL min^{-1}) and the anolyte recirculation flask (45 - 135 mL min^{-1}), respectively. The absorber consisted of a 35 cm height by 12 cm^2 area glass cylinder through which pure CO_2 was sparged, in the opposite direction to the liquid flow, bottom-up, at a flow of 0.44 - 0.65 mL min^{-1} controlled by a mass flow controller (5800 Series Smart Mass Flow Controllers, BROOKS, USA). The headspace of the absorber was then connected to a flow meter (µFlow unit, Bioprocess Control, Sweden) which quantified the total amount of gas that went through and which, in turn, was connected to a gas bag (Cali-5-BondTM) to collect the gas. Gas samples were taken from this gas bag.

The anolyte recirculation flask was continuously flushed with N_2 in order to remove the produced and (possibly) leaked-in oxygen. The headspace of the this flask was open to air. The N_2 amount was controlled at 20 - 40 mL min^{-1} by a mass flow controller (5800 Series Smart Mass Flow Controllers, BROOKS, USA).

Electrolyte and inocula

As introduced, two different electrolyte compositions were used during this study. At first both B1 and B2 were start-up under "standard" phosphate electrolyte and after a few months of operation the electrolyte was switched to a haloalkaline electrolyte.

The "standard" phosphate electrolyte was composed of 50mM phosphate buffer. Additionally, for the catholyte 0.2 g L^{-1} NH_4Cl and 1 mL L^{-1} of both vitamin and mineral 10x concentrated stock solutions were added.[35] The standard anolyte consisted of 50mM phosphate buffer alone.

The haloalkaline electrolyte (catholyte and anolyte) composition ranged between 0.6M and 1M bicarbonate buffer with the addition of 50mM phosphate ($NaH_2PO_4x2H_2O$). For the majority of the operation 0.6M was used (details in section 2). Additionally, to the catholyte 0.2 g L^{-1} NH_4Cl (or 0.296 g L^{-1} NH_5 CO_3), 1 mL L^{-1} of both vitamin and mineral 10x concentrated stock solutions,[35] 6.78 mg L^{-1} $MgSO_4x7\,H_2O$ and 3.99 mg L^{-1} $CaHPO_4x2\,H_2O$ was added.

The inocula was retrieved from the anaerobic digester of the waste water treatment facility at the paper mill company in Eerbeek (Eerbeek, The Netherlands). The Eerbeek sludge was "washed" by following a few centrifuging steps (at least 2 times) at 10 000 rpm in order to remove the volatile fatty acids and other organic compounds in the sludge. The pellet was then re-suspended in electrolyte each time.

Experimental operation and analysis

Both set-ups were inoculated at the cathode side with 10% (V/V) Eerbeek sludge (The Netherlands) and then start-up galvanostatically at a constant current of -4.5 A m^{-2}, with the use of an Ivium-n-Stat (Ivium Technologies, Eindhoven, The Netherlands). For the remaining of the run the current density was increase and the electrolyte changed as discussed in section 2.

During operation samples were taken twice a week (on average) from the gas phase of the catholyte recirculation (gas bag) and from the liquid phase of both the anode recirculation flask and the catholyte recirculation column. By sampling the gas bag it was possible to quantify methane by Gas Chromatography as described in previous work [21, 24]. In addition the total amount of gas quantified by the flow meter (and confirmed by emptying the gas bag with a syringe) allows us to calculate the total amount of methane produced. With the same GC method it was possible to also detect H_2, CO_2, N_2 and O_2.

Conductivity, pH were measured in the liquid samples as well as regular measurements of ammonium on the supernatant fraction of the electrolyte.

Equations

Methane production rate (equation 3.1), faradaic efficiency (equation 3.2), voltage efficiency (equation 3.3) and energy efficiency (equation 3.4) are the main performance indicators we have focused on when analysisng the performance of the two methane producing BESs and were calculated as follows.

$$Methane\ production\ rate\ (NL\,m^{-2}\,d^{-1}) = \frac{CH_4 \times gas\ flow\ rate}{100 \times A_{CC}} \tag{3.1}$$

Where CH_4(in %) is the methane concentration in the gas bag which is quantified by gas chromatography, gas flow rate (in NL d^{-1}) is the combination of the amount of gas in normalised volume (NL) and the time between samples (days) which are both quantified via the gas flow meter connected prior to the gas bag, and A_{CC} (in m^2) is the area of the current collector, in this case the graphite plate (0.002 m^2).

$$Faradaic\,efficiency(\%) = \frac{CH_4 \times gas\,flow \times P}{100 \times R \times T} \times \frac{8 \times F}{I} \tag{3.2}$$

Where gas flow is in NL (see above), P is the atmosferic pressure (101.33 kPa), R is the ideal gas constant (8.31 kPa L mol^{-1} K^{-1}), T is the temperature (in K) which is measured every sampling day, 8 is the fraction of electrons needed per molecule of CH_4 (in mol_{e^-} $mol_{CH_4}^{-1}$), F is the faraday constant (96485 C $mol_{e^-}^{-1}$) and I (in C) is the amount of current

applied/fixed in the system (in A) times the amount of time between sampling days (in s).

$$Voltage\,efficiency(\%) = \frac{\Delta G_{CH_4}}{cell\ voltage \times 8 \times F} \tag{3.3}$$

$$Energy\,efficiency(\%) = \frac{CH_4\,produced \times \Delta G_{CH_4}}{I \times cell\ voltage} \tag{3.4}$$

Where CH_4 produced is in mol_{CH_4}, ΔG_{CH_4} is the energy density per mole of CH_4 (-890.4 x 10^3 J $mol_{CH_4}{}^{-1}$) and cell voltage (in V) is the experimental cell voltage measured with a multimeter.

The distribution of losses, shown in section 2.1, was calculated according to literature and as follows.[25] The resulting cell voltage is composed of the following losses, the equilibrium voltage (E_{eq}), the cathode overpotential (E_{Cat}), the anode ovepotential (E_{An}), the electrolyte resistances (E_{Ion}) and the other transport losses (E_T). All calculated as shown in equations 3.5 to 3.9.

$$E_{eq} = E_{Cat\,theoretical} - E_{An\,theoretical} \tag{3.5}$$

$$E_{Cat} = E_{Cat\,theoretical} - E_{Cat\,measured} \tag{3.6}$$

$$E_{An} = E_{An\,measured} - E_{An\,theoretical} \tag{3.7}$$

Where $E_{Cat_{theoretical}}$ and $E_{An_{theoretical}}$ are the expected cathode and anode potentials (in V) based on the experimental conditions (temperature, pH, and reactants and products concentrations), and $E_{Cat_{measured}}$ and $E_{An_{measured}}$ are the potentials (in V) measured with a multimeter.

$$E_{ion} = I_{ions} \times \left(\frac{d_{An}}{2A_{CC}\sigma_{An}} + \frac{d_{Cat}}{2A_{CC}\sigma_{Cat}}\right) \tag{3.8}$$

Where I_{Ions} is the flow of ions through the electrolyte (in A m^{-2}, same as the current density), d_{An} and d_{Cat} is the distance between the respective electrode material and the membrane, and σ_{An} and σ_{Cat} is the conductivity of the respective electrolyte (in S m^{-1}).

$$E_T = E_{cell} - (E_{eq} - E_{Cat} - E_{An} - E_{ion}) \tag{3.9}$$

The ratio between each component (equations 3.5 to 3.9), in V, and the current density ($I_{density}$), in A m^{-2}, is equal to the resistance associated to each component in Ohm m^2. Note that equation 3.5 includes the resistances due to pH gradients, which can be extrapolated as follows in equation 3.10.

$$R_{\Delta_{pH}} = \frac{E_{\Delta_{pH}}}{I_{density}} = \frac{\frac{RT}{F} \times \ln(10^{(pH_{Cathode} - pH_{Anode})})}{I_{density}} \tag{3.10}$$

Acknowledgements

We would like to acknowledge Shell Global Solutions International B.V. and Paqell B.V. for funding the research. We would also like to acknowledge Jan Klok for the scientific contribution to this work, and thank Nicolas Tsesmetzis for the fruitful discussions. Additionally, we would like to thank Jelmer Vroom for the SEM imaging.

References

[1] V. Masson-Delmotte, P. Zhai, H.-O. Pörtner, D. Roberts, J. Skea, P. R. Shukla, et al. *Global Warming of 1.5° C: IPCC Special Report on Impacts of Global Warming of 1.5° C above Pre-industrial Levels in Context of Strengthening Response to Climate Change, Sustainable Development, and Efforts to Eradicate Poverty*. Cambridge University Press, 2022. DOI: 10.1017/9781009157940.

[2] IRENA. *World Energy Transitions Outlook: 1.5°C pathway*. Tech. rep. IRENA, Abu Dhabi, United Arab Emirates, 2021.

[3] K. Hashimoto. "Metastable metals for "green" materials for global atmosphere conservation and abundant energy supply". *Materials Science and Engineering: A* 179 (1994), 27–30.

[4] D. Stolten and V. Scherer. *Transition to renewable energy systems*. Chapter 39. John Wiley & Sons, 2013.

[5] G. Centi, E. A. Quadrelli, and S. Perathoner. "Catalysis for CO 2 conversion: a key technology for rapid introduction of renewable energy in the value chain of chemical industries". *Energy & Environmental Science* 6.6 (2013), 1711–1731.

[6] J. Zhu, L. Lv, S. Zaman, X. Chen, Y. Dai, S. Chen, G. He, D. Wang, and L. Mai. "Advances and Challenges in Single-Site Catalysts towards Electrochemical CO2 Methanation". *Energy & Environmental Science* (2023).

[7] J. Mao, Y. Liu, H. Chen, Y. Yang, C. Jiao, W. Zhu, Y. Zhang, X. Wu, and Z. Zhuo. "Atomically Inner Tandem Catalysts for Electrochemical Reduction of Carbon Dioxide". *Energy & Environmental Science* (2023).

[8] U. Schröder and F. Harnisch. "Life electric—nature as a blueprint for the development of microbial electrochemical technologies". *Joule* 1.2 (2017), 244–252.

[9] F. Enzmann, F. Mayer, M. Rother, and D. Holtmann. "Methanogens: biochemical background and biotechnological applications". *Amb Express* 8 (2018), 1–22.

[10] R. G. Grim, Z. Huang, M. T. Guarnieri, J. R. Ferrell, L. Tao, and J. A. Schaidle. "Transforming the carbon economy: challenges and opportunities in the convergence of low-cost electricity and reductive CO 2 utilization". *Energy & Environmental Science* 13.2 (2020), 472–494.

[11] X. Ning, R. Lin, R. O'Shea, D. Wall, C. Deng, B. Wu, and J. D. Murphy. "Emerging bioelectrochemical technologies for biogas production and upgrading in cascading circular bioenergy systems". *Iscience* 24.9 (2021), 102998.

[12] Z. Huang, R. G. Grim, J. A. Schaidle, and L. Tao. "The economic outlook for converting CO 2 and electrons to molecules". *Energy & Environmental Science* 14.7 (2021), 3664–3678.

[13] F. Geppert, D. Liu, M. van Eerten-Jansen, E. Weidner, C. Buisman, and A. Ter Heijne. "Bioelectrochemical power-to-gas: state of the art and future perspectives". *Trends in biotechnology* 34.11 (2016), 879–894.

[14] W. Cai, K. Cui, Z. Liu, X. Jin, Q. Chen, K. Guo, and Y. Wang. "An electrolytic-hydrogen-fed moving bed biofilm reactor for efficient microbial electrosynthesis of methane from CO2". *Chemical Engineering Journal* 428 (2022), 132093.

[15] A. G. Vidales, S. Omanovic, and B. Tartakovsky. "Combined energy storage and methane bioelectrosynthesis from carbon dioxide in a microbial electrosynthesis system". *Bioresource Technology Reports* 8 (2019), 100302.

[16] H. Zhou, D. Xing, M. Xu, Y. Su, J. Ma, I. Angelidaki, and Y. Zhang. "Optimization of a newly developed electromethanogenesis for the highest record of methane production". *Journal of Hazardous Materials* 407 (2021), 124363.

[17] T. H. Sleutels, A. Ter Heijne, C. J. Buisman, and H. V. Hamelers. "Bioelectrochemical systems: an outlook for practical applications". *ChemSusChem* 5.6 (2012), 1012–1019.

[18] M. Kim, S. Li, Y. E. Song, D.-Y. Lee, and J. R. Kim. "Electrode-attached cell-driven biogas upgrading of anaerobic digestion effluent CO2 to CH4 using a microbial electrosynthesis cell". *Chemical Engineering Journal* 446 (2022), 137079.

[19] M. C. Van Eerten-Jansen, A. T. Heijne, C. J. Buisman, and H. V. Hamelers. "Microbial electrolysis cells for production of methane from CO2: long-term performance and perspectives". *International Journal of Energy Research* 36.6 (2012), 809–819.

[20] F. Geppert, D. Liu, E. Weidner, and A. ter Heijne. "Redox-flow battery design for a methane-producing bioelectrochemical system". *International Journal of Hydrogen Energy* 44.39 (2019), 21464–21469.

[21] M. B. Lavender, S. Pang, D. Liu, L. Jourdin, and A. Ter Heijne. "Reduced overpotential of methane-producing biocathodes: Effect of current and electrode storage capacity". *Bioresource Technology* 347 (2022), 126650.

[22] D. Liu, M. Roca-Puigros, F. Geppert, L. Caizán-Juanarena, S. P. Na Ayudthaya, C. Buisman, and A. Ter Heijne. "Granular carbon-based electrodes as cathodes in methane-producing bioelectrochemical systems". *Frontiers in bioengineering and biotechnology* 6 (2018), 78.

[23] F. Jensen and F. Schubert. "Hydrogen generation through static feed water electrolysis". In: *Hydrogen Energy: Part A*. Springer, 1975, 425–439.

[24] D. Liu. "Strategies for Improving Methane Production from CO 2 and Electricity in Bioelectrochemical Systems". PhD thesis. Wageningen University and Research, 2018.

[25] T. H. Sleutels, H. V. Hamelers, R. A. Rozendal, and C. J. Buisman. "Ion transport resistance in microbial electrolysis cells with anion and cation exchange membranes". *International Journal of Hydrogen Energy* 34.9 (2009), 3612–3620.

[26] J. Hu, C. Zeng, G. Liu, Y. Lu, R. Zhang, and H. Luo. "Enhanced sulfate reduction accompanied with electrically-conductive pili production in graphene oxide modified biocathodes". *Bioresource technology* 282 (2019), 425–432.

[27] N. Eaktasang, C. S. Kang, H. Lim, O. S. Kwean, S. Cho, Y. Kim, and H. S. Kim. "Production of electrically-conductive nanoscale filaments by sulfate-reducing bacteria in the microbial fuel cell". *Bioresource technology* 210 (2016), 61–67.

[28] X. Zhang, T. Arbour, D. Zhang, S. Wei, and K. Rabaey. "Microbial electrosynthesis of acetate from CO2 under hypersaline conditions". *Environmental Science and Ecotechnology* 13 (2023), 100211.

[29] R. Kiran, R. Yadav, D. Sathe, and S. A. Patil. "Halophilic CO2-fixing microbial community as biocatalyst improves the energy efficiency of the microbial electrosynthesis process". *Bioresource Technology* (2023), 128637.

[30] Q. Shu, L. Legrand, P. Kuntke, M. Tedesco, and H. V. Hamelers. "Electrochemical regeneration of spent alkaline absorbent from direct air capture". *Environmental science & technology* 54.14 (2020), 8990–8998.

[31] T. H. Sleutels, A. ter Heijne, P. Kuntke, C. J. Buisman, and H. V. Hamelers. "Membrane selectivity determines energetic losses for ion transport in bioelectrochemical systems". *ChemistrySelect* 2.12 (2017), 3462–3470.

[32] M. F. Alqahtani, S. Bajracharya, K. P. Katuri, M. Ali, J. Xu, M. S. Alarawi, and P. E. Saikaly. "Enrichment of salt-tolerant CO2–fixing communities in microbial electrosynthesis systems using porous ceramic hollow tube wrapped with carbon cloth as cathode and for CO2 supply". *Science of the Total Environment* 766 (2021), 142668.

[33] D. Sudmalis. "Anaerobic sludge granulation at high salinity". PhD thesis. Chapter 7. Wageningen University and Research, 2020.

[34] I. Vyrides and D. C. Stuckey. "Adaptation of anaerobic biomass to saline conditions: Role of compatible solutes and extracellular polysaccharides". *Enzyme and Microbial Technology* 44.1 (2009), 46–51.

[35] E. Wolin, M. Wolin, and R. Wolfe. "Formation of methane by bacterial extracts". *Journal of Biological Chemistry* 238.8 (1963), 2882–2886.

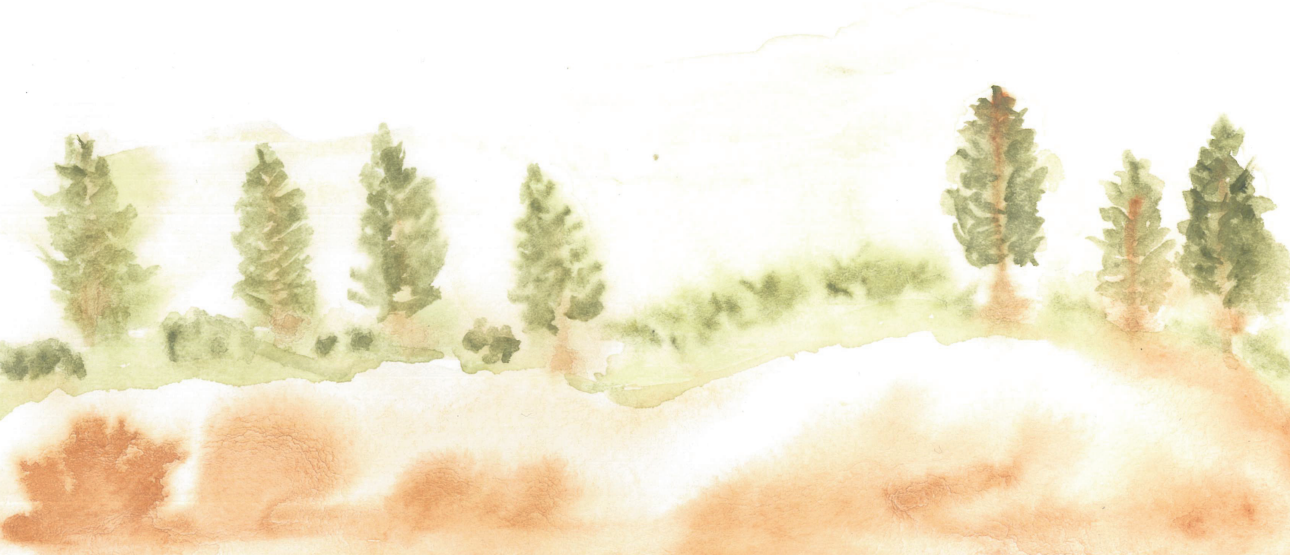

Chapter 4

Designing, building and operating a scale up methane producing BES

Manuscript in preparation by Micaela Brandão Lavender, Jos Steller[1], Dandan Liu, Rieks de Rink, Shiba Tofik & Annemiek ter Heijne.

[1]Shared First Authorship

Abstract

A 17 L scale up methane producing bioelectrochemical system (BES) for power-to-gas application was designed taking into account: 1) use of GAC as cathode material, 2) a design that can be further scale up in modules, and 3) materials which are low cost and/or commercially available. The 17 L BES was operated for 470 days with step wise increase in applied current density between -6 and -125 A m^{-3}_{BES}, with resulting methane production rates between 10 NL m^{-3}_{BES} d^{-1} and 280 NL m^{-3}_{BES} d^{-1}. Throughout the whole experimental time the faradaic efficiency ranged between 80% and 100%. Furthermore, throughout the operation, changes in the electrolyte composition and anode dimensions were made in order to decrease losses associated to the electrolyte and anode reaction, respectively. The distribution of the voltage losses was assessed in this paper, but, in general, the 17 L BES was operated for the majority of the experimental time at around 40% energy efficiency, specifically when operating at 0.2M, 0.4M and 0.6M electrolyte and with an anode surface area of 0.02 m^2 or larger. Beside the BES itself, the reactor design consisted of a bubble column, an oxygen stripping unit and an interchange vessel, all of which essential for the operation of the BES. In general, a stable performance was observed for 400 days, after a start-up period of approximately 70 days.

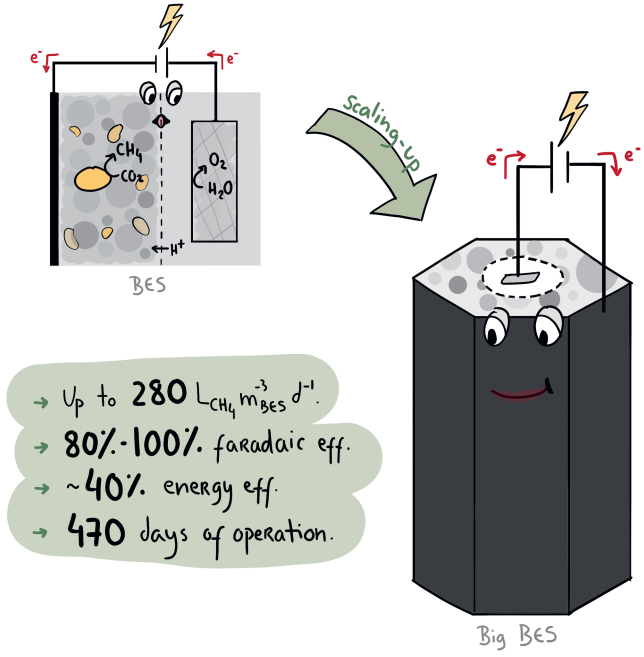

4.1 Introduction

According to the International Renewable Energy Agency, one key barrier in the energy transition is infrastructure, namely 1) limited electricity transport infrastructure (grid), 2) limited electricity storage infrastructure, 3) insufficient adaptation of other distribution infrastructure, such as gas pipelines, and 4) end-users, such as households, unready for electrification.[1] Power-to-methane in a bioelectrochemical system (BES) is an electricity storage technology, alternative to the ones readily available, that can help bypass the presently unprepared infrastructure. In this methane producing BES, carbon dioxide (CO_2) is biologically reduced to methane (CH_4) at the cathode and the electrons needed to drive this reaction are made available through oxidation of water to oxygen at the anode and the consumption of electrical power, hence, converting electrical energy into chemical energy in the form of methane. Methane as a gaseous chemical energy carrier allows for long term and stable storage, and is more energy dense than its alternative, hydrogen, at the same pressure. Moreover, methane as an end product can be transported and stored using the currently existing gas infrastructure, including pipelines, and can serve non-electrified households. Hence, in principle, Power-to-methane in BES can be more easily implemented within the currently existing infrastructure, in comparison to other power-to-gas alternatives. Furthermore, upgrading biogas can be and interesting application for a methane producing BES.

In general, however, scaling-up BESs faces a number of challenges, 1) materials and designs that provide effective large surface areas and good microbe-material interactions are needed in order to achieve high volumetric reaction rates, 2) increasing size normally results in increasing distances between electrodes and thus between reduction and oxidation reaction, and results in increasing diffusion limitations, hence higher energy losses and in turn, less efficient process, 3) the design for scaling-up is largely dependent on application, hence they need to be function-oriented.[2–6] So far, most efforts have focused on researching and summarising scaling-up strategies for waste water treatment applied BESs.[3, 4, 7, 8] However, there are a few studies on scaling-up BES for power-to-gas applications, with either hydrogen as an end product,[9, 10] or, more recently, methane.[11–15] However, in the latter studies, either low rates or low efficiencies were observed.

The goal of the research was to 1) design an efficient BES in terms of energy and rates with focus on application as a power-to-methane technology, and to 2) operate the system for long term and analyse its performance over time.

Design considerations

The main consideration taken into account when creating the scale up BES design were: 1) the use of materials that are commercially available, experience low losses and have large surface areas (specially at the cathode), 2) the use of a membrane separating the

anode and cathode, whilst allowing for easy maintenance, and 3) a final design that can be further scaled up in modules.

The use o granular activated carbon (GAC) as cathode material in lab scale methane producing BES has resulted in low cathode overpotential (see Chapter 2). Moreover, GAC has a larger surface area available for the attachment of microorganisms, in comparison to flat plate electrodes. GAC is also thermally stable material, resistant to corrosion and relatively low in costs, which is relevant for large scale implementation. Although these are promising characteristics, the questions remains on how to scale up efficiently using this 3D electrode. For this , the GAC had to be tightly packed between the membrane and the current collector. In this design, a stainless steal mesh (SS) was used as current collector. For the anode current collector, a commercially available Iridium-Ruthenium coated Titanium electrode was used, once it is state of the art for water oxidation.

A membrane-less configuration is often considered when scaling up BESs in order to avoid diffusion-associated losses across the membrane, and to reduce costs, specially those associated to maintenance of the membrane.[2, 6, 16] However, in a methane producing BES, a membrane-less design is not a good option taking into account the anaerobic nature of the biological reduction reaction at the cathode, and the formation of oxygen at the anode. Hence, a commercially available cation exchange tubular shaped membrane was centred in the BES. The tubular shape of the membrane allows it to be easily removed, provided that between the membrane and the GAC bed a meshed plastic spacer is added, keeping the pressure on the GAC against the current collector when removing the membrane.

Scaling up in modules is currently an important concept that has been under consideration to a large extent in designing BES.[2, 4] Modular-friendly designs allow the system to be further scale up at any point in time and without compromising rates which are associated to the design. Wang et al. [6], designed a flat plate BES that can be scale up in modules by alternating plates. The uniqueness of the design laid on the fact that the flat plates were slightly bent and when stacked they would create the pattern resembling a honeycomb. Hence, merging the concept of a modular flat plate electrode design with a tubular flow-through design. Inspired by this, the current collector, SS, was shaped forming an hexagonal prism (see figure 4.3 in Experimental methods for more details). One side of the hexagonal prism of one BES can be in contact with another side of another hexagonal BES, and so on, mimicking a honeycomb. In this way allowing current to be distributed through the different modules (BES). This would not be possible if the outside current collector was tubular shaped.

Operation and evaluating performance

Once one BES module was assembled, the operation was initiated. The scale up methane producing BES was operated under galvanostatic control for a period of 470 days. During

this time, the performance, in terms of methane production rates and energy efficiency (including faradaic and voltage efficiencies) was assessed. In this work, the performance is initially shown and discussed in comparison to other existing power-to-gas BES designs. Secondly, other important considerations of the built scale up BES are summarized. In the end, based on the previous two, opportunities and challenges of the design are discussed.

4.2 Results

Performance of a 17 L methane producing BES

The 17 L methane producing BES was operated for 470 days under galvanostatic regime. In figure 4.1, the applied current density and the resulting methane production rate was shown throughout the operational time. In general, methane production rates increased proportional to the increase in applied current density. The current density was increased step wise from -6 A m^{-3} to -125 A m^{-3}, and the resulting methane production rates increased between from 10 NL m^{-3}_{BES} d^{-1} to 280 NL m^{-3}_{BES} d^{-1} (in normalised liter per BES volume per day). This is two to ten times lower than reported in lab scale methane producing biocathodes with GAC as cathode material (433 L m^{-3} d^{-1} (in Chapter 2), 470 L m^{-3} d^{-1} (in Chapter 3), and 2150 L m^{-3} d^{-1}).[17] Nevertheless, the limiting methane production rate was not tested in this scale up BES, hence it is possible that higher rates can be reached.

Regarding efficiency of the BES set-up, for the majority of the experimental run, the faradaic efficiency ranged between 80% to 100%. Up to day 100, the resulting energy efficiency stabilised around 20%. At day 100, in an attempt to further decrease the voltage losses, the conductivity of the electrolyte was increased by adding Na^+/K^+ bicarbonate up to a concentration of 0.2 M. This led to an increase in voltage efficiency up to 40% and in energy efficiency up to 35%, whereas the effect on faradaic efficiency was not clear. For the rest of the operational run, the conductivity was increased up to 0.4 M and subsequently to 0.6 M, throughout the majority of which the energy efficiency of the scale up BES remained stable around 40%. Other details of the performance of the scale up methane producing BES are shown in the supplementary information chapter, in figures 13, 14 and 15.

Distribution of losses in a scale up methane producing BES

To better understand what determines the voltage efficiency (and in turn energy efficiency), the different voltage losses in the system were calculated.[18] The overall voltage losses can be distributed over 1) cathode overpotential, 2) anode overpotential, 3) pH losses, 4) ionic losses, and 5) other (transport) losses. The contribution of the different voltage losses to the overall voltage loss is shown in figure 4.2 for different conditions, electrolyte

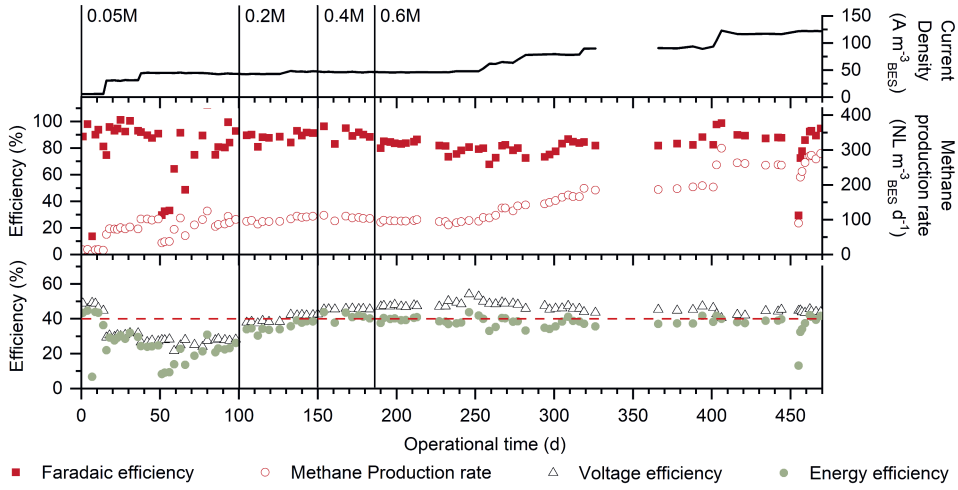

Figure 4.1: Control strategy of the scale up methane producing BES (top), and resulting methane production rate (middle, right axis), faradaic efficiency towards methane (middle, left axis), voltage efficiency (bottom) and energy efficiency (bottom) throughout the operational time. Vertical lines represent the change from operation with standard electrolyte (0.05 M phosphate) to 0.2 M bicarbonate electrolyte, and subsequently to 0.4 M bicarbonate electrolyte, and subsequently to 0.6 M bicarbonate electrolyte.

composition, applied current density and/or anode electrode size. Note that for condition A and B the anode overpotential (2) and other transport losses (5) are not separated, this was due to the fact that during this time there was no reference electrode included at the anode, thus the anode potential (and overpotential) could not be measured.

Comparing A and B shows that changing from the standard electrolyte (A) to haloalkaline electrolyte (0.2 M, B) resulted in a decrease of the overall losses from 95 mΩ m^3 to 62 mΩ m^3, at similar current densities. Furthermore, during the operation under a haloalkaline electrolyte the pH loss became slightly negative and the ionic losses also decreased, in comparison to standard electrolyte. These trends support the previous work at lab scale, where both standard and haloalkaline conditions were tested (in Chapter 3). Overall, the largest contributor to total resistance was for both conditions the combination of anode overpotential and transport losses (that could not be separated due to absence of anode reference electrode).

Further increasing the alkalinity to 0.4 M and 0.6 M, at similar current densities, (C and D) also lead to lower overall losses, although the difference was less pronounced. In C and D, the contributions of anode overpotential and transport losses could be measured separately, revealing that for these conditions the anode overpotential was the biggest

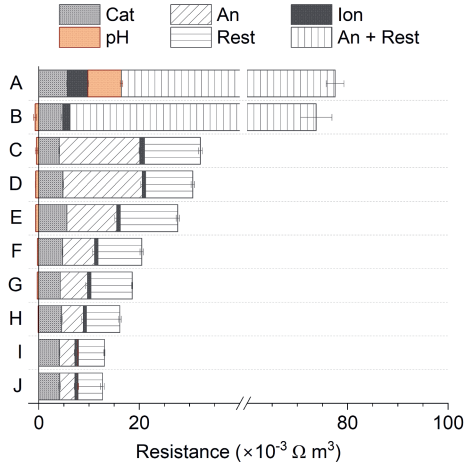

	Electrolyte (M)	Current Density (A m^{-3})	Anode size (m^{-2})
A	0.05	45	0.01
B	0.2	43	0.02
C	0.4	46	0.02
D	0.6	46	0.05
E	0.6	47	0.09
F	0.6	65	0.09
G	0.6	79	0.09
H	0.6	92	0.09
I	0.6	117	0.09
J	0.6	122	0.09

Figure 4.2: Distribution of voltage losses normalised by current density, in Ω m^3_{BES} at different operational conditions. The different operational conditions are summarised to the right of the graph including electrolyte composition (in M), applied current (in A m^{-3}), and anode size (in m^2). The observed total cell voltage is: (A) -4.35 V, (B) -2.93 V, (C) -1.47 V, (D) -1.38 V, (E) -1.28 V, (F) -1.31 V, (G) -1.44 V, (H) -1.47 V, (I) -1.53 V, (J) -1.55 V. The sampling days are: (A) days 38-49, (B) days 108-126, (C) days 160-183, (D) days 190-211, (E) days 233-241, (F) days 263-277, (G) days 301-316, (H) days 366-401, (I) days 434-444, (J) days 456-469. Note that there is an axis break between 40 to 60 x 10^{-3} Ω m^3 for better visualization.

contributor to the overall loss, followed by the other transport losses, and then the cathode overpotential.

Comparing D and E, when increasing the anode surface area from 0.02 m^2 to 0.05 m^2 the anode overpotential decreased drastically, leading to losses similar to the transport losses. A further increase in anode surface area (F) to 0.09 m^2 led to an even further decrease in the anode overpotential related losses. These were accompanied by a reduction of the total loss as well. Hence, the size of the anode electrode can potentially further be increased to further reduce the total losses and increase the voltage efficiency. However, this would also mean increased costs.

Between F and J the current density was step-wise increased from -65 to -122 A m^{-3} and the total voltage loss (in V) also increased. However, between F and I the resulting contribution of the anode overpotential and other transport losses decreased significantly, thus decreasing the total losses normalised by current density. Between I and J, the contribution of the losses did not change much, meaning that the losses increased proportionally to the increase in current density, suggesting that this would be the case if further increasing the current density.

In general, the contribution of ionic losses was low and the contribution of transport losses was the highest (at anode surface area of 0.05 m^2 and above). Moreover, the contribution of cathode overpotential to the overall losses remained fairly stable for all tested conditions, specially F to J where current density was increased. Thus, suggesting a linear relationship between cathode overpotential and current density, where doubling the current density would result in double the losses at the cathode. Moreover, a cathode overpotential of 5×10^{-3} $\Omega\, m^3$ (equal to 0.1 $\Omega\, m^2_{\text{cathode current collector}}$) is three times higher than the contribution of the same losses at the lab scale (with BES size equal to 0.09 dm^3) (see Chapter 3).

4.3 Discussion

Performance of other scale up designs of methane producing BESs

In table 4.1, the performance of scale up methane producing BESs, with cell volumes equal to or above 17 L, is summarised. In contrast to our design, the summarised work include, a 50 L tubular reactor with 3 m^2 carbon laying cathode,[11] a 45 L moving bed reactor with fixed 0.05 m^2 stainless steel mesh cathode,[12] and a 20 L continuous stirred tank (CSTR) with an inserted tubular BES of 0.35 L with a 0.03 m^2 stainless steel mesh cathode.[13] For the last case the 20 L volume is taken into account in the table because it is assumed that the conversion of CO_2 into methane takes place in the entire volume of the CSTR. For a schematic representation of each design please check the referred work.

The 50 L tubular cathode was the first study to run a scale up BES with pure culture *Methanococcus maripaludis*.[11] The reported faradaic efficiency averaged above 100%. Authors suggested that methane formation occurred from additional electron sources but did not describe which. Although the resulting energy efficiency ranged around 27%, low methane production rates were reported, 5.2 L_{CH_4} m^{-3} d^{-1}, due to the resulting low current density when applying -3.1 V over the cell.

In the moving bed reactor type, an energy efficiency up to 43% was observed,[12] slightly higher than in this work, 40%. However, this occurred at the expense of lower methane production rates, 49 L_{CH_4} m^{-3} d^{-1}, in comparison to this work, 280 L_{CH_4} m^{-3} d^{-1}. Further increasing the current density, leading to higher methane production rates such as 116 L_{CH_4} m^{-3} d^{-1}, consequently led to a decrease in energy efficiency to 30% and faradaic efficiency to 46%, with formation of by-products such as hydrogen and acetate.

The tubular BES inserted in the continuous stirred tank showed overall best rates, reporting methane production rates of 521 and 757 L_{CH_4} m^{-3} d^{-1}.[13] However, this came at the expense of large voltages, -6.5 V and -8.0 V, respectively, hence the resulting energy efficiency was comparatively low up to 20%. Larger voltages most probably resulted from hydrogen mediated methanogenesis, once hydrogen was detected as a by-product, and the

Table 4.1: Performance overview of scale up BES for power-to-methane application.

BES volume (L)	Area cathode current collector (m^2)	Current density (A m^{-2})	Current density (A m^{-3})	Methane prod. rate (NL m^{-3}_{BES} d^{-1})	Faradaic eff. (%)	Cell voltage (V)	Voltage eff. (%)	Energy eff. (%)	Ref
50	3.00	8×10^{-2}	5	5	114	-3.1	NR	27	[11]
45	0.05	22	18	49	96	NR	NR	43	[12]
45	0.05	44	36	83	92	NR	NR	40	[12]
45	0.05	111	91	116	46	NR	NR	30	[12]
20	0.03	120	197	521	95	-6.5	NR	20	[13]
20	0.03	180	295	757	45	-8.0	NR	14	[13]
17	0.31	6.4	118	280	88	-2.6	45	40	this

distance between the reactive surface area of the cathode and reaction sight in the CSTR can be large.

The larger trade off between energy efficiency and rates reported in the previous two studies,[12, 13] in contrast to this work, are probably a consequence of ten times smaller cathode current collector surface area (see table 4.1).

Challenges

Larger losses in comparison to the lab scale

This scale up BES design resulted in lower energy efficiency, in comparison to the lab scale, up to 70% (in Chapter 3). However, the main contributors in the scale up were losses associated to transport over the membrane and cathode overpotential, whereas in the lab scale the main contribution was anode overpotential. In this scale up the anode overpotential was initially high, but was decreased by increasing its surface area up to 0.09 m^2. Similarly, other reactor configurations might need to be adjusted in order to decrease the losses associated to cathode overpotential and transport.

In order to decrease the transport losses the distance between the electrodes and between the electrodes and the membrane should be minimised. In order to do so the diameter of the tubular membrane could be decreased for a better fit around the anode, whilst maintaining the area of the membrane by increasing the height of the reactor. Optionally, bringing the cathode current collector closer to the center as well, and creating a thinner GAC bed might reduce transport resistance that might be formed over the depth of the GAC bed. However, because the local condition at the cathode are unknown, it limits our understanding of how cathode overpotential can be decreased. In a study on chain

elongation biocathodes, H_2, pH and ORP local measurements were made with microsensors in order to identify rate limiting factors present at the biocathode.[19] Once gradients were observed in the previous study, the process conditions were adjusted to optimise rates. Similarly, conducting local measurements at methane producing GAC based biocathodes might give indications of what needs to be avoided when scaling up, and what can possibly be the cause for larger cathode overpotentials in the scale up, e.g. vertical gradients in height or horizontal gradients in depth.

Changing conductivity during operation with haloalkaline electrolyte

Although operation under haloalkaline led to a lower sum of voltage losses, it also led to significant changes in conductivity of the anolyte and catholyte, once cations travel from the anode to the cathode in consequence of the electron flow (in Chapter 3). In this work, an interchange vessel was added in order to mix the catholyte and the anolyte together to decrease conductivity changes in time, specially when operating with haloalkaline electrolyte (for more details please see the Experimental section). By using this strategy, referred to as "interchange strategy", the conductivity and pH of the electrolyte recirculating through the anode and the cathode was kept stable (see supplementary information chapter, figure 15). However, using the interchange vessel, to mix the catholyte and anolyte, led to CH_4 losses via the gas outlet in the interchange vessel, which was continuously sparged with N_2 to maintain low oxygen conditions. Therefore, either the use of the interchange strategy has to be minimised or another strategy has to be implemented. A possible alternative strategy could be feeding the bleed of the cathode recirculation to the anode recirculation and vice versa, without using the interchange vessel, however further experiments would be needed.

Opportunities

Long term stable performance

Overall, the 17 L scale up methane producing BES was operated for 470 days at stable performance, with energy efficiency above 35% and around 40% for the majority of the run, after the start-up period of around 70 days. At 40% energy efficiency, large rates of methane production up to 280 NL m^{-3}_{BES} d^{-1} were reached. Larger rates found in literature on scale up methane producing BES were only reached at the expense of energy efficiency (below 20%). Moreover, the limiting rates of the scale up were not tested. Since, 1) faradaic efficiency remained high throughout the operation, 2) no H_2 was detected in the outlet gas, and 3) ten times larger rates have been reached in lab scale methane producing GAC-based biocathodes,[17] it is possible that larger rates can still be reached with this design.

CO_2 absorption

In this scale up BES the catholyte was recirculated between the cathode chamber and a bubble column (for more details please see the Experimental methods). In this way, CO_2 was sparged in the bubble column and the liquid was recirculated to the cathode, where CO_2 in the liquid phase was converted to CH_4, which was then recirculated back to the bubble column, where the CH_4 composition of the liquid was replaced by CO_2 and the CH_4 could escape via the gas outlet of the bubble column. The use of a haloalkaline electrolyte allows more CO_2 to be dissolved, in comparison to standard electrolyte. Moreover, it buffers pH changes resulting from dissolving CO_2 and conversion, allowing a more stable environment for microorganisms (in terms of pH). Here, by setting the CO_2 inflow rate at approximately 5.5 NL d^{-1}, the CH_4 concentration in the gas outlet reached 75% when operating at -125 A m^{-3} and with 0.6 M haloalkaline electrolyte (see supplementary information chapter, figure 14). Therefore, operation at haloalkaline electrolyte and with a simple bubble column design leads to up to 75% CH_4 in the outlet gas. CO_2 absorption columns are commonly implemented in biogas upgrading technologies at industrial scale, and yield CH_4 concentrations around 98%.[20] Therefore, further improving the bubble column design, and therefore the CH_4 content, at an industrial scale is not perceived as an issue. Moreover, currently implemented biogas upgrading technologies rely on physical removal of CO_2 from biogas, rather than the conversion of CO_2. The removed CO_2 is more often than not released back to the atmosphere. Utilising methane producing BES to treat these CO_2-rich streams presents a promising initial application. This approach not only decreases the amount of CO_2 released to the atmosphere, but also enhances the production of biomethane.

Economic assessment

At this stage, a techno economic assessment of the current design is crucial in order to understand how competitive this scale up methane producing BES is in comparison to other power-to-gas alternatives, and other electricity storage alternatives. This techno economic assessment should take into account, 1) the value of (bio)methane as an end product, 2) the value of using CO_2-rich streams which are currently polluting the environment, 3) and the value of supporting the function of electrical frameworks, e.g. by taking up electricity from the grid when its production surpasses demand.

4.4 Conclusion

The galvanostatic controlled scale up BES design resulted in the largest methane production rates, 280 L m^{-3} d^{-1}, at 40% energy efficiency. Larger rates have been reported in literature but only at the expense of energy efficiency. Nevertheless, the limiting rates of this BES design were not yet tested. Moreover, the majority of the voltage losses in this design

accounted for transport losses across the membrane. Decreasing the distance between the anode electrode and the membrane, whilst maintaining the area of the membrane, is suggested to further improve the energy efficiency of the current design. Overall, this work shows that the current design is promising for scaling up bioelectrochemical systems.

4.5 Experimental methods

Reactor design

Bioelectrochemical cell

A 17 L hexagonal prism shaped bioelectrochemical cell was built, a schematic representation of the BES and the used materials are shown in figure 4.3, including the dimensions of the BES. The hexagonal housing was made of PVC and a tubular cation exchange membrane (CE-2, RisingSun membrane technology, Beijing, China) with a projected surface area of 0.12 m^2 was centered separating the anode chamber inside (3L) from the cathode chamber outside (14L).

The cathode chamber contained a current collector and a granular activated carbon (GAC) packed bed. The current collector was stainless steel mesh with projected surface area of 0.34 m^2. GAC (Norit® PK 1-3, Cabot Norit activated carbon, Amersfoort, The Netherlands) with a bulk density of 290 kg m^{-3} was used as cathode electrode material and filled the entire volume of the cathodic chamber with exception of a small thin layer at the bottom (6.5cm in height) which was filled with glass beads in order to ensure good liquid distribution. Around the tubular membrane, a fiberglass (PTFE) mesh with the pore size of 1.1mm × 1.3mm and a layer of graphite felt attached with carbon string were placed to ensure no damage to the membrane due to the GAC. Good compactness of the GAC bed is important to ensure contact between current collector and granule bed, as confirmed by measuring the capacitance, which was 363 F g^{-1}. At the top of the GAC bed, an Ag/AgCl (in 3M KCl) reference electrode was placed. All potentials are reported vs this Ag/AgCl reference electrode (equivalent to -0.29 V vs SHE).

The anode chamber contained an Iridium-Ruthenium coated Titanium meshed electrode (Baoji Zhufeng Metal Processing Co., Ltd., China) that was bent into a cylindrical shape and had a projected surface area of 0.01m^2. At day 147, an Ag/AgCl reference electrode (in 3M KCl) was also inserted in the anode chamber. To test the area of the electrode on the losses associated to the anodic reaction the size of the anode electrode was increased 2, 5 and 10 times throughout the run.

Set-up

The bioelectrochemical system was connected through a series of liquid flows to the rest of the set-up, which consists of an bubble column, an oxygen stripping unit and an interchange

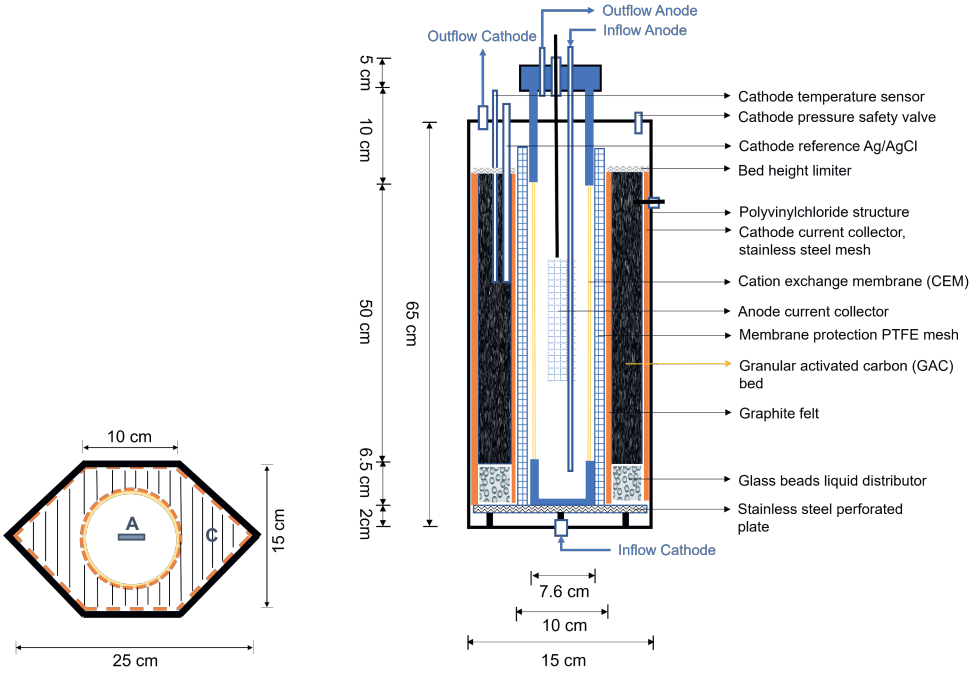

Figure 4.3: Schematic representation of the scale up BES from above (left), and of the interior from a side perspective (right), with indication of the different components and sizes.

vessel, as shown in figure 4.4. The catholyte was recirculated between the cathode chamber, the bubble column and the interchange vessel. The anolyte was recirculated between the anode chamber, the oxygen stripping unit and the interchange vessel.

The bubble column had a total volume of 4.3L and dimensions of 6cm × 160cm (diameter × height). In the bubble column, CO_2 gas was sparged in counter flow to the electrolyte flow at a rate of approximately 2.1 L h^{-1}. The CO_2-rich electrolyte was then circulated to the cathode, via pump P2. The electrolyte at the outlet of the cathode was separated in two flows, with a glass T-piece, one to the top of the bubble column and the other one recirculated back to the cathode, via P1. The glass T-piece allows the separation of the formed gas from the electrolyte, and directs it to the bubble column. P1 was used for internal recirculation of the electrolyte over the cathode chamber.

The oxygen stripping unit had a total volume of approximately 0.8L and dimensions 3cm × 81cm (diameter × height). In the oxygen stripping unit, N_2 gas was sparged in counter flow to the electrolyte flow at a rate of 5.1 L h^{-1}. The electrolyte coming from the anode chamber was circulated to the oxygen stripping unit, by P4, so that the produced oxygen from the BES was stripped away before the electrolyte was circulated back to the anode.

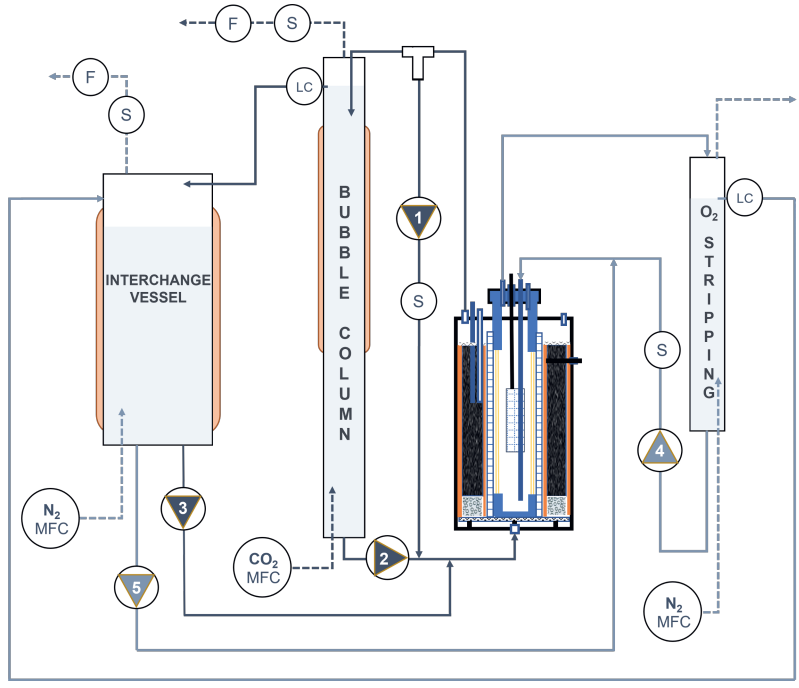

Figure 4.4: Schematic overview of the experimental set-up, including interchange vessel, bubble column, BES cell and oxygen stripping unit from left to right. The dark coloured lines represent the cathode recirculation, the light coloured lines represent the anode recirculation; the dashed lines represent the gas flows. F stands for flow meter, S stands for sampling point (both liquid and gas), LC stands for level controller (though overflow), and MFC stands for mass flow controller (both for CO_2 and N_2).

Before starting experiments it was observed that an hydraulic retention time (HRT) of 1 min is sufficient to remove at least 90% of the produced O_2.

The interchange vessel had the purpose of mixing together the electrolyte recirculating through the cathode chamber and electrolyte recirculating through the anode chamber. The interchange vessel could hold up to 3.4 L of electrolyte. Throughout operation of a BES, specially at haloalkaline conditions (see Chapter 3), cations are transported across the cation exchange membrane from the anode to the cathode to balance the transport of electrons from the anode to the cathode. As a result, the conductivity of the catholyte increases and the conductivity of the anolyte decreases, respectively with time. Therefore, mixing anolyte and catholyte was used as a strategy to keep the conductivity of the catholyte and the anolyte constant. This constant conductivity was needed in order to keep the system stable, which becomes especially important for long term operation. The electrolyte recirculating through the cathode chamber would overflow to the interchange

vessel with the use of a level controller overflow in the bubble column (LC, see figure 4.4), and the electrolyte recirculating through the anode chamber would overflow to the interchange vessel from the oxygen stripping unit. The (mixed) electrolyte in the interchange vessel would then be pumped to the cathode chamber via pump P3, and to the anode chamber via pump P4. For simplicity, throughout the paper we call this the "interchange strategy".

Operation and analysis

Inocula and electrolyte

The set-up was inoculated (at day 0) with 2L anaerobic granular sludge from an up flow anaerobic sludge blanket (UASB) reactor. This UASB treats papermill wastewater and was located in Eerbeek (The Netherlands). The granular sludge was grinded into flocculent sludge by a disperser (IKA T25 digital ULTRA-TURRAX), and then washed with tap water before addition to the set-up . The total volatile suspended solids (VSS) of the washed sludge was 50.77±5.47 g L^{-1}.

Initially, up to day 100, the system was operated under "standard conditions", mimicking the previous work with the lab scale methane producing BES (see Chapter 3). The standard electrolyte consists of 50 mM phosphate electrolyte (13.6 g L^{-1} KH_2PO_4 and 56.7 g L^{-1} Na_2HPO_4) with 0.3 g L^{-1} NH_5CO_3, 1 mL L^{-1} Wolfe's vitamin solution and 1 mL L^{-1} Wolfe's mineral solution.[21] At the anode, the same electrolyte solution was used but without the addition of ammonium, vitamin and minerals.

At day 100, the alkalinity of the electrolyte was increased to 0.2 M with bicarbonate electrolyte by adding both $NaHCO_3$ and $KHCO_3$ at a 4:1 ratio. Additionally, 0.3 g L^{-1} NH_4HCO_3, 1 mL L^{-1} Wolfe's vitamin solution,[21] 1 mL L^{-1} Wolfe's mineral solution,[1] 6.78 mg L^{-1} of $MgSO_4x7\,H_2O$ and 3.99 mg L^{-1} of $Na_2HPO_4x2\,H_2O$ were added to the "haloalkaline" electrolyte. At a later stage, the alkalinity of the electrolyte was further increased in a step wise approach up to 0.6M. This and other control strategies are summarised in table 4.2.

Start-up and operation

Before start-up and inoculation at day 0, the GAC packed reactor was "charged" by applying a current density of about -69 A m^{-3}, until a cathode potential of -0.53 V vs Ag/AgCl was reached, the potential which resulted in methane production at the cathode in previous work on methane producing BES (Chapter 2).

After inoculation, the set-up was controlled at -6 A m^{-3}. During the whole experimental run, the reactor was operated under galvanostatic conditions (fixed current density) controlled by a potentiostat (HP 96 – 20, Bank Elektronik - Intelligent Controls GmbH, Pohlheim). An online data logging system (Labview) was used to record the applied current and the

Table 4.2: Details of the operation of the scale up methane producing BES throughout the 470 days of operation.

Days of operation	Fixed current density	electrolyte composition	Interchange strategy
0 - 14	6 A m^{-3}	0.05M phosphate	OFF
14 - 36	31 A m^{-3}	0.05M phosphate	OFF
36 - 51	43 A m^{-3}	0.05M phosphate	OFF
51 - 100	43 A m^{-3}	0.05M phosphate	P3 and P5 on
100 - 150	43 - 48 A m^{-3}	0.2M bicarbonate	P3 and P5 on
150 - 183	46 A m^{-3}	0.4M bicarbonate	P3 and P5 on
183 - 233	46 A m^{-3}	0.6M bicarbonate	P3 and P5 on
233 - 277	48 - 69 A m^{-3}	0.6M bicarbonate	P3 and P5 on
277 - 400	80 - 90 A m^{-3}	0.6M bicarbonate	P3 and P5 on
400 - 444	105 - 117 A m^{-3}	0.6M bicarbonate	P3 and P5 on
444 - 470	122 A m^{-3}	0.6M bicarbonate	P3 and P5 on

resulting cathode potential at 1 minute intervals. In this paper we report the applied current normalised to the BES volume (0.017 m^3). During start-up, the interchange strategy was not yet used, so the catholyte and anolyte were separated. The changes in current density, electrolyte composition and interchange strategy after start-up are summarised in table 4.2. In general, throughout the experimental run, the electrolyte composition was changed three times, from standard electrolyte to 0.2 M haloalkaline electrolyte on day 100, to 0.4 M haloalkaline electrolyte on day 150 and to 0.6 M haloalkaline electrolyte on day 183. From day 233 onwards, the current density was step-wise increased up to -122 A m^{-3} and the interchange strategy was tested under standard conditions from day 51, and then maintained at haloalkaline conditions.

Throughout the operation of the reactor, vitamin, minerals, ammonium and water were added regularly. Moreover, The temperature of the reactor was maintained at around 30°C by using a water bath (with a set point of 40°C) that was circulated over water jackets that were added around the pump tank and the bubble column.

Analysis

The bubble column gas outflow was sampled twice per week for the quantification of carbon dioxide, methane, nitrogen, oxygen and hydrogen content using a gas chromatography (Chapter 2). Taking into account the percentage of methane in the vent gas and the amount of gas produced, calculated with a gas flow meter (μ Flow unit, Bioprocess Control, Sweden), the methane production rate was calculated. From day 98 onwards, a small amount of methane ended up in the outflow of the interchange vessel. Hence, during

interchange the amount of methane in the outflow of the interchange vessel was also quantified. In this paper, the total methane production rate was normalised by the total volume of the BES (0.017 m^3).

The resulting cathode potential and anode potential were monitored every minute using an online data logging collection system (Labview). Furthermore, the cathode potential, anode potential and cell voltage was measured manually with a multimeter twice per week. pH (PHM210, MeterLab®), conductivity (HQ440d multi, Hach), and the ammonium content (Hach Lange (LCK305), Hach) of the electrolyte were measured once or twice a week by sampling the inlet to the cathode and anode chambers.

Methane production rate (1.1), faradaic efficiency (1.2), voltage efficiency (1.3), and energy efficiency (1.4) were calculated as introduced in Chapter 1. Moreover, the contribution of losses over the cathode, anode and membrane to the overall energy efficiency were calculated as done in Chapter 3.[18] The only difference is that here the pH loss was calculated separately from the cathode overpotential and anode overpotential.

Acknowledgments

We would like to acknowledge Shell Global Solutions International B.V. and Paqell B.V. for funding the research. We would like to thank Jan Klok for the scientific contribution to this work. We would like to thank Nicolas Tsesmetzwas for the fruitful discussions. Additionally, we would like to acknowledge Vinnie de Wilde, Michiel van den Broek and Bert Willemsen for helping with the design and construction of the experimental set-up.

References

[1] IRENA. *World energy transitions outlook: Executive Summary and Introduction*. 2023. (Visited on 2024).

[2] R. M. Alonso, M. I. San-Martín, R. Mateos, A. Morán, and A. Escapa. "Scale-up of bioelectrochemical systems for energy valorization of waste streams". In: *Microbial Electrochemical Technologies*. CRC Press, 2020, 447–459.

[3] A. Janicek, Y. Fan, and H. Liu. "Design of microbial fuel cells for practical application: a review and analysis of scale-up studies". *Biofuels* 5.1 (2014), 79–92.

[4] D. A. Jadhav, S.-G. Park, S. Pandit, E. Yang, M. A. Abdelkareem, J.-K. Jang, and K.-J. Chae. "Scalability of microbial electrochemical technologies: Applications and challenges". *Bioresource Technology* 345 (2022), 126498.

[5] F. Enzmann, M. Stöckl, A.-P. Zeng, and D. Holtmann. "Same but different–Scale up and numbering up in electrobiotechnology and photobiotechnology". *Engineering in life sciences* 19.2 (2019), 121–132.

[6] A.-J. Wang, H.-C. Wang, H.-Y. Cheng, B. Liang, W.-Z. Liu, J.-L. Han, B. Zhang, and S.-S. Wang. "Electrochemistry-stimulated environmental bioremediation: Development of applicable modular electrode and system scale-up". *Environmental Science and Ecotechnology* 3 (2020), 100050.

[7] H. Hiegemann, D. Herzer, E. Nettmann, M. Lübken, P. Schulte, K.-G. Schmelz, S. Gredigk-Hoffmann, and M. Wichern. "An integrated 45 L pilot microbial fuel cell system at a full-scale wastewater treatment plant". *Bioresource technology* 218 (2016), 115–122.

[8] P. Liang, R. Duan, Y. Jiang, X. Zhang, Y. Qiu, and X. Huang. "One-year operation of 1000-L modularized microbial fuel cell for municipal wastewater treatment". *Water Research* 141 (2018), 1–8.

[9] L. Singh, A. G. Miller, L. Wang, and H. Liu. "Scaling-up up-flow microbial electrolysis cells with a compact electrode configuration for continuous hydrogen production". *Bioresource Technology* 331 (2021), 125030.

[10] E. S. Heidrich, S. R. Edwards, J. Dolfing, S. E. Cotterill, and T. P. Curtis. "Performance of a pilot scale microbial electrolysis cell fed on domestic wastewater at ambient temperatures for a 12 month period". *Bioresource technology* 173 (2014), 87–95.

[11] F. Enzmann and D. Holtmann. "Rational Scale-Up of a methane producing bioelectrochemical reactor to 50 L pilot scale". *Chemical Engineering Science* 207 (2019), 1148–1158.

[12] W. Cai, K. Cui, Z. Liu, X. Jin, Q. Chen, K. Guo, and Y. Wang. "An electrolytic-hydrogen-fed moving bed biofilm reactor for efficient microbial electrosynthesis of methane from CO2". *Chemical Engineering Journal* 428 (2022), 132093.

[13] G. Shang, K. Cui, W. Cai, X. Hu, P. Jin, and K. Guo. "A 20 L electrochemical continuous stirred-tank reactor for high rate microbial electrosynthesis of methane from CO2". *Chemical Engineering Journal* 451 (2023), 138898.

[14] A. Ceballos-Escalera, D. Molognoni, P. Bosch-Jimenez, M. Shahparasti, S. Bouchakour, A. Luna, A. Guisasola, E. Borràs, and M. Della Pirriera. "Bioelectrochemical systems for energy storage: A scaled-up power-to-gas approach". *Applied energy* 260 (2020), 114138.

[15] M. Kim, S. Li, Y. E. Song, D.-Y. Lee, and J. R. Kim. "Electrode-attached cell-driven biogas upgrading of anaerobic digestion effluent CO2 to CH4 using a microbial electrosynthesis cell". *Chemical Engineering Journal* 446 (2022), 137079.

[16] A.-J. Wang, D. Cui, H.-Y. Cheng, Y.-Q. Guo, F.-Y. Kong, N.-Q. Ren, and W.-M. Wu. "A membrane-free, continuously feeding, single chamber up-flow biocatalyzed electrolysis reactor for nitrobenzene reduction". *Journal of hazardous materials* 199 (2012), 401–409.

[17] D. Liu, M. Roca-Puigros, F. Geppert, L. Caizán-Juanarena, S. P. Na Ayudthaya, C. Buisman, and A. Ter Heijne. "Granular carbon-based electrodes as cathodes in methane-producing bioelectrochemical systems". *Frontiers in bioengineering and biotechnology* 6 (2018), 78.

[18] T. H. Sleutels, H. V. Hamelers, R. A. Rozendal, and C. J. Buisman. "Ion transport resistance in microbial electrolysis cells with anion and cation exchange membranes". *International Journal of Hydrogen Energy* 34.9 (2009), 3612–3620.

[19] S. M. de Smit, J. J. Langedijk, J. H. Bitter, and D. P. Strik. "Alternating direction of catholyte forced flow-through 3D-electrodes improves start-up time in microbial electrosynthesis at applied high current density". *Chemical Engineering Journal* 464 (2023), 142599.

[20] L. N. Nguyen, J. Kumar, M. T. Vu, J. A. Mohammed, N. Pathak, A. S. Commault, D. Sutherland, J. Zdarta, V. K. Tyagi, and L. D. Nghiem. "Biomethane production from anaerobic co-digestion at wastewater treatment plants: A critical review on development and innovations in biogas upgrading techniques". *Science of The Total Environment* 765 (2021), 142753.

[21] E. Wolin, M. Wolin, and R. Wolfe. "Formation of methane by bacterial extracts". *Journal of Biological Chemistry* 238.8 (1963), 2882–2886.

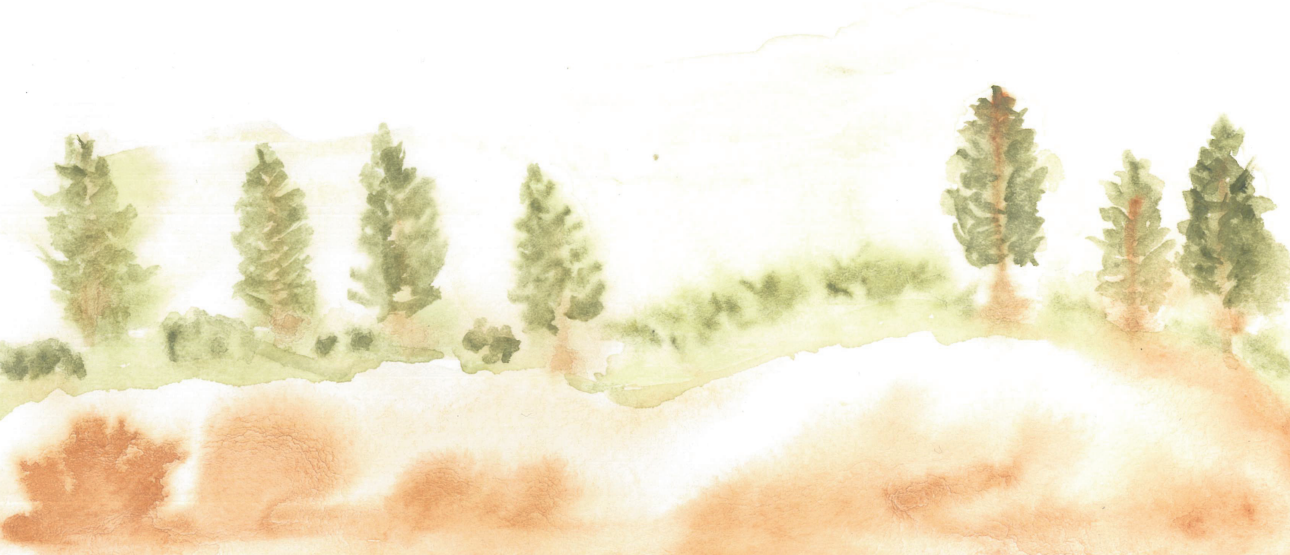

Chapter 5

Identifying local gradients in a methane producing GAC based biocathode

Manuscript in preparation by Micaela Brandão Lavender, Jasper Groot, Annemiek ter Heijne & Sanne de Smit.

Abstract

Methane producing bioelectrochemical systems (BES) with granular activated carbon (GAC) as cathode material are a promising alternative to convert CO_2 and electricity into methane, power-to-methane. Nevertheless, not much is know about the local conditions, and possibly local gradients, formed within the GAC bed at methane producing biocathodes. Observing local conditions can give better insights on possibly existing limitations at methane producing biocathodes. By considering the limitations, process conditions and/or reactor design can be changed to improve rates and efficiency. Here, microsensors were used to measure H_2, pH and ORP, within the GAC bed of methane producing biocathodes and at different depths. Firstly, H_2 was detected locally at cathode potentials of -0.63 V (vs Ag/AgCl), whereas no H_2 was detected in the outlet gas of the methane producing BES, suggesting an efficient use of hydrogen. Secondly, it was identified that there are gradients in all three parameters, being that with increasing depth (away from the current collector and towards the membrane) there is an increase in H_2 and in pH, and a decrease in ORP (becoming more negative).

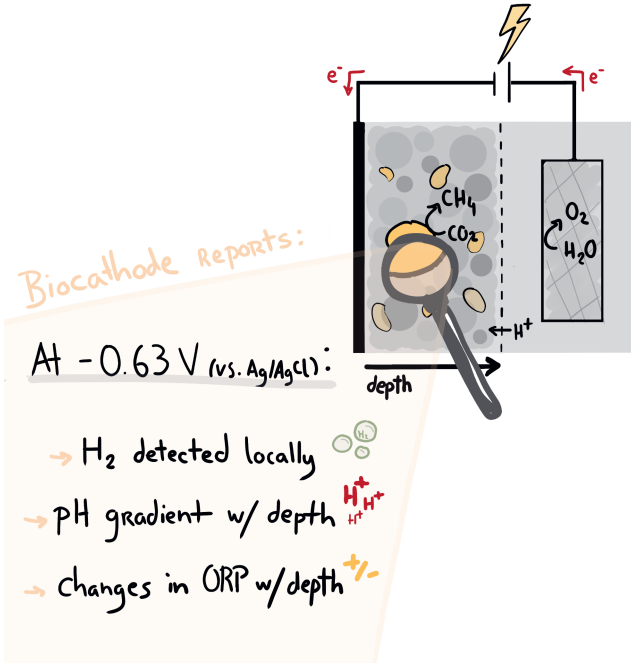

5.1 Introduction

A methane producing bioelectrochemical system (BES) is a Power-to-Methane technology that makes use of microorganisms to catalyse the conversion of CO_2 into CH_4. This offers a sustainable alternative to the expenditures of conventional chemical methods, such as metal catalysts, high temperatures, and/or high pressures. In these systems, CO_2 is biologically reduced to CH_4 at the cathode. Protons and electrons needed for this conversion are supplied by the oxidation of water (with release of oxygen) at the anode. Protons diffuse to the cathode through a cation exchange membrane separating both chambers and electrons flow through an electrical circuit by supplying power.

In order to fully assess the performance of a methane producing BES, energy efficiency (including faradaic and voltage efficiency) and methane production rates must be assessed. On the one hand, high energy efficiency in methane producing BES, up to 70% (in Chapter 3), has been reported as a result of 1) low cathode overpotential by using granular activated carbon (GAC) as cathode material,[1, 2] and of 2) decreased electrolyte associated resistances (Chapter 3). However, also in Chapter 3 low reaction rates had to be set, with resulting methane production around 11 L $m^{-2}_{cathode}d^{-1}$, in order to operate at high energy efficiency. On the other hand, high methane production rates, up to 408 L $m^{-2}_{cathode}d^{-1}$, have been reached in methane producing biocathodes, but at the expense of energy efficiency (14%).[3] Thus, in practice there is a trade-off between rates and energy efficiency at methane producing biocathodes. In this way, knowing the local conditions at methane producing biocathodes, such as reactant and product concentrations, can give more insights on the possible local limitations, such as low concentrations of reactants, leading to lower conversion rates. However, to the best of our knowledge, local conditions at the surface of methane producing biocathodes, such as pH, and/or product and reactant concentrations are not often investigated.

Local concentrations of H_2 at methane producing,[4] acetate producing,[5] and chain elongation biocathodes,[6, 7] have been recently investigated using H_2 microsensors. Moreover, in the last two studies, pH and oxidation reduction potentials (ORP) were also measured locally using similar microsensors.[6, 7] The combination of the three measurements gave better insights on existing mass-transfer limitations, such as pH gradients above the recirculation pH, and places of local H_2 accumulation.[6] These insights were used to design and improve recirculation strategy to prevent occurrences of zones with elevated pH or low local H_2 availability.[7]

Inspired by these studies, the aim of this work was to measure H_2, pH and ORP at different depths in the GAC bed of methane producing biocathodes, and to understand if, based on these profiles, conclusions can be made about possibly existing limitations at methane producing biocathodes using GAC as electrode material. In previous experiments, H_2 was not detected at the gas outlet of the methane producing biocathodes and low cathode

overpotentials, up to -0.50 V vs Ag/AgCl, were observed (including Chapter 3).[2] However, hydrogenotrophic methanogens, such as *methanobacterium*, are often found at methane producing biocathodes operated at similar conditions, pH 7 and low conductivity (below 10 mS cm^{-1}), and inoculated with similar sludge.[8] Moreover, *Methanobacterium* species can have hydrogen thresholds as low as 65Pa[9] and, considering these low thresholds, hydrogen evolution at -0.50 V cannot be excluded.[10] The local investigation of the presence of H_2 at methane producing biocathodes can give better insights on the electron transfer mechanisms, such as discriminating between hydrogen mediated electron transfer and/or direct electron transfer (DET). In theory, DET would lead to lower cathode overpotential, in contrast to hydrogen mediation, thus possibly leading to higher energy efficiency.

ORP and pH are also important measurements, since ORP give a general indication of the distribution of reductive and oxidative chemical species with depth of the GAC bed, and pH is a measurement of local proton concentration and the reduction of CO_2 to CH_4 comes at the expense of proton consumption. Moreover, microorganisms are sensitive to pH changes and, if local pH values vary widely from the pH of the recirculation electrolyte, it might hamper biological activity.

In this work, two methane producing BES, with GAC as cathode material were set-up and operated for 170 days similarly to what has been done in previous work, including fixed current at -2.5 A m^{-2} and with 0.05M phosphate electrolyte.[1, 2] Adaptations were made to the profiling method set up from de Smit et al. [6] to allow measurements within the GAC bed. These adaptations are summarised in the experimental section. H_2, pH and ORP measurements at different depths in the GAC bed were done to report the local conditions during operation of B1 and B2. Abiotic profiles, A3 and A4, were conducted for comparison. Moreover, CH_4 and H_2 measurements of the gas outlet were conducted in order to evaluate the overall performance of these set-ups, in terms of product formation rates. By conducting these profiles, H_2, pH and ORP gradients in the GAC bed of methane producing biocathodes were identified and as a result, possible limitations are proposed. In this way, new insights into methane producing biocathodes that use GAC as electrode material are generated, which can ultimately aid in decision making towards appropriate design (and operation) changes with the aim of increasing conversion rates.

5.2 Results & Discussion

The investigation of the local presence of local H_2 in a methane producing GAC bed

H_2 is a possible mediator at methane producing biocathodes and, although its absence in the gas outlet of methane producing BES (in both Chapter 2 and 3), its presence locally at GAC-based biocathodes has not been studied. In this work, both methane producing BES, B1 and B2, were operating with fixed -2.5 A m^{-2}, and initially the resulting cathode

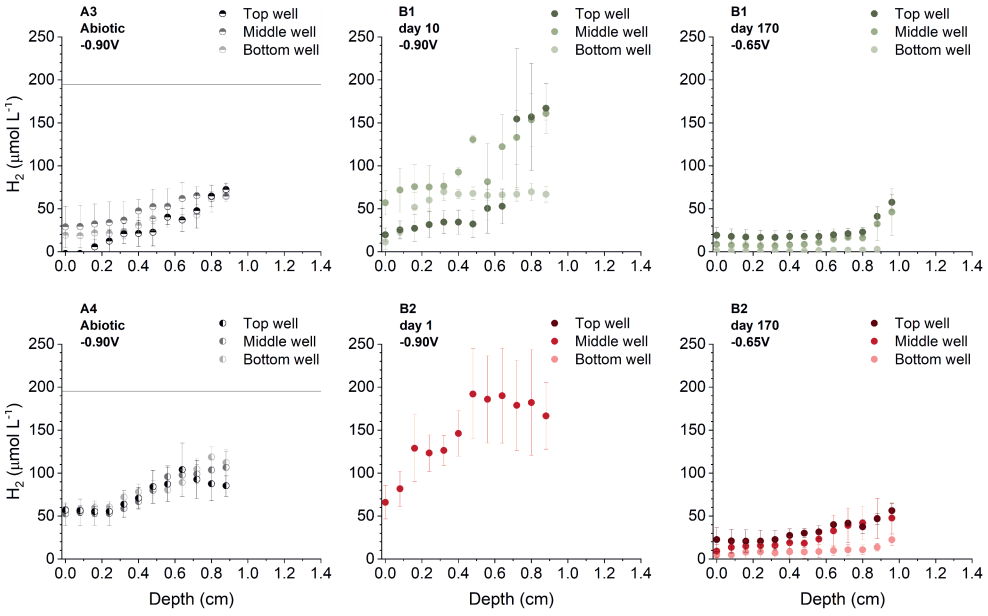

Figure 5.1: Local H_2 profiles (in μmol L^{-1}) throughout the depth of the granular activated carbon (GAC) bed (in cm). Depth 0cm corresponds to the current collector and depth 1.4cm corresponds to the membrane. On the left, profiles of two abiotic reactors, A3 and A4 (black, half full circle) with cathode potential -0.90 V. In the middle, profiles of two biotic reactors, B1 (green, top) and B2 (red, bottom), shortly after inoculation and at cathode potential -0.90 V. On the right, profiles for the same two biotic reactors, B1 and B2, at day 170 and at cathode potential -0.65 V. Data was collected at three different heights, bottom, middle and top, and is represented from lighter to darker colour. Duplicate results are shown in supplementary information chapter, figure 16.

potential of -0.90 V was observed, subsequently increasing to -0.65 V and stabilising, similarly to previously observed.[2] The presence of local H_2 was evaluated at these two different cathode potentials, -0.90 V (day 1-10) and -0.65 V (day 170). Additionally, local H_2 was quantified during the abiotic operation of two reactors, A3 and A4, in order to compare the rates of abiotic hydrogen evolution to the biotic rates (if detected) in the presence of methanogenesis. The cathode potential of -0.90 V was observed during galvanostatic operation (fixed -2.5 A m^{-2}) of A3 and A4. The hydrogen profiles with depth of the GAC bed are shown in figure 5.1, with the GAC bed having a total depth of 1.4 cm, where 0 cm corresponds to the cathode current collector and 1.4 cm corresponds to the cation exchange membrane. Profiles were measured at three different heights of the GAC bed, bottom (closer to the inlet flow), middle, and top (closer to the outlet flow). See Experimental methods for more details.

During abiotic operation of A3 and A4, hydrogen concentrations between 0 to 120 μmol L^{-1} were found locally between depth 0 and 0.9 cm. Moreover, an increasing trend of hydrogen concentration with increasing depth can be observed, suggesting possibly higher concentrations of hydrogen closer to the membrane (0.9-1.4 cm), which in turn suggests that hydrogen formation is limited either by 1) the availability of protons produced at the anode side, or 2) the lower internal resistances closer to the membrane, or 3) both. There were no clear differences between profiles done at the bottom, middle and top well for both reactors up to the depth of 0.9 cm. Taking into account that the liquid flow rate through the cathode chamber was set at 8 ml min^{-1}, and if assuming 100% faradaic efficiency towards hydrogen, the expected average hydrogen concentration for the entirety of the volume of the GAC bed would be 194 μmol L^{-1}, this is visualised in the figures as the black horizontal line. Depths between 0.9 cm and 1.4 cm were not measured in order to avoid breaking the microsensors against the membrane.

A few days after inoculation of set-ups B1 and B2 (day 10 and 1, respectively), H_2 profiles were measured. At this point in time, H_2 was detected locally in the GAC bed of both reactors, and also with increasing hydrogen concentration with increasing depth (away from the current collector). Additionally, in B1, H_2 concentration in the bottom well (the one closest to the liquid inlet) were lower overall in comparison to the other two wells. For B2, only the middle well was measured due to technical issues with the microsensor. In comparison to the abiotic measurements of A3 and A4, the H_2 concentration for B1 and B2 at -0.90 V, was in general higher, with the highest observed H_2 concentration around 190 μmol L^{-1}. This suggests, that either the presence of microorganisms affects the way hydrogen is distributed in the GAC bed, and/or the microorganisms themselves promote hydrogen evolution, which has been demonstrated for certain species of hydrogenotrophic microorganisms,[11, 12] or the sole presence of microorganisms affects cathode potential. In addition, the way that the GAC is distributed and how compact/tight the GAC bed is, can influence the distributions of hydrogen. The amount of GAC added to the abiotic reactors, A3 and A4, was lower than that added for B1 and B2 (see Experimental Methods section). Thus, it is possible that differences in tightness of the GAC bed, lead to differences in hydrogen distribution along the depth. Hence, biotic results at a specific depth can't be directly compared to the abiotic results at the same depth, but trends can.

Approximately 160 days later, H_2 profiles were measured again for B1 and B2 when cathode potential was registered at -0.65 V. These profiles, similar to the ones made at day 10 and 1, show an increasing concentration with depth, and that the concentration at the bottom well were lower in comparison to the middle and top well. However, in contrast to when cathode potential was -0.90 V, the local H_2 concentration at -0.65 V were significantly lower, up to 70 μmol L^{-1}.

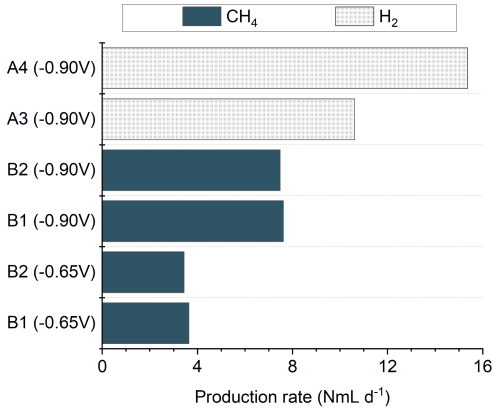

Figure 5.2: Product formation rate (in normalised mL d^{-1}) based on H_2 and CH_4 concentration found in the gas outlet of two abiotic reactors (top two bars), A3 and A4, with resulting cathode potential of -0.90 V, and two biotic reactors, B1 and B2 at resulting cathode potential of -0.90 V (middle two, day 10), and -0.65 V (bottom two, day 170).

In addition to local H_2 concentrations, H_2 and CH_4 concentrations in the outlet gas of B1 and B2 (as well as for A3 and A4), were measured in order to calculate the product formation rates. This results are shown in figure 5.2.

At day 10 after inoculation, CH_4 production rates close to 8 NmL d^{-1} were detected in the gas outlet of both B1 and B2 (middle two bars, figure 5.2). In addition, hydrogen concentrations below the quantification limit of the gas chromatography were observed, meaning that hydrogen in the outlet corresponded to less then 1.2% faradaic efficiency (value for the quantification limit). At day 170 (bottom two bars), H_2 was not detected in the headspace of the methane producing BES and CH_4 production rates rounded 3.5 NmL d^{-1}. In comparison, CH_4 was not detected in the headspace of the abiotic experiments, A3 and A4, as expected and H_2 production rates of 10.5 NmL d^{-1} for A3, and 15.5 NmL d^{-1} for A4, were observed (top two bars). It is important to note that, overall, the faradaic efficiency in all set-ups was low in comparison to previous studies (see supplementary information chapter, figure 17). This might be a result of the adaptations to the BES that had to be made in order to conduct the microsensor profiles, such as measuring wells, that might not have been as leak proof to gases as expected (see Experimental Methods for more details). Additionally, H_2 leakages across the membrane can not be excluded, both biotically and abiotically, but this would not explain the difference in faradaic efficiency in contrast to the previous work (Chapter 3), since similar experimental methods were used.

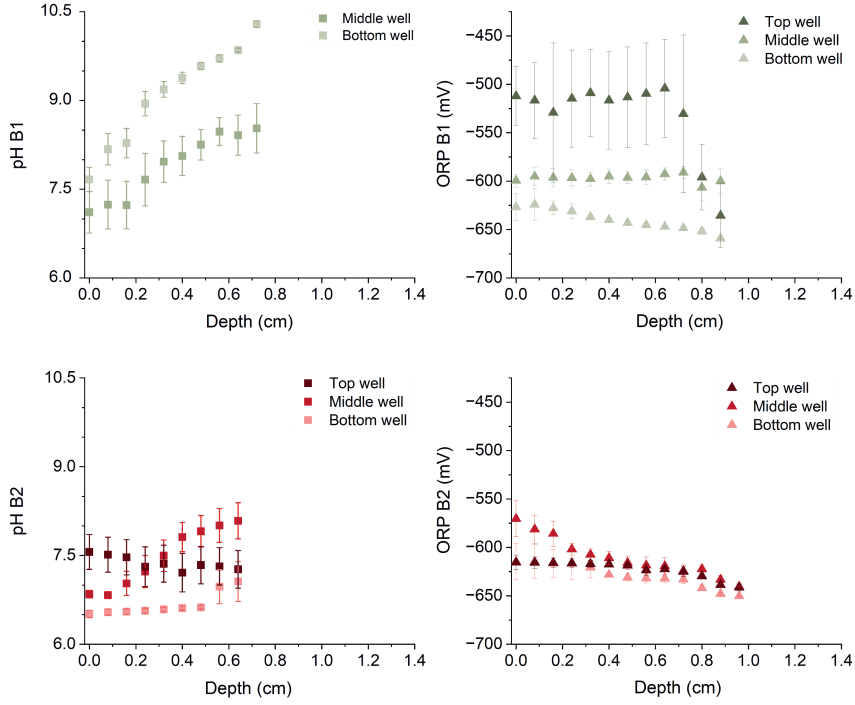

Figure 5.3: pH (full square, left) and ORP (full triangle, right) profiles throughout the depth (in cm from the current collector) of B1 (top, green) and B2 (bottom, red) at day 170. Bottom, middle and top well measurements are shown with lighter to darker colours. Note that no pH measurement is shown for the top well of B1, this is because the sensor broke in between measurements.

The investigation of pH and ORP in a methane producing GAC bed

At day 170, pH and ORP profiles were also measured for B1 and B2, these are shown in figure 5.3. In general, there was an increasing trend in pH and a decreasing trend in ORP (becoming more negative) with increasing depth away from the current collector, both of which are in line with the higher concentrations of hydrogen with increasing depth, and consumption of protons.

The pH gradient in the middle well of both reactors increased between 7 and 8 with depth. In the bottom well the increase in pH was more significant in B1, reaching above pH 10 around 0.7 cm, in comparison to B2, reaching pH 7 at 0.7 cm. Only for the top well of B2 was a decrease in pH observed with increasing depth. These differences in pH deviations between the two reactors, are most certainly due to uneven liquid recirculation around the GAC, resulting possibly from the addition of the measuring tube only used in the pH profiles (see Experimental Methods). For comparison, the recirculation pH was measured.

For B1 pH at the inlet was measured to be 6.60 and at the outlet 6.66, and for B2 the measured pH at the inlet was 6.81 and at the outlet 6.86, evidencing a slight increase in pH when the electrolyte flows through the cell. After, the liquid is recirculated from the cathode to the absorber, where sparging with CO_2 probably decreases back the pH. Note that, large differences in pH along the GAC bed, in comparison to recirculation liquid and inoculum conditions, can lead to zones where there is low activity either because 1) there is no biological growth and/or 2) other competitive microorganisms proliferate.

Interestingly, having measured pH profiles at biotic conditions, we can no longer be certain of the assumption that the hydrogen production is limited by the availability of protons (as was suggested for the abiotic data), since the pH is lower closer to the current collector. However, pH profiles were not conducted at abiotic conditions, and these could be different to biotic conditions. At biotic conditions lower concentration of H_2 closer to the current collector could result at the expense of higher rates of H_2 consumption. However, this is also not certain because even at abiotice conditions the rates of H_2 formation were lower near the current collector, and no H_2 consumption is expected.

More negative ORP with increasing depth means that the presence of reduced species (reduction potential) is higher with increasing depth away from the cathode current collector. For comparison, the measured cathode potential at the cathode current collector with the IVIUM potentiostat was -0.63 V for B1 and -0.64 V for B2 at the time of the measurements, which is approximately close to what is measured at depth 0 for the bottom well of B1 and at depth 0 for the bottom well and the top well of B2.

5.3 Outlook

This study set out to identify possible gradients that are formed within the GAC bed of methane producing biocathodes in order to foresee possible limitations that can be overcome to reach higher rates and efficiency in methane producing BES. With this in mind, H_2 concentrations, pH and ORP measurements were conducted at different depths in the GAC bed in order to profile these parameters and conclude possible limitations. These findings led to the following outlook points, related to electron transfer mechanisms, and possible limitations.

The electron transfer mechanisms: Can't exclude H_2 mediation nor DET

Although H_2 is not present in the outlet gas stream of a methane producing BES, the results in this paper show that H_2 is present locally at the biocathode and that its concentration varies with the depth of the GAC bed and resulting cathode potential. H_2 concentrations, as low as 5 μmol L^{-1}, were detected even at low cathode overpotential, with cathode potential of -0.63 V (vs Ag/AgCl). The local presence of H_2 suggests that, to a certain extent, hydrogen mediated methanogenesis occurs, both at -0.63 V and -0.90 V. Moreover,

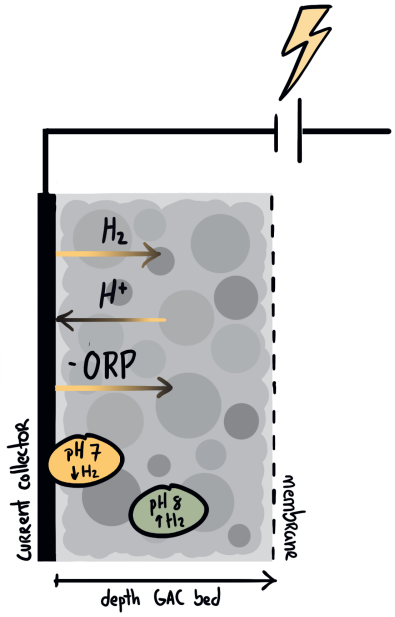

Figure 5.4: Schematic representation of the gradients in H_2, protons (inverse of pH), and (negative) ORP throughout the depth of the GAC bed. The hypothetical different microorganisms depending on the different local conditions are also represented.

it suggests that in this kind of BES, there is an efficient use of hydrogen for methanogenesis, since no H_2 is detected as by-product in the gas outlet, and up to 90% faradaic efficiency has been observed in similar set-ups at similar cathode potentials (Chapter 3). In the previous mentioned work, similar methane production rates were observed (at same fixed current density) at both larger and lower cathode overpotentials (Chapter 3).

However, the presence of H_2 locally can not exclude DET pathways either. Because the hydrogen profiles were not executed for the entirety of the depth of the GAC bed, it is not possible to determine if H_2 concentrations matches fully methane production. Moreover, a shift in cathode potential from -0.90 V to -0.63 V, could be related to a shift in pathways.[2] This means that, at -0.90 V hydrogen mediating pathways could be more prominent, and at -0.63 V DET could be more prominent. Specially, since lower H_2 concentrations were found (for the same depths) at -0.63 V, in comparison to -0.90 V. Microorganisms that can perform both hydrogen mediated electron transfer and direct electron transfer with other species (DIET) have been reported.[13] Nevertheless, one other possible explanation for lower cathode overpotentials over time, is that the increase in microorganisms may favor the overall catalysis for H_2 evolution.[11, 14]

The possible electron transfer mechanisms at methane producing biocathodes, including direct electron transfer (DET) and mediated electron transfer (by use of mediators, such as hydrogen,[15] or extracellular enzymes[11]), has been reviewed.[15] Although many studies suggested the presence of DET in methane producing biocathodes,[14, 16, 17] the true involvement of DET pathways has been, in general, doubted throughout the scientific community. Only recently has a handful of studies reported some species of methanogenic archaea to be capable of DIET.[13, 18–20] These studies and the probable mechanisms underlying DIET have been reviewed,[21] but only one study reports a species with the ability of DIET belonging to the *Methanobacterium* cluster (*YSL* strain).[20] Additionally, in the previous study, it is hypothesized that the presence of GAC, as a conductive material, aided the DIET.[20] Nevertheless, it is still not certain to which extent these species would be able to directly take up electrons from a solid electrode, if the DET-capable species were not present.

With the observations of this study, it has been identified that throughout the GAC bed there are different conditions, in terms of H_2, pH and ORP, which are summarised in figure 5.4. These gradients can lead to, as an example, different adaptations in the local microbial community, possibly leading to the distribution of different communities along the GAC bed. An interesting future research direction would be to try to identify if there are any (and which) changes in microbial community and activity with depth.

Possible limitations and proposed design considerations

Low H_2 concentrations near the current collector

Local concentrations of hydrogen near the current collector are quite low, as low as 5 μmol L^{-1}. If assuming hydrogen mediated methanogensis is preferred in these systems, this means that this might hamper biological activity due to low reactant concentrations. Hence it is possible that a thinner GAC bed has to be considered in future designs.

pH deadzones

Large pH differences were observed at the bottom well of reactor B1, ranging from pH 7.5 close to the current collector, to pH 10.5 at depth 0.7 cm. Although this was only observed for B1, such large pH differences most certainly hamper biological activity or performance. Additionally, these large pH differences are probably related to low recirculation flow rates in this measurement area of the GAC bed, which is probably due to the packing of the GAC bed, since recirculation rates were the same for both B1 and B2. A tightly packed bed will probably lead to a better distribution of the liquid flow rate in comparison to a less tight bed. To prevent dead zones in (larger scale) methane producing biocathodes, the recirculation flow rate should be high enough to ensure homogeneous distribution of electrolyte, without compromising the attachment of microorganisms at the electrode. Making a pH profile can be used to assess if electrolyte is homogeneously distributed.

5.4 Experimental Methods

Reactor

Two reactors, B1 and B2, were built similarly to previous work,[2] with the bioelectrochemical cell at their core and recirculation vessels for the recirculation of the catholyte and anolyte over the cell. Adjustments were made to the bioelectrochemical cell to be able to conduct the microsensor measurements at the cathode side. A schematic representation of the reactor is shown in figure 5.5. In addition, the same two reactors with different packed GAC bed, were also operated under abiotic conditions, these were named A3 and A4.

Bioelectrochemical cell

Two methane producing BES were built. The BES, which is centred in figure 5.5, comprised of seven layers, with silicon spacers positioned between each layer. Starting from the left, the first layer (light gray) was a plexiglass plate and the second layer (dark gray) was a graphite plate acting as the cathode current collector and with a surface area of 21.6 cm^2. In both these layers three holes were made, in a way that each hole in each layer aligned with the hole in the other layer. These holes were made in order to execute the microsensor profiles (movement represented by dotted yellow arrow) at three different heights, and caps were added at the plexiglass plate, that could easily be screwed open and closed. The third layer was the catholyte compartment and it consisted of a plexiglass plate with a hole in the middle (33 cm^3). To this layer, tightly packed granular activated carbon (GAC) (black dots) was added, with 1–3mm in diameter (Cabot Norit Nederland B.V., Zaandam, the Netherlands). In total 11.0g of GAC were added to B1 and 10.5g to B2, and for the abiotic experiments 7.6g was added to B3 and 7.3g to B4. This GAC bed (layer 3) had a total thickness of 1.4 cm, and along with the graphite plate comprised the cathode electrode material. In addition two connections to fit two Ag/AgCl (3M KCl) reference electrodes (QM710X, ProSense Qis, Oosterhout, The Netherlands; +0.210 V vs. NHE) (yellow circles) were added in this layer, at heights 6 cm and 9 cm from the bottom of the cell (inlet) and at depth 0.7 cm from the current collector. The forth layer (yellow) consisted of a cation exchange membrane (FumaTech GmbH, Ingbert, Germany), with a surface area of 22 cm^2. The fifth layer was the anolyte compartment, where a plexiglass plate with a hole in the middle (33 cm^3) was filled with glass beads (white circles) to ensure similar pressure on both sides of membrane. The sixth layer (dark gray) consisted of a Ti/Pt-Ir MMO flat anode electrode, with 1mm thickness (Magneto Special Anodes BV, Netherlands) and a surface area of 22 cm^2. The seventh layer (light gray) was a final plexiglass plate.

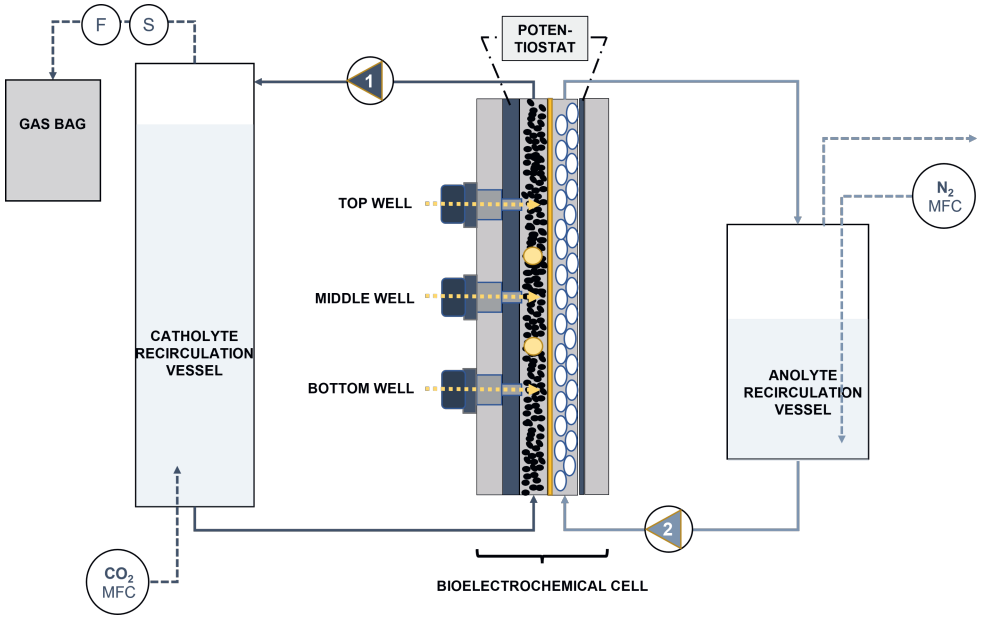

Figure 5.5: Schematic representation of the set up, with overview of the gas flows (dashed lines), liquid flows (solid lines), and electrical connection (alternating dot and dashed line). Flows at the cathode side are represented in dark blue and flows at the anode side in light blue. The bioelectrochemical cell is at the centre of the scheme. MFC-mass flow controller, S-sampling T-piece, and F-flow meter.

Set-up and gas sampling

The catholyte was recirculated bottom-up through the cathode side of the cell at 8 mL/min, using a pump (120U/DV, Watson Marlow, Falmouth, United Kingdom), to the top of catholyte recirculation bottle (left side, figure 5.5). In the catholyte recirculation CO_2 was sparged bottom-up at 0.65 mL/min through approximately 250 mL of catholyte, leaving a headspace volume of approximately 25 mL. An oxygen dot sensor (SP-PSt3-NAU-D5-YOP, PreSens GmbH, Germany) was added to the headspace of the bottle to confirm that the amount of oxygen was below 2%, which we consider to be sufficiently anaerobic. The headspace was connected to T-piece (closed with a rubber stoper) which was then connected to a gas flow meter (BPC instruments, Lund, Sweden), which quantified the gas flow and the time period, which was then connected to a 5L multi-layer foil gas bag (Medisense, Groningen, the Netherlands) where the gas was collected for sampling. At the T-piece, gas samples were taken for quantification of H_2 via gas chromatography with a μ-TCD (HP 6890 GC and HP Molsieve 5A column, Hewlett-Packard Company, Palo Alto, United States). At the gas bag, gas samples were taken for quantification of CH_4

via gas chromatography with a flame ionisation detector (HP 6890 GC, Hewlett-Packard Company, Palo Alto, United States; RT-Q-BOND column, Restek, Germany).

The anolyte was recirculated bottom-up through the anode side of the cell at approximately 12 mL/min, using a pump (120U/DV, Watson Marlow, Falmouth, United Kingdom), to the top of anolyte recirculation bottle (right side, figure 5.5) The anolyte recirculation bottle was sparged bottom-up with N_2 at a rate of 6.65 mL/min to strip away the produced oxygen and keep the chamber anaerobic (below 2% of O_2). The anolyte recirculation bottle had a liquid volume of 250 mL and a headspace volume of 150 mL which was open to air. An oxygen dot sensor (SP-PSt3-NAU-D5-YOP, PreSens GmbH, Germany) was added to the headspace of the bottle to confirm the amount of oxygen.

Inoculation and Operation

The inoculum for B1 and B2 was obtained from the anaerobic digester at the waste water treatment facility of the paper factory in Eerbeek (Industriewater Eerbeek B.V., Eerbeek, The Netherlands) in 2023 and stored at -10°C. The sludge was pre-treated with the following steps before addition to the reactors. The first step was separating the organic matter in the liquid from the granules by sieving the granules in tap water, with a pore size sieve of 500 μm. After sieving, the granules were placed in a plastic bottle that was continuously flushed with a high flow of nitrogen to maintain an anaerobic environment. Next, the granules were mashed using a dispersing instrument (Janke & Kunkel ultra turrax T25, IKA-Werke GmbH & Co. KG, Germany). During this process, 30 ml of catholyte was added (see below), and the granules were mashed until they reached a liquid consistency, still under N_2 flush. 30 ml of the resulting liquid was drawn up using a syringe and then added to the inlet of the catholyte recirculation bottle, at the top. Both electrolytes, catholyte and anolyte, were composed of 50 mM phosphate buffer (2.77 g L^{-1} $NaH_2PO_4.2H_2O$ and 4.58 g L^{-1} Na_2HPO_4), with approximately pH 7. Neither nitrogen, vitamins, nor minerals were added to avoid depositions on the electrode (electrode passivation), and because short experimental times were investigated.

The two methane producing BES were operated at a fixed current density of -2.5 A $m^{-2}_{\text{cathode area}}$ using a potentiostat (Ivium n-Stat with IviumSoft v2.462, Eindhoven, The Netherlands). During this time the cathode potential was registered by the software of the potentiostat. Anode potential and cell voltage were measured every week or every two weeks with a multimeter. Throughout the entirety of the run the reactors were in a temperature-controlled cabinet at 22-27°C. Note that the abiotic operation of A3 and A4 was done as described above, excluding inoculation.

Microsensor measurements

Microprofiling set-up and method

The microsensors measurements were conducted following thoroughly the methodology set by Smit et al. [6], with the use of a motor tool, which automatically moved the sensors in a 90°alignment with the bioelectrochemical cell (Unisense A/S, Denmark). An overview of the motor tool and other details of the measurement setup can be found in the Results section of the previously mentioned work.[6] With the motor tool, it was able to measure starting at the current collector (depth 0) and up to 0.9 cm in depth in the GAC bed, with a measurement step of 0.08 cm. For each measurement step (0.08 cm), a 20s wait period and a 10s measuring period was set for each microsensor. Depths above 0.9 cm and up to 1.4 cm (where the membrane is located) were not measured to exclude the risk of breaking the sensor against the membrane or puncturing the membrane with the sensor. The measurements were done at three different heights in the GAC bed, bottom, middle, and top well, at heights 4.3 cm, 8 cm, and 11.7 cm from the inlet, respectively. In order to conduct the measurements, the cap at the certain well had to be unscrewed, the measuring sleeve had to be screwed in, and the sensor had to be centred in the measuring sleeve. All these steps were conducted manually and had to be conducted as fast as possible to minimise oxygen intrusion. After the sensor was properly centred in the measuring sleeve, with vacuum grease to avoid leakages, the recirculation of the BES was re-started in order to remove possible oxygen contamination. After a while (few minutes), the profiling cycles were started and 3 to 5 profiles were executed per measuring well.

In contrast to previous work, where glass microsensors were used to measure in graphite felt,[6] here, needle versions of these microsensors were used (with exception for pH, as discussed later)(Unisense A/S, Denmark). This was done to avoid breaking the glass sensors against the GAC. Prior to the experiment, the set-up was tested with dummy sensors. These dummy sensors were made of the same glass as the real sensors but without the electrodes present in the real sensor (Unisense A/S, Denmark). Details of each microsensor used are described in the following sections.

Needle H_2, EP, and ORP microsensors

The needle H_2 microelectrode (H_2-NP) was used for measuring and profiling H_2 (Unisense A/S, Denmark). At each measuring day, a new calibration was made beforehand to correspond the current signal (in mV) to the amount of hydrogen. The calibration was made in the same electrolyte used for operating the system, and 0 μmol L^{-1} corresponded to the signal when the flask with the electrolyte was open to air, and 778.8 μmol L^{-1} (saturation of H_2 at electrolyte salinity and cabinet temperature) corresponded to the signal when the flask was continuously flushed with H_2. For the latter, we assumed saturation when the mV signal did not change for 5 min, or longer, during continuous flushing of H_2.

Because both the needle of the microsensor and the GAC bed are conductive, it could be possible that, during measuring, the granules that were not at the tip of the microsensor, but that were in contact with the needle at another end, could interfere with the signal at the tip of the needle via conductive contact. To prevent this, the majority of the surface of the needle microsensor was covered with PEEK tubing, as a strategy to avoid conductive contact. The non-conductive PEEK tubing had an outer diameter of 0.16 cm and an inner diameter of 0.08 cm, wide enough to fit the needle sensor, and covered the majority of the needle with the exception of 0.2–0.3 cm of the tip.

The needle electric potential microelectrode (EP-NP) was used for measuring the electric potential for correction of electric field disturbance of the pH and ORP mV signals (Unisense A/S, Denmark), as described by Smit et al. [6]. This microelectrode measures the electric potential difference between the microsensor and the reference electrode, located in the bioelectrochemical cell at a specific depth (0.7cm from the current collector in our study).

The ORP microelectrode (RD-NP) was used for measuring and profiling the oxidation reduction potential (Unisense A/S, Denmark). Similar to the H_2 microsensor, PEEK tubing was added to the needle part of both EP and ORP microsensors, with exception of the tip.

Glass pH microsensor

Glass pH microsensors (pH-25, pH-50 and pH-100) were used for measuring pH (Unisense A/S, Denmark). The reason why glass pH microsensors were used over needle alternatives, as done for the previous sensors, is because the needle pH sensors took very long (several hours) for the signal stabilization of the mV signal, especially at high pH (8-14). In contrast, the glass sensor tip surface has a greater area exposed to the measured liquid, allowing for a faster signal response (bellow 10s). The pH microsensor was calibrated every measuring day. This was done by submerging the microelectrode and the reference (used in the BES) in so lutions of pH 3, pH 6, pH 7, pH 9, and pH 10, and corresponding each to a mV signal.

Because for the pH measurements glass microsensors were used, and these would break if directly plunged through GAC, it was necessary to print a 3D channel to fit in the GAC bed, so that the microelectrode would not be in direct contact with the GAC but with the liquid surrounding the GAC. The design of this 3D printed channel is shown in figure 5.6. The cylindrical shape had an inner diameter of 0.35 cm, through which the sensor would easily go through, and an outer diameter of 0.96 cm. The total length of the channel was of 4.8 cm, but the measuring section of the channel had 1.5 cm (1.4 cm in the GAC bed). In addition, in this measuring section multiple 0.1 cm wholes were made to allow the flow of liquid perpendicularly to the positioning of the channel. PLA was used as material to 3D print these channels.

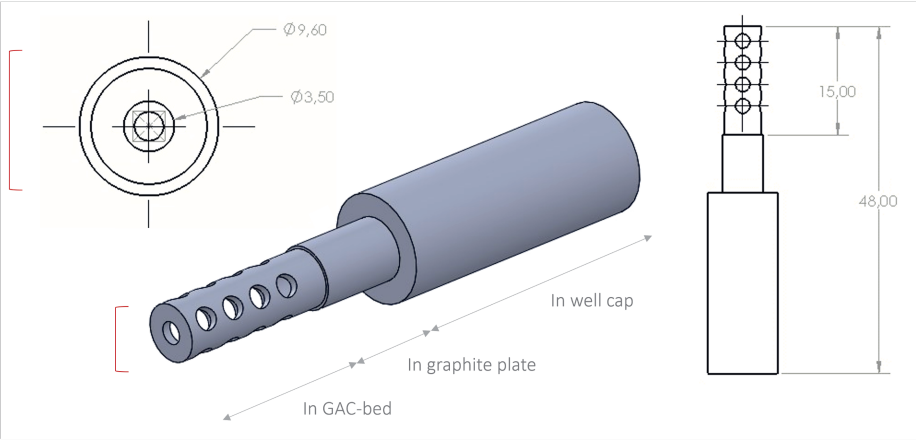

Figure 5.6: Schematic representation of 3D printed well for microsensor profiling in the GAC bed with pH glass microsensor. Numbers in the figure in mm.

Acknowledgments

We would like to acknowledge Paqell B.V. for funding the work.

References

[1] D. Liu, M. Roca-Puigros, F. Geppert, L. Caizán-Juanarena, S. P. Na Ayudthaya, C. Buisman, and A. Ter Heijne. "Granular carbon-based electrodes as cathodes in methane-producing bioelectrochemical systems". *Frontiers in bioengineering and biotechnology* 6 (2018), 78.

[2] M. B. Lavender, S. Pang, D. Liu, L. Jourdin, and A. Ter Heijne. "Reduced overpotential of methane-producing biocathodes: Effect of current and electrode storage capacity". *Bioresource Technology* 347 (2022), 126650.

[3] G. Shang, K. Cui, W. Cai, X. Hu, P. Jin, and K. Guo. "A 20 L electrochemical continuous stirred-tank reactor for high rate microbial electrosynthesis of methane from CO2". *Chemical Engineering Journal* 451 (2023), 138898.

[4] W. Cai, W. Liu, B. Wang, H. Yao, A. Guadie, and A. Wang. "Semiquantitative detection of hydrogen-associated or hydrogen-free electron transfer within methanogenic biofilm of microbial electrosynthesis". *Applied and Environmental Microbiology* 86.17 (2020), e01056–20.

[5] T. Sandfeld, L. V. Grøn, L. Munoz, R. L. Meyer, K. Koren, and J. Philips. "Considerations on the use of microsensors to profile dissolved H2 concentrations in microbial electrochemical reactors". *Plos one* 19.1 (2024), e0293734.

[6] S. M. de Smit, J. J. Langedijk, L. C. van Haalen, S. H. Lin, J. H. Bitter, and D. P. Strik. "Methodology for in situ microsensor profiling of hydrogen, pH, oxidation–reduction potential, and electric potential throughout three-dimensional porous cathodes of (bio) electrochemical systems". *Analytical Chemistry* 95.5 (2023), 2680–2689.

[7] S. M. de Smit, J. J. Langedijk, J. H. Bitter, and D. P. Strik. "Alternating direction of catholyte forced flow-through 3D-electrodes improves start-up time in microbial electrosynthesis at applied high current density". *Chemical Engineering Journal* 464 (2023), 142599.

[8] D. Liu. "Strategies for Improving Methane Production from CO 2 and Electricity in Bioelectrochemical Systems". PhD thesis. Wageningen University and Research, 2018.

[9] F. Karadagli and B. E. Rittmann. "Thermodynamic and kinetic analysis of the H 2 threshold for Methanobacterium bryantii MoH". *Biodegradation* 18 (2007), 439–452.

[10] J. Philips. "Extracellular electron uptake by acetogenic bacteria: does H2 consumption favor the H2 evolution reaction on a cathode or metallic iron?" *Frontiers in Microbiology* 10 (2020), 483184.

[11] J. S. Deutzmann, M. Sahin, and A. M. Spormann. "Extracellular enzymes facilitate electron uptake in biocorrosion and bioelectrosynthesis". *MBio* 6.2 (2015), 10–1128.

[12] M. Villano, L. De Bonis, S. Rossetti, F. Aulenta, and M. Majone. "Bioelectrochemical hydrogen production with hydrogenophilic dechlorinating bacteria as electrocatalytic agents". *Bioresource technology* 102.3 (2011), 3193–3199.

[13] D. J. Walker, K. P. Nevin, D. E. Holmes, A.-E. Rotaru, J. E. Ward, T. L. Woodard, J. Zhu, T. Ueki, S. S. Nonnenmann, M. J. McInerney, et al. "Syntrophus conductive pili demonstrate that common hydrogen-donating syntrophs can have a direct electron transfer option". *The ISME journal* 14.3 (2020), 837–846.

[14] M. Villano, F. Aulenta, C. Ciucci, T. Ferri, A. Giuliano, and M. Majone. "Bioelectrochemical reduction of CO2 to CH4 via direct and indirect extracellular electron transfer by a hydrogenophilic methanogenic culture". *Bioresource technology* 101.9 (2010), 3085–3090.

[15] F. Geppert, D. Liu, M. van Eerten-Jansen, E. Weidner, C. Buisman, and A. Ter Heijne. "Bioelectrochemical power-to-gas: state of the art and future perspectives". *Trends in biotechnology* 34.11 (2016), 879–894.

[16] S. Cheng, D. Xing, D. F. Call, and B. E. Logan. "Direct biological conversion of electrical current into methane by electromethanogenesis". *Environmental science & technology* 43.10 (2009), 3953–3958.

[17] P. F. Beese-Vasbender, J.-P. Grote, J. Garrelfs, M. Stratmann, and K. J. Mayrhofer. "Selective microbial electrosynthesis of methane by a pure culture of a marine lithoautotrophic archaeon". *Bioelectrochemistry* 102 (2015), 50–55.

[18] A.-E. Rotaru, P. M. Shrestha, F. Liu, M. Shrestha, D. Shrestha, M. Embree, K. Zengler, C. Wardman, K. P. Nevin, and D. R. Lovley. "A new model for electron flow during anaerobic digestion: direct interspecies electron transfer to Methanosaeta for the reduction of carbon dioxide to methane". *Energy & Environmental Science* 7.1 (2014), 408–415.

[19] M. O. Yee and A.-E. Rotaru. "Extracellular electron uptake in Methanosarcinales is independent of multiheme c-type cytochromes". *Scientific reports* 10.1 (2020), 372.

[20] S. Zheng, F. Liu, B. Wang, Y. Zhang, and D. R. Lovley. "Methanobacterium capable of direct interspecies electron transfer". *Environmental Science & Technology* 54.23 (2020), 15347–15354.

[21] K. Gao and Y. Lu. "Putative extracellular electron transfer in methanogenic archaea". *Frontiers in Microbiology* 12 (2021), 611739.

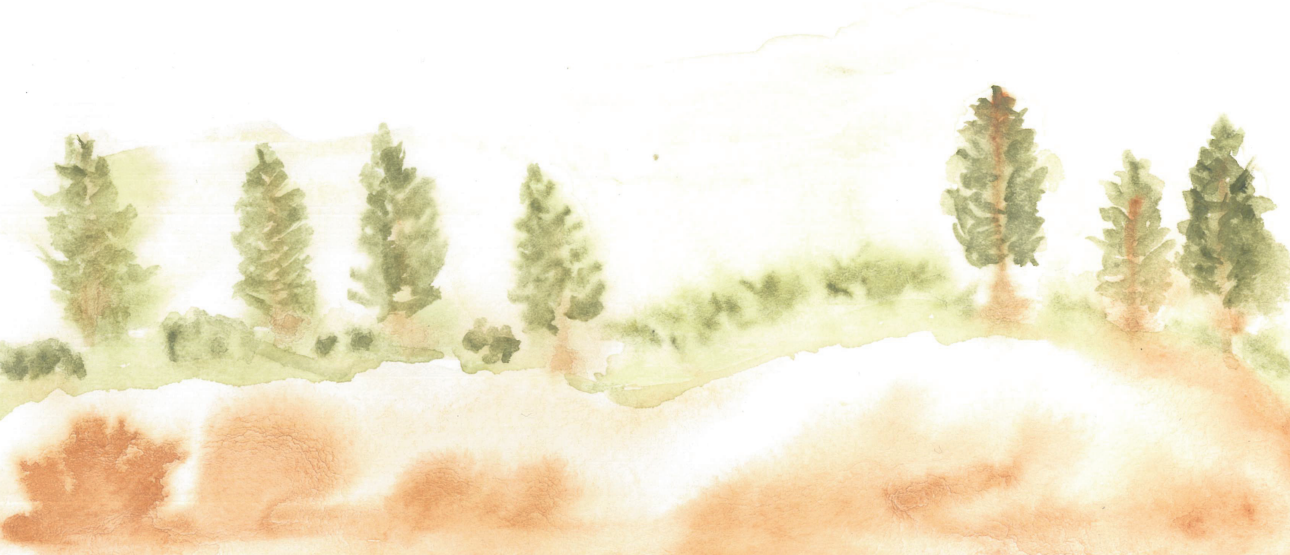

Chapter 6

General Discussion

6.1 Power-to-methane in BES, *Quid factum est*

This thesis set out to understand the limitations of methane producing BESs, and how to overcome these, in order to improve energy efficiency. In this section, the main research outcomes are summarised (see table 6.1). Overall, three focus points were addressed: 1) decreasing overpotentials and electrolyte associated resistances, 2) understanding the resulting trade-off between energy efficiency and methane production rates, and 3) the losses associated with scaling-up.

Reaching for high energy efficiency: reducing voltage losses

Tackling overpotentials by selecting appropriate electrode materials and operating at fixed current

Most experiments on methane producing BESs have been controlled by fixing cathode potential, setting a more negative cathode potential than theoretically expected (e.g. between -0.60 V and -1.1 V vs Ag/AgCl),[1–5] aiming to provide enough driving force for the biological CO_2 reduction to methane to occur. Alternatively, in this thesis, we opted for the operation of methane producing BES under fixed current density, galvanostatic control. Moreover, in this thesis, granular activated carbon (GAC) was chosen as the cathode material, since methane producing biocathodes with GAC have reported the lowest cathode overpotentials.[6] It was observed that by controlling the rate of electrons it allowed the resulting cathode potential to increase over time from values around -0.90 V (at t=0) to values between -0.51 V and -0.63 V vs Ag/AgCl depending on the study (see table 6.1). Although this increasing trend was observed in all three chapters, the rate at which it occurred was not always the same. The local conditions leading to the increase in cathode potential are further discussed later on in this chapter.

Although the resulting cathode overpotential was -0.52 V vs Ag/AgCl in Chapter 2, the energy efficiency remained quite low, being around 21%. Therefore, from Chapter 2 to Chapter 3 the anode electrode was changed to a commercially available and state-of-the-art electrode for water splitting and the overall reactor set-up (including recirculation vessels) was improved in order to minimise gas leakages. As a result, the energy efficiency in Chapter 3 reached 42% using a standard electrolyte, 50 mM phosphate, with a resulting cathode pH around 7 and a resulting anode pH around 2. Taking into account the theoretical potentials in table 6.2, at 42% energy efficiency (pH 7) the cathode overpotential accounted for around 0.09 V (-0.42 V - -0.51 V), the anode overpotential for 0.25 V (1.15 V - 0.90 V) and the overall cell overpotential accounted for 0.51 V (-1.32 V - -1.83 V), while the electrolyte associated losses accounted for 0.17 V ((-0.51 V - 1.15 V) - -1.83 V).

Table 6.1: Performance of methane producing biocathodes with GAC as the electrode material (NM-not measured. NR-not reported. Note that Chapter 4, is the scale up chapter).

Cathode (V vs Ag/AgCl)	Anode (V vs Ag/AgCl)	Cell voltage (V)	Energy eff. (%)	Methane prod. rate (NL m^{-2}_{CC} d^{-1})	Methane prod. rate (NL m^{-3}_{BES} d^{-1})	Electrolyte	Ref.
-0.52	NR	NR	NR	65	2150	0.05M phosphate	[6]
-0.52	2.14	-2.77	21	13	433	0.05M phosphate	Ch. 2
-0.51	1.15	-1.83	42	40	470	0.05M phosphate	Ch. 3
-0.69	0.93	-1.70	54	10	109	0.6M bicarbonate	Ch. 3
-0.62	0.76	-1.43	**70**	11	120	1M bicarbonate	Ch. 3
-0.66	NM	-4.14	25	5	95	0.05M phosphate	Ch. 4
-0.60	1.30	-2.70	39	6	110	0.2M bicarbonate	Ch. 4
-0.64	1.35	-2.50	41	5	100	0.4M bicarbonate	Ch. 4
-0.99	0.96	-2.60	40	15	280	0.6M bicarbonate	Ch. 4

Tackling electrolyte associated resistances by changing the operation to an haloalkaline electrolyte

Energy efficiency was improved substantially, namely up to 70% (Chapter 3) by changing the standard electrolyte to an haloalkaline electrolyte - in this case 1M bicarbonate - with an observed cathode pH around 8 and an observed anode pH around 10 (see table 6.2). The resulting cathode potential increased slightly to -0.62 V and so did the overpotential from 0.09 V at standard electrolyte to 0.15 V (-0.47 V - -0.62 V) at haloalkaline electrolyte. Moreover, the anode potential decreased to 0.76 V but the anode overpotential increased from 0.25 V at standard electrolyte to 0.36 V (0.76 V - 0.40 V) at haloalkaline electrolyte. Although the resulting cell voltage decreased to -1.43 V, the cell overpotential slightly increased from 0.51 V at standard electrolyte to 0.56 V (1.43 V - 0.87 V) at haloalkaline electrolyte. Nevertheless, the electrolyte associated losses (ionic and transport) decreased substantially, in comparison to standard electrolyte, to 0.05 V ((-0.62 V - 0.76 V) - -1.43

Table 6.2: Cathode, anode and overall chemical equations and their respective theoretical potential/voltage (E) based on process conditions. Top equations at standard electrolyte, assumed 0.05M HCO_3^-, with concentrations of methane in the μmol L^{-1} range and 1M O_2. Bottom equations at haloalkaline electrolyte, assumed 1M HCO_3^-, concentrations of methane in the μmol L^{-1} range and 1M O_2.

	Equation	pH	E (V vs Ag/AgCl)
Cathode	$HCO_3^- + 9\,H^+ + 8\,e^- \longrightarrow CH_4 + 3\,H_2O$	7	-0.42
Anode	$2\,O_2 + 8\,H^+ + 8\,e^- \longrightarrow 4\,H_2O$	2	+0.90
Cell	$HCO_3^- + H_2O + H^+ \longrightarrow 2\,O_2 + CH_4$	-	-1.32
Cathode	$HCO_3^- + 9\,H^+ + 8\,e^- \longrightarrow CH_4 + 3\,H_2O$	8	-0.47
Anode	$4\,H_2O + 2\,O_2 + 8\,e^- \longrightarrow 8\,OH^-$	10	+0.40
Cell	$HCO_3^- + H_2O + H^+ \longrightarrow 2\,O_2 + CH_4$	-	-0.87

V). These results show that changing to an alkaline electrolyte efficiently reduced the losses associated to ion and other transport across the membrane. In fact, these losses accounted for a total ohmic resistance of 11 mΩ $m^2_{membrane}$ at haloalkaline electrolyte in comparison to 39 mΩ $m^2_{membrane}$ at standard electrolyte. Lower ohmic resistances, in the order of 2 mΩ $m^2_{membrane}$ have only been achieved by using zero-gap bioelectrochemical cell designs, to the best of our knowledge.[7] Up to 42% energy efficiency has been reached, when operating a zero-gap BES for CO_2 reduction to methane fed with a waste water derived electrolyte.[8] However, it is not only the low ionic and transport losses over the membrane that lead to the lower cell voltage at alkaline electrolyte but also the lower theoretical (and real) anode potentials. It would be interesting to investigate if operation at haloalkaline electrolyte of a zero gap methane producing cell could yield higher energy efficiency rather than using GAC.

Voltage losses associated to scaling-up

The energy efficiency of the scale up BES (Chapter 4) is lower than the energy efficiency of the lab scale for the same operational conditions with standard electrolyte and 0.6M electrolyte (table 6.1). All three parameter cathode overpotential, anode overpotential and cell overpotential were larger in the scale up BES than the lab scale. Nevertheless, the cell voltage was decreased significantly from -4.14 V to -2.70 V, when the size of the anode was increased at the same time that the electrolyte was switched from 0.05M phosphate to 0.2M bicarbonate. At 0.6M haloalkaline electrolyte the ionic and transport losses in the scale up version accounted for 0.65 V ((-0.99 V - 0.96 V) - -2.60 V), which is far larger than the lab scale version 0.08 V ((-0.69 V - 0.93 V) - -1.70 V). These larger losses are most probably due to increased distances between electrodes and between the electrodes and the membrane. Decreasing these will most probably lead to higher energy efficiency in the

scale up. Other scale up methane producing BES designs reported slightly lower energy efficiency at similar rates up to 30% (see Chapter 4 for more information).[9] Therefore, this design remains to date the most energy efficient scale up design (40%) with 280 L_{CH_4} m^{-3}_{BES} d^{-1} produced.

The trade-off between energy efficiency and methane production rates.

Results in Chapter 3 suggest a trade-off between methane production rates and energy efficiency (see table 6.1). At standard electrolyte up to 470 L m^{-3}_{BES} d^{-1} of methane was produced at 42% energy efficiency. At haloalkaline electrolyte lower rates had to be set in order to keep cathode overpotential to a minimum. The resulting energy efficiency ranged between 55% and 70% and methane production rates were around 120 L m^{-3}_{BES} d^{-1}. In contrast, in the scaled up BES rates were increased after switching to an haloalkaline electrolyte from 95 L m^{-3}_{BES} d^{-1} to 280 L m^{-3}_{BES} d^{-1}. Here, instead of an abrupt change of electrolyte, as was done in the lab scale (Chapter 3), a gradual increase in salinity was tested (see Chapter 4), which suggests that microorganisms struggle to adapt to an abrupt change in conductivity in the lab scale, even after long periods of operation (up to 590 days). Whereas, a gradual increase in conductivity in the scale up showed better results regarding biological activity under haloalkaline conditions. However, during this period the cathode overpotential was high with cathode potential at -0.99 V and the resulting energy efficiency was low at 40% in contrast to 70% in the lab scale.

In this thesis, a maximum methane production rate of 40 L m^{-2}_{CC} d^{-1} was reached. However, slightly higher rates up to 65 L m^{-2}_{CC} d^{-1} have been observed in methane producing BESs with GAC, as the cathode material.[6] In comparison, the above mentioned zero-gap methane producing BES reported the highest production rates in literature of up to 669 L_{CH_4} m^{-2}_{CC} d^{-1} to the best of our knowledge.[8] It was suggested that such high rates were achieved due to an efficient H_2 supply resulting from the use of the $Fe_3Ni_3Co_3S_8$ catalyst at the cathode. Nevertheless, these rates were obtained by applying a cell voltage of -2.2 V, thus resulting in a 42% energy efficiency. The main limitation in BESs and specifically in this thesis remains the trade-off between energy efficiency and methane production rates.[10] Can a better understanding of local conditions in methane producing biocathodes explain the trade-off between energy efficiency and methane production rates?

Understanding how local conditions affect the resulting low cathode overpotential at standard electrolyte.

In BESs operated at fixed current density, the resulting cathode overpotential is highly influenced by local conditions, such as pH, temperature and product and reactant concentrations.[11] Additionally, in the case of the presence of microorganisms acting as catalysts, cathode overpotential also depends on biological activity and density, which in turn depends on process conditions as well. Therefore, in this thesis the local conditions at

the methane producing biocathodes were investigated with the prospect of gaining insights on possible existing limitations.

The exact local conditions leading to the increase in cathode potential over time are still unknown. However, in Chapter 2 it was observed that by depleting CO_2 the cathode potential, which before depletion was at around -0.50 V, would decrease back to values around -0.90 V (see figure 2.4). Additionally, in Chapter 5, experiments show that the local concentration of H_2 at -0.90 V is higher than those at less negative cathode potentials of -0.63 V (160 days after the measurement at -0.90 V) (see figure 5.1). Thus, the combination of these results show that cathode potential in a methane producing BES is highly dependent on the availability of CO_2 and H_2, since the overpotential is lower when CO_2 is available (and consumed) and lower concentrations of H_2 are present.

Understanding how local conditions relate to methanogenic activity at standard electrolyte.

In addition to the previous facts, in Chapter 5 it was observed that throughout the depth of the GAC bed there are gradients of H_2, pH and ORP. Larger concentrations of H_2 and lower pH were found further away from the current collector than closer to it. However, the measurements were done only up to half-way in the GAC bed from depth 0 (current collector) to depth 0.7 cm, as the total depth of the GAC bed was 1.4 cm (distance where the membrane is located). It is hypothesized that towards the membrane the hydrogen concentration keeps on increasing, since proton availability at the anode is higher (pH 2) than at the cathode (pH 7), while ion and transport resistances are lower closer to the membrane (see figure 6.1).[11] Although the H_2 production and, therefore, proton consumption increases from depth 0 to depth 0.7 cm away from the current collector, it is suggested that the pH increases (from 0 to 0.7 cm), rather than decreases, because the rate of formation and entrapment of H_2 bubbles is larger than the rate of proton transport.[12] Here it is hypothesized that closer to the membrane, once the rate of proton diffusion is higher (due to lower transport resistances) than the rate of hydrogen formation (and entrapment), the pH will decrease significantly. However, this measurement was not conducted. Last, ORP becomes more negative in the direction towards the membrane, which means that the presence of reductive species increases towards the membrane.

Overall, these results suggest that hydrogen formation is more favourable closer to the membrane. However, the question remains if this is also the case for the biological conversion of CO_2 to CH_4? Are places with the larger H_2 formation rates also the ones where methane formation is higher? Can the hypothetical pH drop close to the membrane negatively impact methanogenic activity?[13] Also, does a more negative ORP mean a larger concentration of H_2 and methane or does it mean larger concentrations of H_2 in relation to methane, since the reductive potential of hydrogen is higher than that of methane?

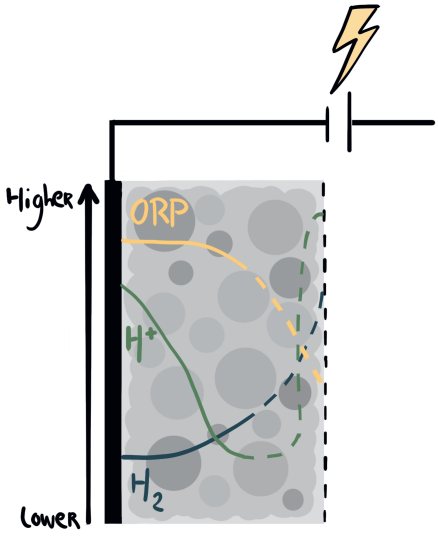

Figure 6.1: Schematic representation of the measured (solid lines) and hypothesized (dashed lines) local conditions at methane producing biocathodes throughout the depth of GAC.

In order to answer if higher H_2 concentrations are a good indicator for methanogenic activity, it would be relevant for future studies to explore techniques to visualise the growth and identify the activity of microorganisms at the methane producing biocathodes, with time and at different depths. *In-vivo* visualization techniques of microorganisms at electrodes can be extensive.[14] Two interesting methods would be: 1) optical coherence tomography, which allows one to follow the growth and attachment of the microorganisms over time and 2) Raman microscopy, which allows one to visualise and quantify compounds of interest at biocathodes, such as in this case CH_4.[14] In addition, collecting GAC samples for RNA sequencing followed by next generation sequencing analysis can give insights on the composition of microorganisms and activity. This could be done at different points in time and at different depths, although the latter might be easier on a larger scale. Moreover, investigating local pH and CO_2 in addition to H_2 throughout the operational time might contribute to a better understanding of why the cathode potential changes over time, and why it stabilises at different potentials (within the range of -0.66 V to -0.51 V in this thesis). In theory, with this understanding process conditions can be adjusted to achieve consistently low cathode overpotentials and at faster rates, thus decreasing the start-up time. Note that, choosing the optimal process condition in order to promote biological activity also depends on which electron transfer pathway is present. Because we have not conducted biological activity measurements (as suggested above), we can only hypothesise what are the electron transfer pathways currently prevailing in this thesis.

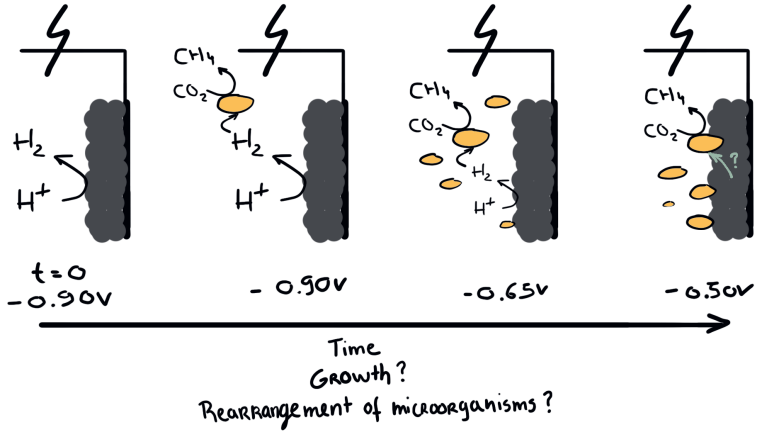

Figure 6.2: Schematic representation of the hypothetical shift in electron transfer pathways in methane producing BESs over operational time, possibly depending on growth factors, as well as, the rearrangement of microorganisms at the GAC surface. The question mark possibly represents DET and/or DIET and/or extracellular enzymatic mediators and/or H_2 concentrations below 5 μmol L^{-1}.

Hypothetical shift in electron transfer pathways at standard electrolyte.

The correlation between the electron transfer pathways present in CO_2 reducing biocathodes and cathode potential is under exploration.[15] However, this correlation has not yet been well established for methane producing biocathodes. In principle, either H_2 mediated electron transfer or direct electron transfer (DET) are most likely to occur.[16] Evidences suggesting direct electron uptake by methanogens from a solid electrode are slim,[4, 17–19] and include mutated species, low cathode overpotential with cathode potential less negative than -0.70 V vs. Ag/AgCl or not detecting H_2 in the headspace of the methane producing BES. However, it was observed in this thesis that, even at a cathode potential of -0.63 V vs Ag/AgCl and with no detection of H_2 in the headspace, extremely low concentrations of H_2 (as low as 5 μmol L^{-1}) were detected locally in methane producing biocathodes with GAC as electrode material. Not only can methanogens,[20] and other hydrogenotrophic microorganisms,[21] grow at these extremely low hydrogen concentrations (as low as 2 μmol L^{-1} [20]) but low concentrations of hydrogen in the order of μmol L^{-1} can also explain cathode potentials as high as -0.45 V vs. Ag/AgCl (see E below).

$$2\,H^+ + 2\,e^- \longrightarrow H_2 \qquad E = \text{-0.45 V vs. Ag/AgCl, at pH} = 7$$

Evidences suggesting the possibility of interspecies electron transfer (DIET) between methanogens and other species known to be able to perform DET e.g. *Geobacter*, [22–25] are more prominent and this includes one study on a hydrogenotrophic methanogen.[25] Since the methane producing BESs in this thesis were inoculated with mixed cultures,

interspecies electron transfer can not be excluded either. Overall, neither DET nor DIET nor H_2 mediation can be clearly excluded.

Nevertheless, the change in cathode potential over time from -0.90 V to -0.63 V, as a result of or resulting in decreasing H_2 concentrations over time, can be explained both/either by 1) larger H_2 consumption rates, due to e.g. biological growth and/or 2) lower H_2 production, due to a shift in pathways from H_2 mediated electron transfer to DET or DIET. Taking into account that H_2 was detected locally at -0.63 V, it is not possible to conclude a complete shift in pathways at -0.63 V. However, in Chapter 2 even lower cathode overpotentials were observed, namely up to -0.50 V. Since -0.50 V (-0.30 V vs SHE), which is close to the thermodynamic limit for H_2 evolution at pH 7 (see equation above),[21] and it is possible that at this potential direct electron transfer pathways are predominant. This hypothetical shift in electron transfer pathways is schematised in figure 6.2.

How can changing to an alkaline electrolyte affect the local conditions and resulting activity?

Local measurements at methane producing biocathodes at haloalkaline conditions were not done in this thesis. Nevertheless, when changing to a haloalkaline electrolyte the following changes are expected: 1) increased catholyte pH (7 to 8) and anolyte pH (2 to 10), 2) increased buffer capacity, 3) increased concentration of carbon species (aqueous CO_2 and HCO_3^-) and 4) increased concentration of cations.

The effect of the increased recirculation pH (1) on the theoretical potentials and cell voltage has been discussed in the previous section. In general, the pH change at haloalkaline electrolyte results in a less negative theoretical cell voltage, since lower theoretical anode potential is expected, which offsets the slightly more negative theoretical cathode potential (see table 6.2). However, cathode, anode and cell overpotentials are larger with the haloalkaline electrolyte, in comparison to standard. Therefore, recirculation pH alone is not responsible for these overpotentials. Since local conditions were not measured for the haloalkaline electrolyte, we are incapable of investigating the effect local pH has on the resulting overpotentials. However, since the buffer capacity of the haloalkaline electrolyte is larger, it is hypothesized that local pH gradients at haloalkaline conditions are not so prominent, as the ones observed with the standard electrolyte. Fewer pH changes also mean lower chances for microbial toxicity, as a result of acidification.

The change in pH also affects the carbonate speciation. At 0.05M phosphate electrolyte and pH 7 around 8 mM CO_2 (aq.) (15%) and around 43 mM in the HCO_3^- (aq.) (85%) form is expected. When operating with 1 M haloalkaline electrolyte and pH 8 around 20 mM CO_2 (aq.) (2%) and 980 mM HCO_3^- (aq.) (98%) is expected. Thus, either carbon species should be present at higher concentrations in the alkaline electrolyte. Larger

concentration of reactants when using the haloalkaline electrolyte does not explain larger overpotential at the cathode.

Lastly, the increased concentration of cations can lead to increased osmotic stress at the biocathode,[26] thus jeopardising methanogenic activity. Lower methanogenic activity and possibly resulting increased concentrations of hydrogen at the biocathode can be a possible explanation as to why overpotential is higher at haloalkaline electrolyte. However, hydrogen was not detected in the headspace, which still suggests an efficient use of H_2 towards methane (biologically).

Performing local measurements, such as suggested above, at biocathodes operated with haloalkaline electrolyte might give insights as to why cathode potential is different to operation with standard electrolyte.

6.2 Power-to-methane in BES, *Quo vadis*

This section focuses on 1) the perspective of the methane producing BES, as an alternative process to biological conversion of CO_2 and H_2 to CH_4, and 2) the perspective of the scale up BES design in this thesis, and 3) the remaining limitations that need to be overcome. Lastly, the thesis is located within the broader context of future CO_2 valorisation.

Perspectives of methane producing BES in the context of biological conversion of CO_2 and H_2 to CH_4

The field of biomethanation, biological conversion of CO_2 and H_2 to CH_4 (see equation below) is more developed than the bioelectrochemical conversion of CO_2 to CH_4. Here we compare both fields and discuss what still needs to be done to level out both fields.

$$CO_2 + 4\,H_2 \longrightarrow CH_4 + 2\,H_2O \qquad \Delta G^\circ = -130.7 \text{ kJ mol}^{-1}{}_{CH_4}$$

Methane production rates

Biological conversion of CO_2 and H_2 to methane has been a well researched topic with various reactor configurations investigated, including continuous stirred tank reactors (CSTR), membrane biofilm based reactors, up-flow systems, bubble column systems, biofilm plug flow reactors and trickle bed reactor (TBR) to name a few.[27] Up to now, the best performing lab scale reactor (up to 1 L volume) uses a biofilm plug flow design with methane production rates reaching 17 x 10^2 L_{CH_4} $m^{-3}{}_{reactor}$ h^{-1}.[28] In contrast, in this work up to 19 L_{CH_4} $m^{-3}{}_{BES}$ h^{-1} were reached in the lab scale (Chapter 3), which is 100 times lower.

Moreover, at a larger reactor scale of 10 to 20 L up to 17 x 10^1 L_{CH_4} $m^{-3}{}_{reactor}$ h^{-1} were reached in CSTR and bubble column type reactors.[29, 30] In contrast, here, 11 L_{CH_4} $m^{-3}{}_{BES}$ h^{-1} was reached, in the scale up reactor (Chapter 4), which is approximately 20

times lower in comparison to the previous similar scale alternatives. Moreover, up to 64 x 10^1 L_{CH_4} $m^{-3}_{reactor}$ h^{-1} was reached in a TBR configuration with 3 times the volume (60 L).[31]

At a pilot scale, 1 to 14 x 10^3 L_{CH_4} $m^{-3}_{reactor}$ h^{-1} rates were achieved at biomethanation plants by MicrobEnergy (Viessmann group) and Electrochaea GmbH, respectively.[32] These rates are 1000 times bigger than those observed in this thesis.

H_2 mediation/usage

The main bottleneck in biomethanation is the low solubility of H_2 and the resulting limitations in H_2 gas to liquid transfer, when H_2 is produced *ex-situ*.[27] Among others, operation at increased temperatures and pressures promotes the gas to liquid transfer of H_2, as well as CO_2. Hence, biomethanation studies often resort to temperature control between 35°C to 70°C and pressures above 5 bar.[27] Mesophilic or thermophilic temperatures not only improve gas solubility but in most cases also improve biological activity. In contrast, methane producing BESs do not need to make use of increased pressures (above atmospheric pressure), since H_2 is produced and consumed in the same "stage", *in-situ*. Moreover, the rapid consumption of H_2 after its production minimises losses of H_2 gas in the overall process in comparison to biomethanation.

In addition to H_2 mediation in methane producing BESs it is hypothesised in this thesis that interspecies electron transfer (DIET) might also play a role to some extent, by acting as an additional electron transfer mechanism. The transfer of electrons via DIET has been thought to occur faster in comparison to the transfer through mediators present in solution, such as H_2.[33–35] Moreover, it is argued that via DIET rates are less susceptible to limitations resulting from substrate accumulation.[36] Thus, it is possible that larger methane production rates can be achieved, if DIET is stimulated.

Energy efficiency

In the Electrochaea process the power requirement is 1.6 MJ $mol_{CH_4}^{-1}$,[37] thus the energy efficiency of the process is 56%, since the amount of heat released by the combustion of CH_4 is 0.9 MJ $mol_{CH_4}^{-1}$ (see Chapter 1). Similarly, in general, stable performance at 45% to 50% energy efficiency was obtained throughout this thesis and during long operational times of up to 600 days. Moreover, this thesis, suggests that operation with haloalkaline electrolyte is a promising strategy to increase energy efficiency up to 70%.

Methane content in the outlet gas

The CH_4 content in the outlet gas of biomethanation reactors easily reaches concentrations from 96% to 99%,[27] whereas in this thesis only up to 75% was obtained (see supplementary information chapter, figure 14). In biomethanation studies several optimisations were done

in order to improve CH_4 content in the outlet gas and the conversion efficiency of CO_2 including applying gas recirculation and the use of gas diffusers.[27] Similarly, improving the absorber column of the methane producing BES line-up with a state-of-the-art gas diffuser and adding a recirculation loop of the gas phase may allow an improvement of the CH_4 content in the outlet gas and also improve the CO_2 conversion efficiency.

Perspective of the BES design in this thesis

The use of GAC as the cathode electrode material

The main reasons why granular activate carbon (GAC) was used as the cathode material in this thesis were the high surface area available for biological interaction and the reported low cathode overpotentials when using GAC.[6] GAC is a relatively low cost material, resistant to corrosion and thermally stable and all are relevant for larger scale implementation. In addition, since the start of this thesis, the advantageous use of GAC in methanogenic processes, including biomethanation and BESs, has been extensively studied and reviewed.[38] The advantages of GAC rely on the following properties: conductivity, surface area, adsorption and high capacitance.[38] These are further explained below and are schematized in figure 6.3.

BESs always rely on conductive materials at the anode and at the cathode for electron transfer but biomethanation processes do not. The addition of conductive materials, such as GAC, in biomethanation processes has led to increased rates, due to the promotion of direct interspecies electron transfer, which is also discussed above.[34]

The porous structure of GAC facilitates the immobilisation and attachment of microorganisms and the high surface area per reactor volume theoretically should lead to a higher density of microorganisms without the need for thick layers of microorganisms (biofilm). These two factors are considered to benefit conversion rates.[38] Moreover, the micro porous structure of GAC allows for the entrapment of substrates, especially those in gaseous form such as H_2 and possibly CO_2 in this case,[39] which can also result in faster conversion rates. Nevertheless, in the same way, products could also be entrapped, impacting rates.

Last, the capacitance property of GAC allows the homogeneous distribution of electrons throughout the large surface area and to store these electrons in the form of an electric double layer.[40] This capacitance property has shown to: 1) improve the oxidizing ability of microorganisms,[41] and possibly also the reducing capability and 2) possibly lead to smaller fluctuations in cathode potential, when the rate of electron supply (current) is changed.[42] Which means that methane producing biocathodes with GAC, as the electrode material, are less susceptible to a change in biological activity with changes in electron supply. This is of special interest in the sense of how much more adaptable are methane producing GAC biocathodes to intermittent electricity regimes resulting from

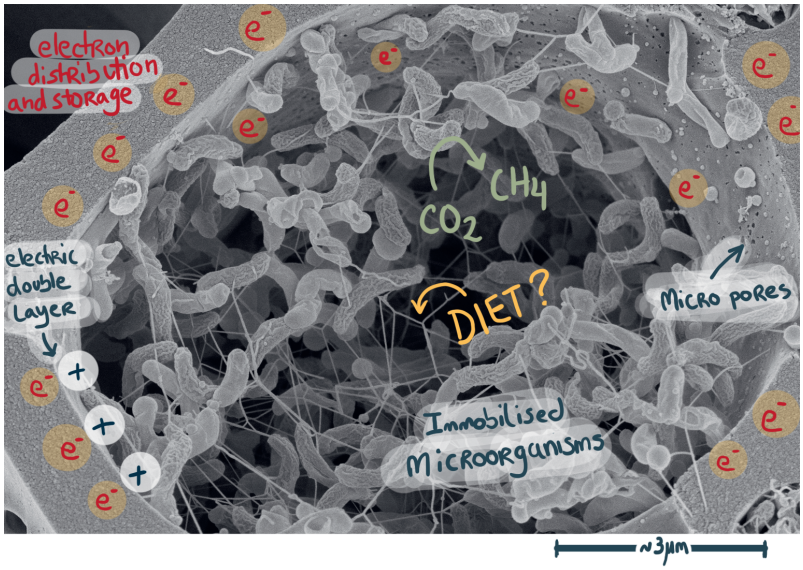

Figure 6.3: Schematic representation of the properties of granular activated carbon (GAC) biocathode present in a methane producing BES (adapted from Chapter 3).

mismatches between electricity supply and demand (see Chapter 1). Therefore, it would be interesting to investigate in the future the effect of intermittent regimes of electron supply on biological activity and process robustness.

CO_2 supply to biocathode

CO_2 converting bioelectrochemical systems commonly operate at neutral pH and make use of a recirculation bottle, where CO_2 is sparged through. The dissolved CO_2 is then recirculated to the cathode side of the BES. However, because the solubility of CO_2 is lower at neutral pH than at alkaline pH, this leads to losses of CO_2 (not all is dissolved). Moreover, dissolving CO_2 in an electrolyte with low buffer capacity leads to a pH drop and acidification, which in turn jeopardizes methanogenic activity.[13]

A haloalkaline electrolyte creates more favourable conditions for the dissolution of CO_2 in comparison to the ones described above. The alkaline nature increases the dissolution of CO_2 and the pH buffering both prevents acidification and preserves the alkaline environment for dissolving CO_2. In this way, this two step process, which includes dissolving CO_2 and recirculating it over the biocathode for conversion to methane, becomes more efficient.

This first step in this two step process resembles adsorption or absorption columns for the production of CO_2 rich streams already used on an industrial scale in processes, such as biogas upgrading,[43] and gas treatment (e.g. biological desulfurisation).[44, 45] Thus,

on the one hand, the adsorption/dissolution of CO_2 can be easily adjusted and improved to fit the BES needs on a larger scale. On the other hand, methane producing BES can be easily implemented with these processes that currently produce CO_2 rich streams. As an example, upgrading biogas to biomethane currently relies on CO_2 removal and not so much its conversion. Thus, commonly the adsorbed CO_2 in solution (after the adsorption column step) is regenerated as a gas and, by default, it is released to the atmosphere. Although other possible revenues for it would be its usage in carbonated beverages or farms, these options are less sought since purification and liquefaction steps are required and are extra expenditures. Alternatively, the CO_2 rich stream can be fed to the methane producing BES for conversion into methane, thus not requiring regeneration, purification (depending on the source) or liquefaction, hence increasing the amount of biomethane produced. In this way, operation with haloalkaline electrolyte is a good strategy to trap CO_2 and avoid pH changes.

The modular scale up

The hexagonal prism shape with the outside as a current collector (conductive shell) allows the methane producing BES to be further up scaled in modules, since the conductive shell of one prism in contact with the conductive shell of another allows electrons to flow through different modules. Scaling up in modules is an important concept in BES technology, since: 1) construction of the different parts of the reactor, such as electrodes and membranes, on a larger scale can be challenging and 2) increasing the size of one reactor usually leads to different properties, such as larger distances between electrodes, which influences the overall internal resistances and in turn voltage losses.[46] Another possibility for scaling up in modules is the use of flat plate designs. However, in comparison flat plate designs do not easily accommodate different electrode areas/sizes for the anode and the cathode, which can be disadvantageous, if one reaction, such as at the cathode, is more limiting than the other. Another issue with flat plate designs is that increasing the membrane area is limited by the pressure exerted on both sides of the membrane, as larger areas are more susceptible to deformations resulting from pressure.[47] All in all, the geometrical robustness of a cylindrical membrane is a major advantage over a flat design, when scaling up.

Oxygen as a possible additional revenue

The line-up at the anode side consists of an O_2 stripping unit, which in this work for simplicity consisted of an unit, where N_2 was sparged through. However, for the larger scale it might be interesting to look at other ways of stripping O_2, such as a vacuum filter or a gas/liquid membrane, allowing for the separation of O_2 at higher content in the gas phase. This gas stream rich in O_2 can then be used, as an extra revenue for oxygen demanding processes, such as combustion processes, metal manufacturing or health care, depending upon the requirement for O_2 purity.

Future research: Overcoming current limitations

There are two main limitations that still need to be overcome at the end of this thesis. The first, being increasing the voltage efficiency of the scale up design to values close to the ones obtained in the lab scale. The second being improving biological activity at haloalkaline electrolyte in order to achieve rates comparable to industrial biomethanation process (100 times higher).

Tackling voltage losses in a scale up design

In the scale up BES the voltage losses across the membrane - both ionic and transport - were greater than those in the lab scale. Reducing the distance between electrodes including the distance between the anode current collector and the membrane and the distance between the cathode current collector and the membrane could greatly reduce these voltage losses across the membrane. Therefore, decreasing the diameter of the tubular membrane to have a closer fit around the anode electrode and decreasing the depth of the GAC bed (distance between current collector and the membrane) is essential to tackle these losses. In contrast, the reactor height could be increased in order to maintain similar operational volume.

In Chapter 5 it was observed that local conditions changed more with depth of the GAC bed rather than height and evidence suggests that biological activity is not homogeneously distributed throughout the depth. Thus, it is hypothesised that decreasing the GAC bed will also have a positive impact on biological activity normalised by volume. However, it has been discussed previously that further experiments are needed to test this hypothesis. In addition, it is not known either up to which reactor height are conditions unchanged, since this was only explored in the lab scale. Therefore, the impact that decreasing the GAC bed will have on biological activity remains purely hypothetical and further research on the local conditions of the scale up BES is needed in order to avoid limitations in depth and height.

Strategies to enhance biological activity at haloalkaline conditions

The methane production rates of the scale up BES are still low in comparison to other scale up attempts,[48] and to conventional biomethanation processes. Moreover, the rates achieved with the haloalkaline electrolyte are lower than those reached under standard electrolyte in this thesis. Therefore, the need remains to explore other strategies to develop a biocathode and enhance biological activity at haloalkaline conditions.

The gradual increase in conductivity in the scale up study (Chapter 4) resulted in larger methane-production rates up to 280 NL m^{-3}_{BES} d^{-1} in comparison to the drastic shift from standard to haloalkaline electrolyte in the lab scale (Chapter 3) resulting in 120 NL m^{-3}_{BES} d^{-1}. Nevertheless, the strategy to gradual increase conductivity could still use some further

fine tuning, since the resulting rates are still lower than with the standard electrolyte and industrial biomethanation.

Electrochaea GmbH - an example of industrial biomethanation with high rates - operates using a pure (/enriched) culture methanogens. The use of pure cultures could be more suited to specific conditions, such as high salt and high pH in the haloalkaline electrolyte. However, the question remains, if such culture can be found and, if so, if it can reach high rates of methane production. Moreover, pure culture processes do not have the resilience that mixed culture processes offer. For example, resiliency towards possible oxygen contamination at the biocathode, due to diffusion across the membrane,[49] or pH drop, due to uneven flows/recirculation. Therefore, in this thesis a mixed culture inocula extracted from an anaerobic reactor of a waste water treatment plant was used. One possible strategy could be the pre-acclimation of the mixed cultures to the haloalkaline electrolyte, before inoculation of the BES. Evidence supports the adaptability of methanogenic mixed cultures present in anaerobic digestion reactors to increasing salt concentrations.[50] However, adaptation usually takes time. Alternatively, inoculating with mixed cultures from anaerobic digestion processes running at elevated salinity,[50] or from saline and alkaline natural environments, such as marine sediments,[51] or soda lakes,[52] could yield better results, when starting up and operating with haloalkaline electrolyte.

Last, a few other process conditions can still be optimised in order to promote biological growth and activity. First, addition of specific elements required for growth at high salinity, such as osmotic stress regulators (e.g. osmolytes),[26] or nutrients. Second, slightly higher temperatures, such as 35°C (in this thesis 25°C and 30°C), usually lead to higher biological activity in biomethanation processes.[27] Third, already mentioned above, decreasing the depth of the GAC bed might avoid the formation of H_2, pH and ORP gradients observed in Chapter 5. This might enhance the biological activity normalised by volume of the GAC bed.

The bigger picture: CO_2 valorisation

The decarbonisation, as a strategy to beat global warming, not only depends on an extreme cutback on dependency of fossil fuels but also on the effective use of CO_2, as a replacement for these fossil fuels.[53] As long as CO_2 rich streams are readily available this can be obtained but once these are not there will be the need to capture CO_2 from air, so called direct air capture (DAC).[54] One of the most common DAC processes uses alkaline solutions to dissolve CO_2 from air. However, the regeneration of this solution tends to be the biggest energy expenditure.[55] A possibly interesting next step would be the integration of DAC with CO_2 (bio)conversion processes. Here again the operation at haloalkaline conditions may be attractive, due to its advantages in dissolving CO_2.

Methane is currently one key product of CO_2 but there are many other platform molecules needed for a sustainable CO_2 neutral society now and in the future.[53] Luckily, there are

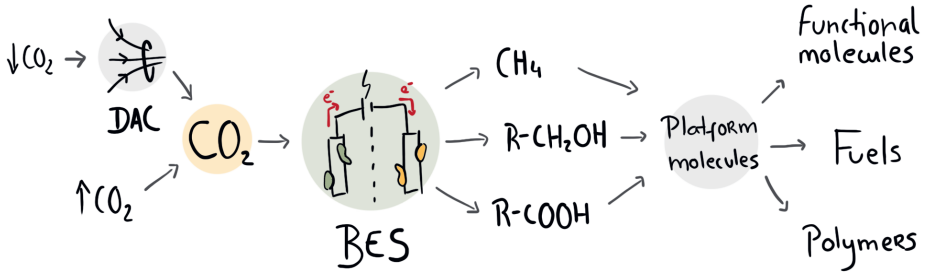

Figure 6.4: Schematic representation of the contribution of BES for future CO_2 valorisation (inspired by Vogt and Weckhuysen [53]).

a variety of opportunities for converting CO_2 into useful products including BESs (see figure 6.4). CO_2 reducing BESs have been shown to produce volatile fatty acids, longer chain fatty acids and alcohols, as well as methane.[56, 57] Due to the diversity in nature of microorganisms, BES might also play an important role in other future CO_2 conversion processes such as the production of biodiesel and bioplastics.[58] Moreover, BESs allow the inter conversion between products and electricity. This can support the transition from linear to circular energy systems by providing electricity storage in the form of conversion processes when there is an electricity surplus, and vice versa, when there is a shortage of electricity. With this said, the research done in this thesis including the limitations and scale up design of bioelectrochemical systems using granular activated carbon as the electrode material, can contribute to future CO_2 valorisation processes.

References

[1] P. Batlle-Vilanova, S. Puig, R. Gonzalez-Olmos, A. Vilajeliu-Pons, M. D. Balaguer, and J. Colprim. "Deciphering the electron transfer mechanisms for biogas upgrading to biomethane within a mixed culture biocathode". *RSC advances* 5.64 (2015), 52243–52251.

[2] Z. Mao, S. Cheng, Y. Sun, Z. Lin, L. Li, and Z. Yu. "Enhancing stability and resilience of electromethanogenesis system by acclimating biocathode with intermittent step-up voltage". *Bioresource Technology* 337 (2021), 125376.

[3] M. C. van Eerten-Jansen, N. C. Jansen, C. M. Plugge, V. de Wilde, C. J. Buisman, and A. ter Heijne. "Analysis of the mechanisms of bioelectrochemical methane production by mixed cultures". *Journal of Chemical Technology & Biotechnology* 90.5 (2015), 963–970.

[4] M. Villano, F. Aulenta, C. Ciucci, T. Ferri, A. Giuliano, and M. Majone. "Bioelectrochemical reduction of CO2 to CH4 via direct and indirect extracellular electron transfer by a hydrogenophilic methanogenic culture". *Bioresource technology* 101.9 (2010), 3085–3090.

[5] G. Zhen, T. Kobayashi, X. Lu, and K. Xu. "Understanding methane bioelectrosynthesis from carbon dioxide in a two-chamber microbial electrolysis cells (MECs) containing a carbon biocathode". *Bioresource technology* 186 (2015), 141–148.

[6] D. Liu, M. Roca-Puigros, F. Geppert, L. Caizán-Juanarena, S. P. Na Ayudthaya, C. Buisman, and A. Ter Heijne. "Granular carbon-based electrodes as cathodes in methane-producing bioelectrochemical systems". *Frontiers in bioengineering and biotechnology* 6 (2018), 78.

[7] G. Baek, R. Rossi, P. E. Saikaly, and B. E. Logan. "High-rate microbial electrosynthesis using a zero-gap flow cell and vapor-fed anode design". *Water Research* 219 (2022), 118597.

[8] R. Rad, T. Gehring, K. Pellumbi, D. Siegmund, E. Nettmann, M. Wichern, and U.-P. Apfel. "A hybrid bioelectrochemical system coupling a zero-gap cell and a methanogenic reactor for carbon dioxide reduction using a wastewater-derived catholyte". *Cell Reports Physical Science* 4.8 (2023).

[9] W. Cai, K. Cui, Z. Liu, X. Jin, Q. Chen, K. Guo, and Y. Wang. "An electrolytic-hydrogen-fed moving bed biofilm reactor for efficient microbial electrosynthesis of methane from CO2". *Chemical Engineering Journal* 428 (2022), 132093.

[10] A. Prévoteau, J. M. Carvajal-Arroyo, R. Ganigué, and K. Rabaey. "Microbial electrosynthesis from CO2: forever a promise?" *Current opinion in biotechnology* 62 (2020), 48–57.

[11] T. H. Sleutels, H. V. Hamelers, R. A. Rozendal, and C. J. Buisman. "Ion transport resistance in microbial electrolysis cells with anion and cation exchange membranes". *International Journal of Hydrogen Energy* 34.9 (2009), 3612–3620.

[12] F. Kracke, J. S. Deutzmann, B. S. Jayathilake, S. H. Pang, S. Chandrasekaran, S. E. Baker, and A. M. Spormann. "Efficient hydrogen delivery for microbial electrosynthesis via 3D-printed cathodes". *Frontiers in Microbiology* 12 (2021), 696473.

[13] M. Sun, B. Liu, K. Yanagawa, N. T. Ha, R. Goel, M. Terashima, and H. Yasui. "Effects of low pH conditions on decay of methanogenic biomass". *Water research* 179 (2020), 115883.

[14] J. Pereira, S. De Nooy, T. Sleutels, and A. Ter Heijne. "Opportunities for visual techniques to determine characteristics and limitations of electro-active biofilms". *Biotechnology Advances* 60 (2022), 108011.

[15] R. Karthikeyan, R. Singh, and A. Bose. "Microbial electron uptake in microbial electrosynthesis: a mini-review". *Journal of Industrial Microbiology and Biotechnology* 46.9-10 (2019), 1419–1426.

[16] F. Geppert, D. Liu, M. van Eerten-Jansen, E. Weidner, C. Buisman, and A. Ter Heijne. "Bioelectrochemical power-to-gas: state of the art and future perspectives". *Trends in biotechnology* 34.11 (2016), 879–894.

[17] Y. Bai, L. Zhou, M. Irfan, T.-T. Liang, L. Cheng, Y.-F. Liu, J.-F. Liu, S.-Z. Yang, W. Sand, J.-D. Gu, et al. "Bioelectrochemical methane production from CO2 by Methanosarcina barkeri via direct and H2-mediated indirect electron transfer". *Energy* 210 (2020), 118445.

[18] P. F. Beese-Vasbender, J.-P. Grote, J. Garrelfs, M. Stratmann, and K. J. Mayrhofer. "Selective microbial electrosynthesis of methane by a pure culture of a marine lithoautotrophic archaeon". *Bioelectrochemistry* 102 (2015), 50–55.

[19] S. Cheng, D. Xing, D. F. Call, and B. E. Logan. "Direct biological conversion of electrical current into methane by electromethanogenesis". *Environmental science & technology* 43.10 (2009), 3953–3958.

[20] F. Karadagli and B. E. Rittmann. "Thermodynamic and kinetic analysis of the H 2 threshold for Methanobacterium bryantii MoH". *Biodegradation* 18 (2007), 439–452.

[21] J. Philips. "Extracellular electron uptake by acetogenic bacteria: does H2 consumption favor the H2 evolution reaction on a cathode or metallic iron?" *Frontiers in Microbiology* 10 (2020), 483184.

[22] A.-E. Rotaru, P. M. Shrestha, F. Liu, M. Shrestha, D. Shrestha, M. Embree, K. Zengler, C. Wardman, K. P. Nevin, and D. R. Lovley. "A new model for electron flow during anaerobic digestion: direct interspecies electron transfer to Methanosaeta for the reduction of carbon dioxide to methane". *Energy & Environmental Science* 7.1 (2014), 408–415.

[23] D. J. Walker, K. P. Nevin, D. E. Holmes, A.-E. Rotaru, J. E. Ward, T. L. Woodard, J. Zhu, T. Ueki, S. S. Nonnenmann, M. J. McInerney, et al. "Syntrophus conductive pili demonstrate that common hydrogen-donating syntrophs can have a direct electron transfer option". *The ISME journal* 14.3 (2020), 837–846.

[24] M. O. Yee and A.-E. Rotaru. "Extracellular electron uptake in Methanosarcinales is independent of multiheme c-type cytochromes". *Scientific reports* 10.1 (2020), 372.

[25] S. Zheng, F. Liu, B. Wang, Y. Zhang, and D. R. Lovley. "Methanobacterium capable of direct interspecies electron transfer". *Environmental Science & Technology* 54.23 (2020), 15347–15354.

[26] D. Sudmalis, S. Millah, M. Gagliano, C. Butré, C. Plugge, H. Rijnaarts, G. Zeeman, and H. Temmink. "The potential of osmolytes and their precursors to alleviate osmotic stress of anaerobic granular sludge." *Water research* 147 (2018), 142–151.

[27] A. Thapa, H. Jo, U. Han, and S.-K. Cho. "Ex-situ biomethanation for CO2 valorization: State of the art, recent advances, challenges, and future prospective". *Biotechnology Advances* (2023), 108218.

[28] S. Savvas, J. Donnelly, T. Patterson, Z. S. Chong, and S. R. Esteves. "Biological methanation of CO2 in a novel biofilm plug-flow reactor: A high rate and low parasitic energy process". *Applied Energy* 202 (2017), 238–247.

[29] M. Voelklein, D. Rusmanis, and J. Murphy. "Biological methanation: Strategies for in-situ and ex-situ upgrading in anaerobic digestion". *Applied Energy* 235 (2019), 1061–1071.

[30] L. Laguillaumie, Y. Rafrafi, E. Moya-Leclair, D. Delagnes, S. Dubos, M. Spérandio, E. Paul, and C. Dumas. "Stability of ex situ biological methanation of H2/CO2 with a mixed microbial culture in a pilot scale bubble column reactor". *Bioresource Technology* 354 (2022), 127180.

[31] D. Strübing, B. Huber, M. Lebuhn, J. E. Drewes, and K. Koch. "High performance biological methanation in a thermophilic anaerobic trickle bed reactor". *Bioresource technology* 245 (2017), 1176–1183.

[32] Y. Rafrafi, L. Laguillaumie, and C. Dumas. "Biological methanation of H 2 and CO 2 with mixed cultures: current advances, hurdles and challenges". *Waste and Biomass Valorization* 12 (2021), 5259–5282.

[33] R. Lin, J. Cheng, J. Zhang, J. Zhou, K. Cen, and J. D. Murphy. "Boosting biomethane yield and production rate with graphene: The potential of direct interspecies electron transfer in anaerobic digestion". *Bioresource technology* 239 (2017), 345–352.

[34] Z. Zhao, Y. Li, Y. Zhang, and D. R. Lovley. "Sparking anaerobic digestion: promoting direct interspecies electron transfer to enhance methane production". *Iscience* 23.12 (2020).

[35] Z. Wang, T. Wang, B. Si, J. Watson, and Y. Zhang. "Accelerating anaerobic digestion for methane production: Potential role of direct interspecies electron transfer". *Renewable and Sustainable Energy Reviews* 145 (2021), 111069.

[36] C. Cruz Viggi, S. Rossetti, S. Fazi, P. Paiano, M. Majone, and F. Aulenta. "Magnetite particles triggering a faster and more robust syntrophic pathway of methanogenic propionate degradation". *Environmental science & technology* 48.13 (2014), 7536–7543.

[37] Electrochaea. *Data Sheet of Applications of Electrochaea's BioCat biomethanation technology*. 2021. (Visited on 2024).

[38] L. Xiao, J. Liu, P. S. Kumar, M. Zhou, J. Yu, and E. Lichtfouse. "Enhanced methane production by granular activated carbon: A review". *Fuel* 320 (2022), 123903.

[39] C. Lu, H. Bai, B. Wu, F. Su, and J. F. Hwang. "Comparative study of CO2 capture by carbon nanotubes, activated carbons, and zeolites". *Energy & Fuels* 22.5 (2008), 3050–3056.

[40] A. Deeke, T. H. Sleutels, T. F. Donkers, H. V. Hamelers, C. J. Buisman, and A. Ter Heijne. "Fluidized capacitive bioanode as a novel reactor concept for the microbial fuel cell". *Environmental science & technology* 49.3 (2015), 1929–1935.

[41] J.-Y. Lee, S.-H. Lee, and H.-D. Park. "Enrichment of specific electro-active microorganisms and enhancement of methane production by adding granular activated carbon in anaerobic reactors". *Bioresource technology* 205 (2016), 205–212.

[42] C. Borsje, D. Liu, T. H. Sleutels, C. J. Buisman, and A. ter Heijne. "Performance of single carbon granules as perspective for larger scale capacitive bioanodes". *Journal of Power Sources* 325 (2016), 690–696.

[43] A. I. Adnan, M. Y. Ong, S. Nomanbhay, K. W. Chew, and P. L. Show. "Technologies for biogas upgrading to biomethane: A review". *Bioengineering* 6.4 (2019), 92.

[44] R. de Rink, J. B. Klok, G. J. van Heeringen, K. J. Keesman, A. J. Janssen, A. Ter Heijne, and C. J. Buisman. "Biologically enhanced hydrogen sulfide absorption from sour gas under haloalkaline conditions". *Journal of hazardous materials* 383 (2020), 121104.

[45] R. de Rink, S. Gupta, F. P. de Carolis, D. Liu, A. ter Heijne, J. B. Klok, and C. J. Buisman. "Effect of process conditions on the performance of a dual-reactor biodesulfurization process". *Journal of Environmental Chemical Engineering* 9.6 (2021), 106450.

[46] R. M. Alonso, M. I. San-Martín, R. Mateos, A. Morán, and A. Escapa. "Scale-up of bioelectrochemical systems for energy valorization of waste streams". In: *Microbial Electrochemical Technologies*. CRC Press, 2020, 447–459.

[47] G. Battaglia, L. Gurreri, G. Airò Farulla, A. Cipollina, A. Pirrotta, G. Micale, and M. Ciofalo. "Membrane deformation and its effects on flow and mass transfer in

the electromembrane processes". *International Journal of Molecular Sciences* 20.8 (2019), 1840.

[48] G. Shang, K. Cui, W. Cai, X. Hu, P. Jin, and K. Guo. "A 20 L electrochemical continuous stirred-tank reactor for high rate microbial electrosynthesis of methane from CO2". *Chemical Engineering Journal* 451 (2023), 138898.

[49] M. Abdollahi, S. Al Sbei, M. A. Rosenbaum, and F. Harnisch. "The oxygen dilemma: the challenge of the anode reaction for microbial electrosynthesis from CO2". *Frontiers in Microbiology* 13 (2022), 947550.

[50] D. Sudmalis, M. Gagliano, R. Pei, K. Grolle, C. Plugge, H. Rijnaarts, G. Zeeman, and H. Temmink. "Fast anaerobic sludge granulation at elevated salinity". *Water research* 128 (2018), 293–303.

[51] M. F. Alqahtani, S. Bajracharya, K. P. Katuri, M. Ali, J. Xu, M. S. Alarawi, and P. E. Saikaly. "Enrichment of salt-tolerant CO2–fixing communities in microbial electrosynthesis systems using porous ceramic hollow tube wrapped with carbon cloth as cathode and for CO2 supply". *Science of the Total Environment* 766 (2021), 142668.

[52] D. Y. Sorokin, B. Abbas, M. Geleijnse, N. V. Pimenov, M. V. Sukhacheva, and M. C. van Loosdrecht. "Methanogenesis at extremely haloalkaline conditions in the soda lakes of Kulunda Steppe (Altai, Russia)". *FEMS microbiology ecology* 91.4 (2015), fiv016.

[53] E. T. Vogt and B. M. Weckhuysen. "The refinery of the future". *Nature* 629.8011 (2024), 295–306.

[54] X. Zhu, W. Xie, J. Wu, Y. Miao, C. Xiang, C. Chen, B. Ge, Z. Gan, F. Yang, M. Zhang, et al. "Recent advances in direct air capture by adsorption". *Chemical Society Reviews* 51.15 (2022), 6574–6651.

[55] Q. Shu, L. Legrand, P. Kuntke, M. Tedesco, and H. V. Hamelers. "Electrochemical regeneration of spent alkaline absorbent from direct air capture". *Environmental science & technology* 54.14 (2020), 8990–8998.

[56] B. Bian, S. Bajracharya, J. Xu, D. Pant, and P. E. Saikaly. "Microbial electrosynthesis from CO2: Challenges, opportunities and perspectives in the context of circular bioeconomy". *Bioresource technology* 302 (2020), 122863.

[57] D. Suri, L. M. Aeshala, and T. Palai. "Microbial electrosynthesis of valuable chemicals from the reduction of CO2: a review". *Environmental Science and Pollution Research* (2024), 1–24.

[58] A. Langsdorf, J. P. Schütz, R. Ulber, M. Stöckl, and D. Holtmann. "Production of polyhydroxybutyrate from industrial flue gas by microbial electrosynthesis". *Journal of CO2 Utilization* 83 (2024), 102800.

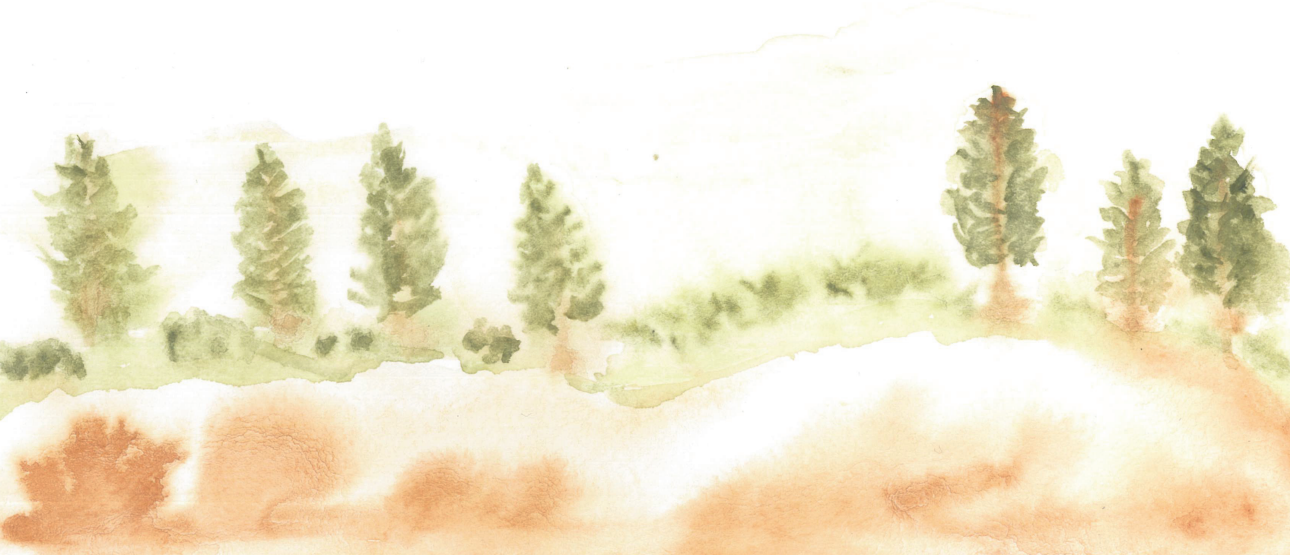

Summary

This thesis investigates bioelectrochemical systems (BESs) for the conversion of CO_2 and electricity to methane.

The alarming prospects of global warming are the main driving force for the decarbonisation of the energy sector. Decarbonisation of the energy sector means cutting down on the use of fossil fuel and increasing the integration of renewable energy sources for electricity supply. However, increasing the share of renewable electricity in the current energy system and infrastructure does not come without its hurdles - the main one being that there are occasional mismatches between the production of electricity (supply) and the demand on electricity by users (consumption), thus, the need for storage emerges. Because electricity can not be stored in its form, it has to be converted. Using bioelectrochemical systems for the conversion of CO_2 and electricity into methane are a promising electricity storage technology, storing electrical energy in a chemical carrier, methane, which is also referred to as power-to-methane. Among others, the main advantage of methane as a chemical carrier is that it can be promptly transported, stored and consumed due to the existing gas pipelines and infrastructure.

Methane producing BESs are still in the development stage and most efforts have focused on improving methane production rates. Nevertheless, in order to fully assess the performance of methane producing BESs the energy efficiency of the system should be investigated and improved, as well as methane production rates. The energy efficiency of a BES is dependant on faradaic efficiency and voltage efficiency. The former, faradaic efficiency, is usually not a limiting factor in methane producing BESs, as it easily reaches values around and above 90%. The latter, voltage efficiency, is usually under reported, and is a measurement of the voltages losses in the BES: 1) cathode overpotential, 2) anode overpotential, and 3) ion and transport losses. The goal in this thesis was to understand and tackle the limitations associated with these three losses with the overall aim of improving the performance of methane producing BESs in terms of energy efficiency.

Cathode overpotential is the excess voltage used for the reduction reaction to occur in comparison to that theoretically expected. In literature on methane producing BESs the lowest cathode overpotential was observed, when using granular activated carbon (GAC) as the electrode material. Therefore, this was the cathode electrode of choice

throughout the thesis. Moreover, the aim in **Chapter 2** was to investigate the role of the control strategy (fixed current density) and the GAC electron storage capacity on the resulting low cathode overpotential. Eight reactors were operated to do so; four reactors were controlled at -5 A m^{-2} and four at -10 A m^{-2}. Additionally, the electrode storage capacity was evaluated by conducting weekly charge/discharge tests on two of each set of four reactors. Results showed that, first, by controlling current density the cathode potential of methane producing BES increases over time, starting at around -0.90 V vs. Ag/AgCl and increasing up to as high as -0.52 V vs. Ag/AgCl. The lowest overpotential observed in literature as expected. Second, the resulting low cathode overpotential is both dependent on applied current density and employment (or not) of charge/discharge tests. Reactors at -10 A m^{-2} without charge/discharge regimes did not result in increasing cathode potential, whereas reactors at -5 A m^{-2} and at -10 A m^{-2} with charge/discharge regimes did. Therefore, suggesting that the chosen control strategy is crucial in order to reach low cathode overpotential. Third, results show that when the CO_2 supply is cut the resulting cathode potential decreases back to values close to -0.90 V. Suggesting that the low overpotentials are associated with the consumption of CO_2, whereas high overpotentials are independent of the presence/consumption of CO_2.

With a better understanding of how to achieve low cathode overpotential in **Chapter 3** the focus shifted towards improving anode overpotential and ion and transport losses. In a first stage, the operation with GAC, as cathode material, was combined with the use of a state-of-the-art electrode for water splitting at the anode an Iridium-Ruthenium coated Titanium electrode. This, in addition to slight improvements in the reactor configuration (in comparison to Chapter 2) led to an energy efficiency of 50% with resulting cell voltage -2.2 V, in comparison to 21% in Chapter 2. In a second stage, the aim was to reduce ion and transport losses over the membrane. Therefore, the electrolyte used in the first stage, standard 0.05 M phosphate electrolyte, was switched to a haloalkaline electrolyte, 0.6 M to 1 M bicarbonate electrolyte. In this second stage, an unprecedented energy efficiency up to 70% was reached with the resulting cell voltage at -1.4 V in comparison to the maximum reported in literature of 40%. Moreover, in this work, the two methane producing BESs were operated for 380 and 590 days at relatively stable performances with energy efficiencies above 40% for the majority of the operations. Thus, displaying testimony of the robustness of the technology. Nevertheless, lower methane production rates had to be set at haloalkaline electrolyte, 11 NL m^{-2}_{CC} d^{-1}, in contrast to 40 NL m^{-2}_{CC} d^{-1} at standard electrolyte, in order to keep low cathode overpotential. Therefore, suggesting that the microorganisms were not able to fully adapt to the abrupt change from standard to haloalkaline electrolyte.

One other crucial bottleneck in the development of bioelectrochemical systems in general is that the performance in the lab scale is usually difficult to mimic on a larger scale. Issues that commonly arise from scaling up BES are: 1) keeping the ratio between electrode surface area available for conversion and volume; 2) increasing voltage losses due to increasing

distances between electrodes; and 3) expensive electrode materials, because bigger versions are not commercially available. With these three issues in mind, in **Chapter 4**, a scale up BES for power-to-gas application was designed with its main features being: 1) use of GAC as cathode material to maintain large surface areas normalised by volume, 2) a design that can be further scaled up in modules to avoid increasing distances, and 3) materials which are relatively low cost and/or commercially available. The built scale up methane producing BES was operated for 470 days and its performance was assessed and compared to the lab scale reactors. Furthermore, the electrolyte was changed from standard to 0.6 M haloalkaline electrolyte in a step wise approach in contrast to the previous chapter (Chapter 3), in an attempt to aid the adaptation of microorganisms to the changing electrolyte. As a result, at 0.6 M haloalkaline electrolyte first the voltage ranged around -2.60 V in contrast to -1.70 V in the lab scale, and second methane production rates up to 280 NL m^{-3}_{BES} d^{-1} were observed in contrast to a maximum of 109 NL m^{-3}_{BES} d^{-1} in the lab scale. The main contributor to the larger voltage (1) in the scales up BES was larger ionic transport losses across the membrane. It is suggested that this can be improved by decreasing the distance between electrodes. The larger methane production rates (2) in the scale up suggest that the gradual increase in salinity is a better strategy than a quick shift

The dominant challenge across the previous research chapters remained the trade off between rates and energy efficiency. In addition, not much is known about the local conditions present in the GAC bed of methane producing biocathodes. Observing local conditions can give better insights on possible existing limitations. Knowing the limitations can help change process conditions or reactor configurations to simultaneously improve rates and efficiency, thus avoiding a trade off. With this in mind, in **Chapter 5** local measurements of H_2, pH and ORP within the GAC bed of methane producing biocathodes were conducted. Results showed that H_2 was detected locally at cathode potentials of -0.63 V (vs Ag/AgCl), whereas no H_2 was detected in the outlet gas at the same point in time, which indicates biological H_2 uptake at this potential. Moreover, it was identified that there are gradients in all three parameters, H_2, pH and ORP, with increasing depth away from the current collector and towards the membrane. H_2 concentration and pH increased and ORP became more negative the further away from the current collector. Overall, the results suggest that rates of H_2 production are higher towards the membrane but the question remains whether the rates of biological conversion of CO_2 to methane follow a similar pattern. To answer this, it is suggested that future research investigates the distribution and activity of microorganisms at the cathode surface.

Overall, although promising results regarding energy efficiency have been achieved in this thesis, the methane production rates remain quite low; namely, up to 19 L m^{-3}_{BES} h^{-1} (Chapter 2), in comparison to biological conversion of CO_2 and H_2 to methane on an industrial scale, 14 x 10^3 L $m^{-3}_{reactor}$ h^{-1} (Electrochaea GmbH). In **Chapter 6** possible future research directions are discussed in order to improve methane production rates at

haloalkaline electrolyte. The main focus would be on 1) improving biological activity at haloalkaline conditions by, for example, using inocula from halophilic environments, and on 2) increasing the knowledge about the local conditions that form at the biocathode, when operating at haloalkaline electrolyte, and the toll they have on the diversity and activity of the microorganisms. Finally, the advantages of specific design rules for the bio-electrochemical system in this thesis, such as the use of GAC and operation at haloalkaline electrolyte, are discussed in the broader context of CO_2 utilisation.

Sumário

Esta tese investiga sistemas bioelectroquímicos (SBEs) para a conversão de CO_2 e eletricidade em metano.

As perspetivas alarmantes do aquecimento global são a principal força para a descarbonização do setor energético. A descarbonização do setor energético implica a redução do uso de combustíveis fósseis e o aumento da integração de fontes de energia renováveis para fornecer eletricidade. No entanto, a presença de energia renovável no sistema energético atual, incluindo a infraestrutura, vem com obstáculos - o principal sendo que há, ocasionalmente, discrepâncias entre a produção de eletricidade (oferta) e a procura de eletricidade pelos utilizadores (consumo), surgindo assim a necessidade de armazenamento. Como a eletricidade não pode ser armazenada na sua forma, tem de ser convertida. Utilizar sistemas bioeletroquímicos para a conversão de CO_2 e eletricidade em metano é uma tecnologia promissora para o armazenamento de eletricidade, convertendo a energia elétrica num produto químico, o metano, processo que também é referido como "power-to-methane". Entre outros, a principal vantagem do metano como produto químico é que pode ser prontamente transportado, armazenado e consumido devido aos gasodutos e outra infraestrutura existente.

Os SBEs produtores de metano ainda estão em fase de desenvolvimento e a maioria dos esforços tem-se concentrado em melhorar as taxas de produção de metano. No entanto, para avaliar plenamente o desempenho dos SBEs produtores de metano, a eficiência energética do sistema deve ser investigada e melhorada, bem como as taxas de produção de metano. A eficiência energética de um SBE depende da eficiência faradaica e da eficiência de voltagem. A primeira, eficiência faradaica, geralmente não é um fator limitante nos SBEs produtores de metano, pois facilmente atinge valores em torno de 90% ou superiores. A segunda, eficiência de voltagem, é geralmente subnotificada, e é uma medida das perdas de voltagem no SBE: 1) sobrepotential do cátodo, 2) sobrepotential do ânodo e 3) perdas associadas a transporte e iões. O objetivo desta tese foi compreender e enfrentar as limitações associadas a estas três perdas, com o objetivo geral de melhorar o desempenho dos SBEs produtores de metano em termos de eficiência energética.

O sobrepotential do cátodo é a voltagem excedente utilizada para que ocorra a reação de redução, em comparação com a voltagem teoricamente esperada. Na literatura sobre SBEs

produtores de metano, menor sobrepotential do cátodo foi observada ao usar "granular activated carbon" (GAC) como material do eletrodo. Portanto, este foi o eletrodo de cátodo escolhido ao longo da tese. Além disso, o objetivo no **Capítulo 2** foi investigar o papel da estratégia de controlo (densidade de corrente) e a capacidade de armazenamento de eletrões no GAC, no resultante reduzido sobrepotential do cátodo. Para isso, oito reatores foram operados; quatro reatores foram controlados a -5 A m^{-2} e outros quatro a -10 A m^{-2}. Adicionalmente, a capacidade de armazenamento do eletrodo foi avaliada realizando testes semanais de carga/descarga de eletrões em dois de cada conjunto de quatro reatores. Os resultados mostraram que, primeiro, ao controlar a densidade de corrente, o potencial do cátodo dos SBEs produtores de metano aumenta com o tempo, começando em cerca de -0,90 V vs. Ag/AgCl e aumentando até um máximo de -0,52 V vs. Ag/AgCl. O menor sobrepotential observada na literatura, conforme esperado. Segundo, o baixo sobrepotential do cátodo resultante depende tanto da densidade de corrente aplicada quanto da realização (ou não) dos testes de carga/descarga. Reatores a -10 A m^{-2} sem regimes de carga/descarga não resultaram em aumento do potencial do cátodo, enquanto reatores a -5 A m^{-2} e a -10 A m^{-2} com regimes de carga/descarga sim. Portanto, sugerindo que a estratégia de controlo escolhida é crucial para alcançar um baixo sobrepotential do cátodo. Terceiro, os resultados mostram que, quando o fornecimento de CO_2 é cortado, o potencial do cátodo resultante diminui novamente para valores próximos de -0,90 V. Sugerindo que as baixas sobretensões estão associadas ao consumo de CO_2, enquanto as altas sobretensões são independentes da presença/consumo de CO_2.

Com uma melhor compreensão de como alcançar um baixa sobrepotential do cátodo no **Capítulo 3**, o foco mudou para a melhoria do sobrepotential do ânodo e das perdas associadas ao transporte e iões. Numa primeira fase, a operação com GAC, como material de cátodo, foi combinada com o uso de um eletrodo de última geração para a oxidação água no ânodo, um eletrodo de Titânio revestido com Irídio-Ruténio. Isto, além de ligeiras melhorias na configuração do reator (em comparação com o Capítulo 2) levou a uma eficiência energética de 50% com uma voltagem da célula resultante de -2,2V, em comparação com 21% no Capítulo 2. Numa segunda fase, o objetivo foi reduzir as perdas de iões e de transporte na membrana. Portanto, o eletrólito utilizado na primeira fase, eletrólito padrão de fosfato 0,05M, foi substituído por um eletrólito haloalcalino, eletrólito bicarbonato de 0,6M a1 M. Nesta segunda fase, uma eficiência energética sem precedentes de até 70% foi alcançada, com uma voltagem da célula resultante de -1,4V, em comparação com o máximo reportado na literatura de 40%. Além disso, neste trabalho, os dois SBEs produtores de metano foram operados por 380 e 590 dias com desempenhos relativamente estáveis, com eficiências energéticas acima de 40% durante a maioria da operação. Assim, exibindo o testemunho da robustez da tecnologia. No entanto, taxas de produção de metano mais baixas tiveram de ser definidas no eletrólito haloalcalino, 11 NL $m^{-2}{}_{CC}$ d^{-1}, em contraste com 40 NL $m^{-2}{}_{CC}$ d^{-1} no eletrólito padrão, para manter um baixo sobrepotential no cátodo. Portanto, sugerindo que os microrganismos não foram capazes

de se adaptar completamente à mudança abrupta do eletrólito padrão para o eletrólito haloalcalino.

Outro obstáculo crucial no desenvolvimento de sistemas bioeletroquímicos em geral é que o desempenho em escala laboratorial geralmente é difícil de replicar numa escala maior. Problemas que normalmente surgem ao aumentar a escala dos SBEs são: 1) manter a proporção entre a área de superfície do eletrodo disponível para conversão e o volume; 2) aumento das perdas de voltagem devido ao aumento das distâncias entre os eletrodos; e 3) materiais caros para a construção de eletrodos, porque versões maiores não estão comercialmente disponíveis. Com estes três problemas em mente, no **Capítulo 4**, um SBE ampliado para aplicação "power-to-gas" foi projetado com as suas principais características sendo: 1) uso de GAC como material de cátodo para manter grandes áreas de superfície normalizadas por volume, 2) uma arquitetura que possa ser ampliada sucessivamente em módulos para evitar o aumento das distâncias entre eletropdos, e 3) materiais que são relativamente de baixo custo e/ou comercialmente disponíveis. O SBE produtor de metano ampliado foi operado por 470 dias e o seu desempenho foi avaliado e comparado com os reatores em escala laboratorial. Além disso, o eletrólito foi alterado de padrão para 0,6M de eletrólito haloalcalino numa abordagem gradual, em contraste com o capítulo anterior (Capítulo 3), numa tentativa de ajudar a adaptação dos microrganismos a mudança. Como resultado, a operação com 0,6M eletrólito haloalcalino, levou a uma voltagem variou de -2,60 V em contraste com -1,70 V em escala laboratorial. Adicionalmente, taxas de produção de metano até 280 NL m^{-3}_{SBE} d^{-1} foram observadas em contraste com um máximo de 109 NL m^{-3}_{SBE} d^{-1} em escala laboratorial. O principal contribuinte para a maior voltagem (1) no SBE ampliado foram maiores perdas de transporte iónico através da membrana. Sugere-se que isso pode ser melhorado diminuindo a distância entre os eletrodos. As maiores taxas de produção de metano (2) na escala ampliada sugerem que o aumento gradual na salinidade é uma melhor estratégia em comparação a uma mudança rápida.

O desafio que dominou os capítulos de pesquisa anteriores foi o compromisso entre as taxas de produção de metano e a eficiência energética. Além disso, pouco se sabe sobre as condições locais presentes no interior do eletrodo (GAC) de biocátodos. Observar as condições locais pode fornecer uma melhor perceção sobre possíveis limitações existentes. Conhecer as limitações pode ajudar a mudar as condições do processo ou as configurações do reator para melhorar simultaneamente as taxas e a eficiência, evitando assim um compromisso. Com isso em mente, no **Capítulo 5** foram realizadas medições locais de H_2, pH e ORP dentro do GAC compondo os biocátodos produtores de metano. Os resultados mostraram que o H_2 foi detetado localmente em potenciais de cátodo de -0,63 V (vs Ag/AgCl), enquanto que nenhum H_2 foi detetado na saída do reator, o que indica o consumo biológico de H_2 neste potencial. Além disso, foi identificado que existem gradientes em todos os três parâmetros, H_2, pH e ORP, com o aumento da profundidade afastando-se do coletor de corrente e em direção à membrana. A concentração de H_2 e o

pH aumentaram e o ORP tornou-se mais negativo à medida que se afastava do coletor de corrente. No geral, os resultados sugerem que as taxas de produção de H_2 são maiores em direção à membrana, mas permanece a questão se as taxas de conversão biológica de CO_2 em metano seguem um padrão semelhante. Para responder a isso, sugere-se que futuras pesquisas investiguem a distribuição e a atividade dos microrganismos na superfície do cátodo.

No geral, embora resultados promissores em termos de eficiência energética tenham sido alcançados nesta tese, as taxas de produção de metano permanecem bastante baixas; nomeadamente, até 19 L m^{-3}_{SBE} h^{-1} (Capítulo 2), em comparação com a conversão biológica de CO_2 e H_2 em metano em escala industrial, 14 x 10^3 L m^{-3}_{reator} h^{-1} (Electrochaea GmbH). No **Capítulo 6** são discutidas possíveis direções futuras de pesquisa para melhorar as taxas de produção de metano no eletrólito haloalcalino. O principal foco seria 1) melhorar a atividade biológica em condições haloalcalinas, por exemplo, usando inóculos de ambientes halofílicos, e 2) aumentar o conhecimento sobre as condições locais que se formam no biocátodo, quando operando em eletrólito haloalcalino, e o impacto que têm na diversidade e atividade dos microrganismos. Finalmente, as vantagens de regras de desenho específicas para o sistema bioeletroquímico nesta tese, como o uso de GAC e operação em eletrólito haloalcalino, são discutidas num contexto mais amplo de utilização de CO_2.

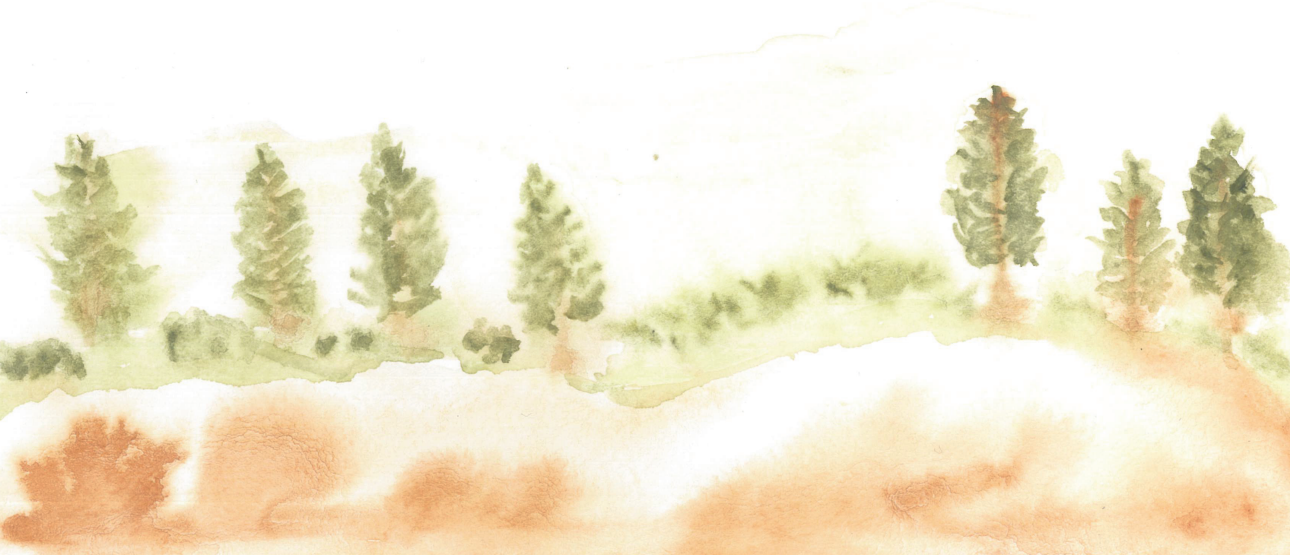

Supplementary Information

Supplementary Information Chapter 3

Operational and performance details of bioelectrochemical system B1 and B2

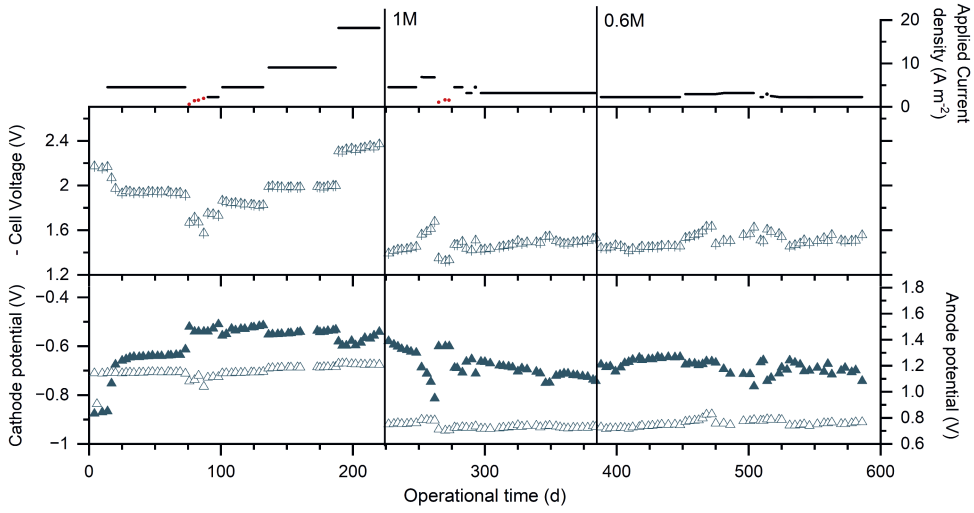

Figure 1: Plot of cell voltage (middle), cathode potential (full dark blue triangles, bottom) and anode potential (empty dark blue triangles, bottom), measured with a multimeter, throughout the operational time of B1. The control strategy, applied current density, is also plotted for reference (top). Vertical lines represent the change from standard electrolyte (0.05 M phosphate) to 1M carbonate/bicarbonate electrolyte and subsequently to 0.6M carbonate/bicarbonate electrolyte. Red dots represent operation at controlled cathode potential.

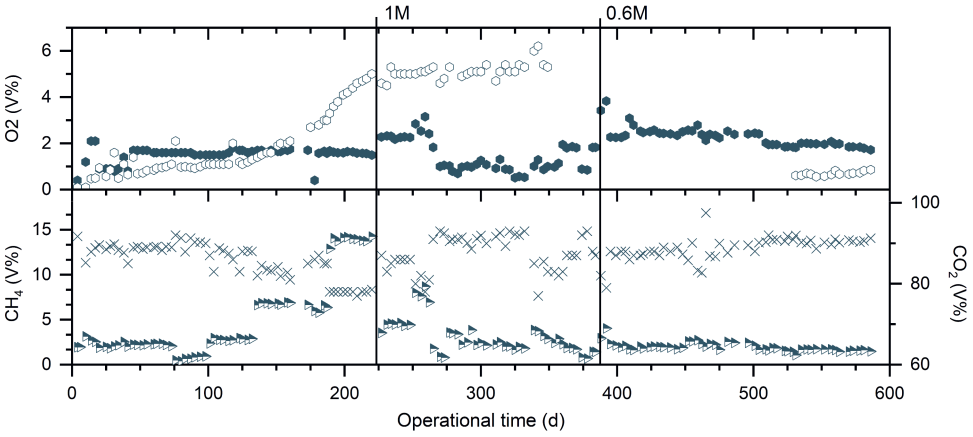

Figure 2: Plot of the oxygen (full dark blue hexagon, top), methane (half full dark blue triangles, bottom) and carbon dioxide (dark blue crosses, bottom) concentration (in V%) in the gas bag connected to the headspace of the catholyte recirculation chamber, and of the oxygen (empty dark blue hexagon, top) concentration (in V%) in the headspace of the anolyte recirculation chamber, throughout the operational time of B1. Vertical lines represent the change from standard electrolyte (0.05 M phosphate) to 1M carbonate/bicarbonate electrolyte and subsequently to 0.6M carbonate/bicarbonate electrolyte.

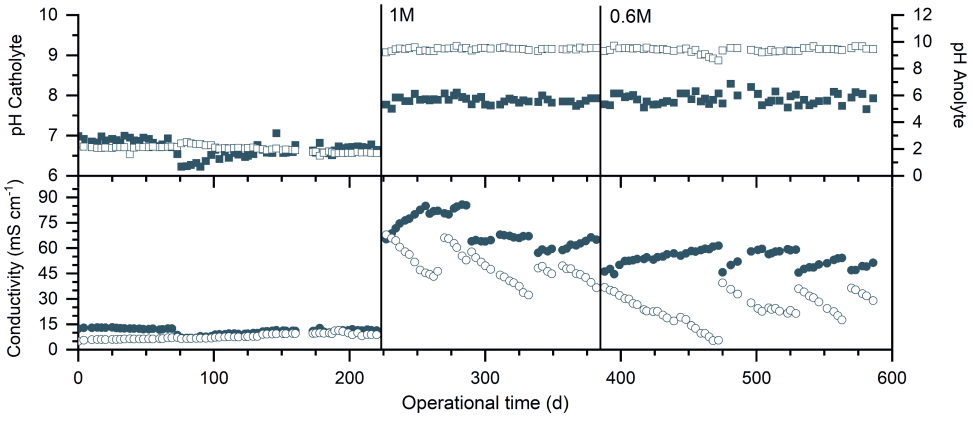

Figure 3: Plot of the pH (top) and conductivity (bottom) of the catholyte (full dark blue squares and circles, respectively) and anolyte (empty dark blue squares and circles, respectively) throughout the operational time of B1. Note that abrupt changes in conductivity are in line with replacement of the electrolyte. Vertical lines represent the change from standard electrolyte (0.05 M phosphate) to 1M carbonate/bicarbonate electrolyte and subsequently to 0.6M carbonate/bicarbonate electrolyte.

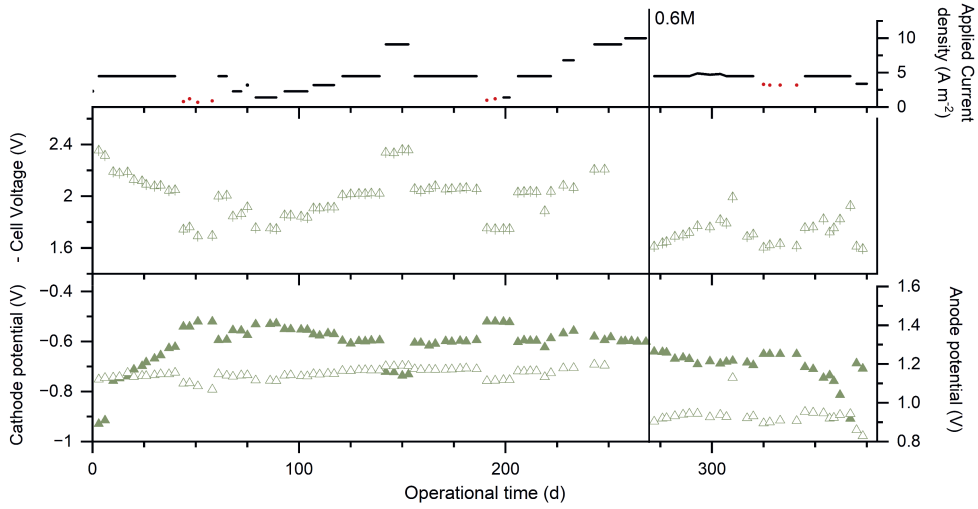

Figure 4: Plot of cell voltage (middle), cathode potential (full green triangles, bottom) and anode potential (empty green triangles, bottom), measured with a multimeter, throughout the operational time of B2. The control strategy, applied current density, is also plotted for reference (empty green hexagon, top). Vertical line represents the change from standard electrolyte (0.05 M phosphate) to 0.6M carbonate/bicarbonate electrolyte. Red dots represent operation at controlled cathode potential.

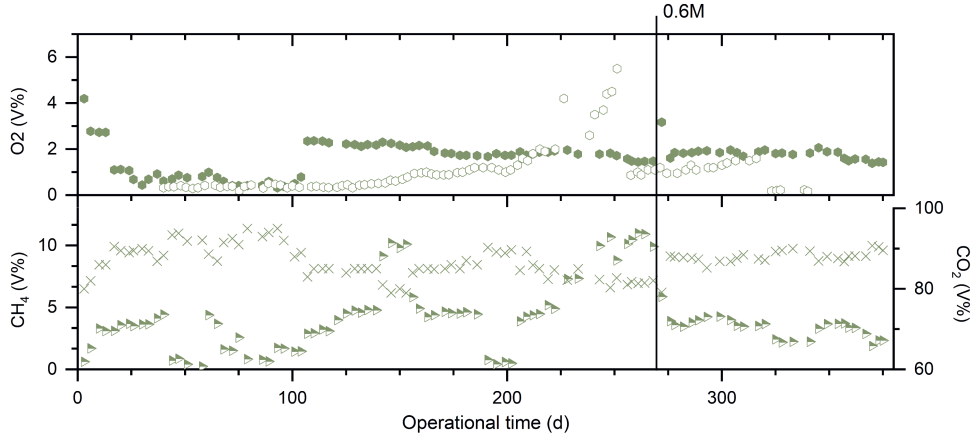

Figure 5: Plot of the oxygen (full green hexagon, top), methane (half full green triangles, bottom) and carbon dioxide (green crosses, bottom) concentration (in V%) in the gas bag connected to the headspace of the catholyte recirculation chamber, and of the oxygen (top) concentration (in V%) in the headspace of the anolyte recirculation chamber, throughout the operational time of B2. Vertical line represents the change from standard electrolyte (0.05 M phosphate) to 0.6M carbonate/bicarbonate electrolyte.

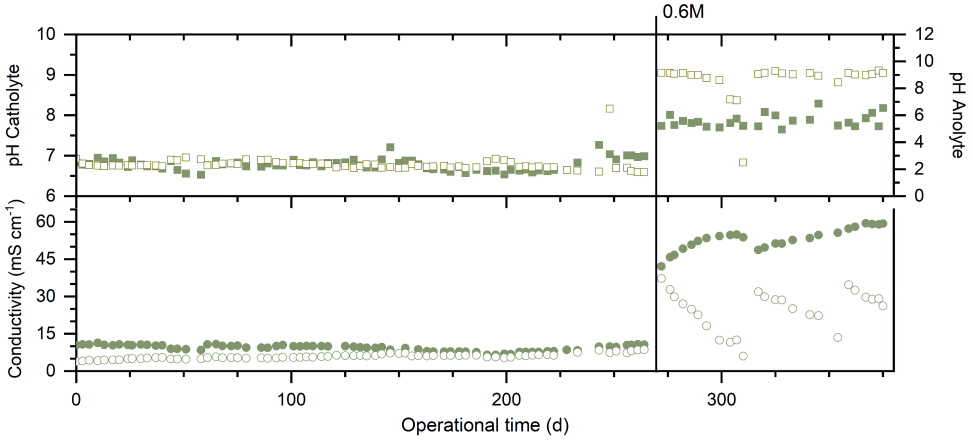

Figure 6: Plot of the pH (top) and conductivity (bottom) of the catholyte (full green squares and circles, respectively) and anolyte (empty green squares and circles, respectively) throughout the operational time of B1. Note that abrupt changes in conductivity are in line with replacement of the electrolyte. Vertical line represents the change from standard electrolyte (0.05 M phosphate) to 0.6M carbonate/bicarbonate electrolyte.

Scanning electron microscopy (SEM) pictures of methane producing biocathodes including scale and other details.

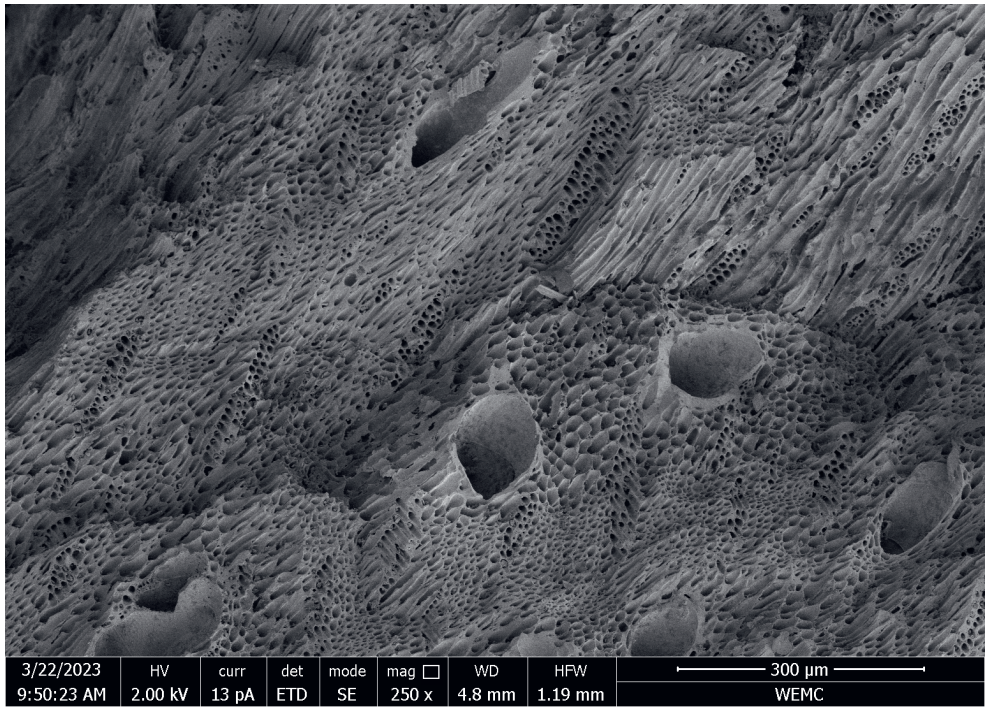

Figure 7: SEM picture taken of granular activated carbon collected from B2.

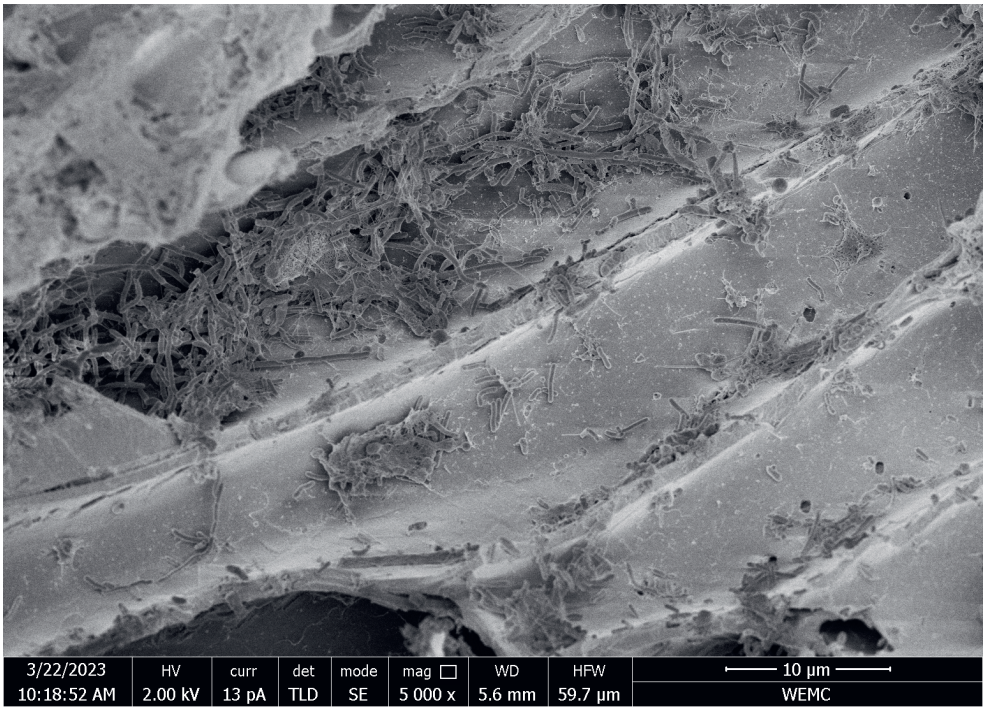

Figure 8: SEM picture taken of granular activated carbon collected from B2.

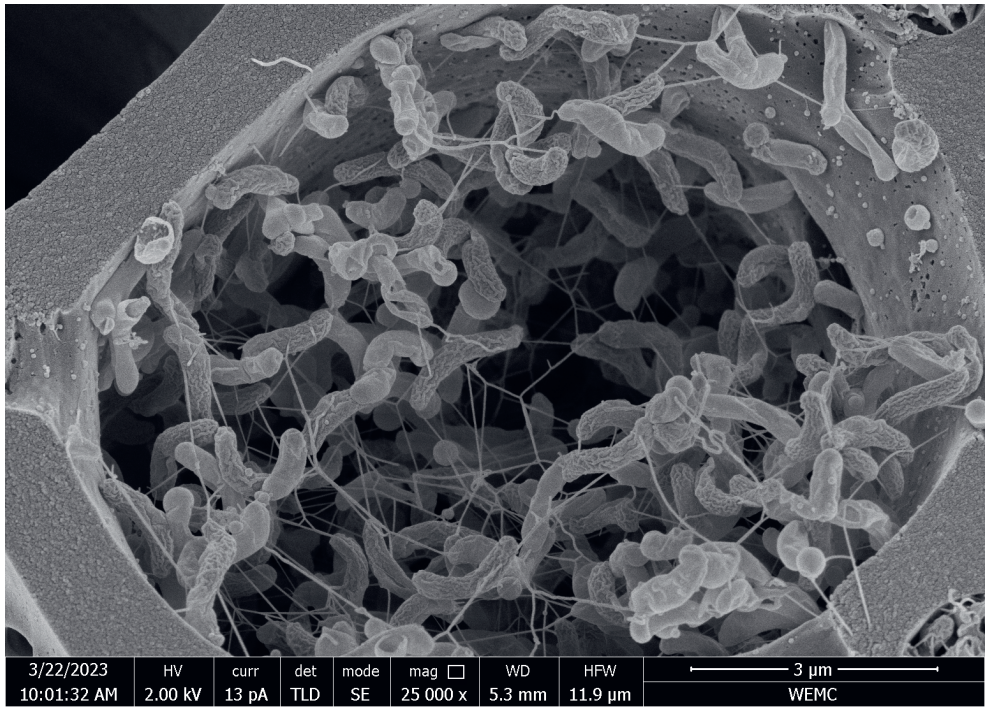

Figure 9: SEM picture taken of granular activated carbon collected from B2.

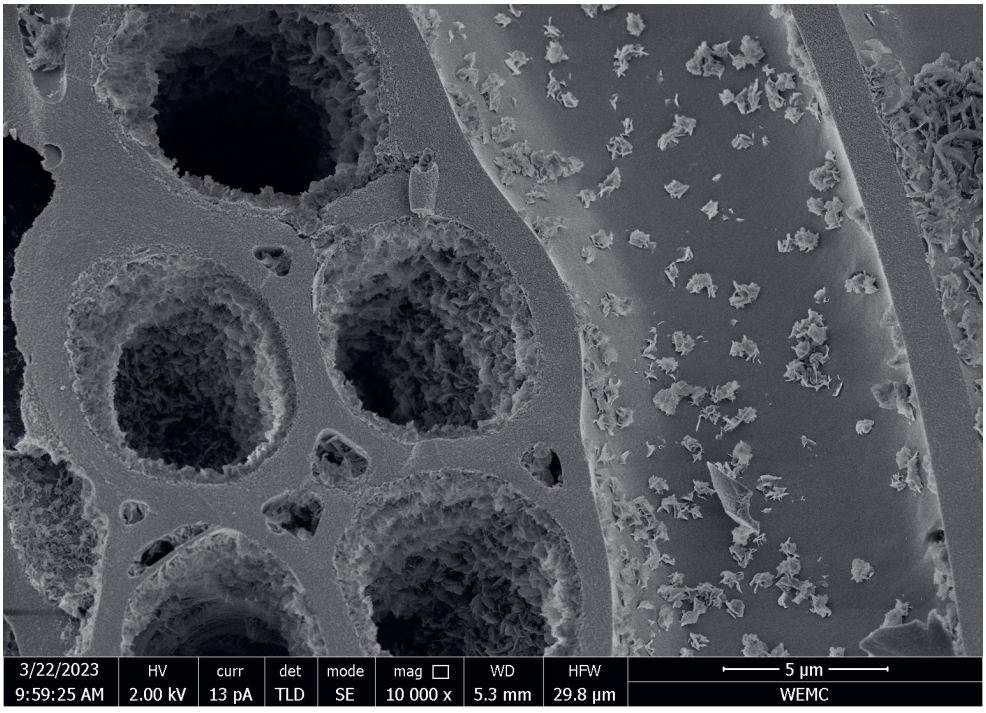

Figure 10: SEM picture taken of granular activated carbon collected from B2.

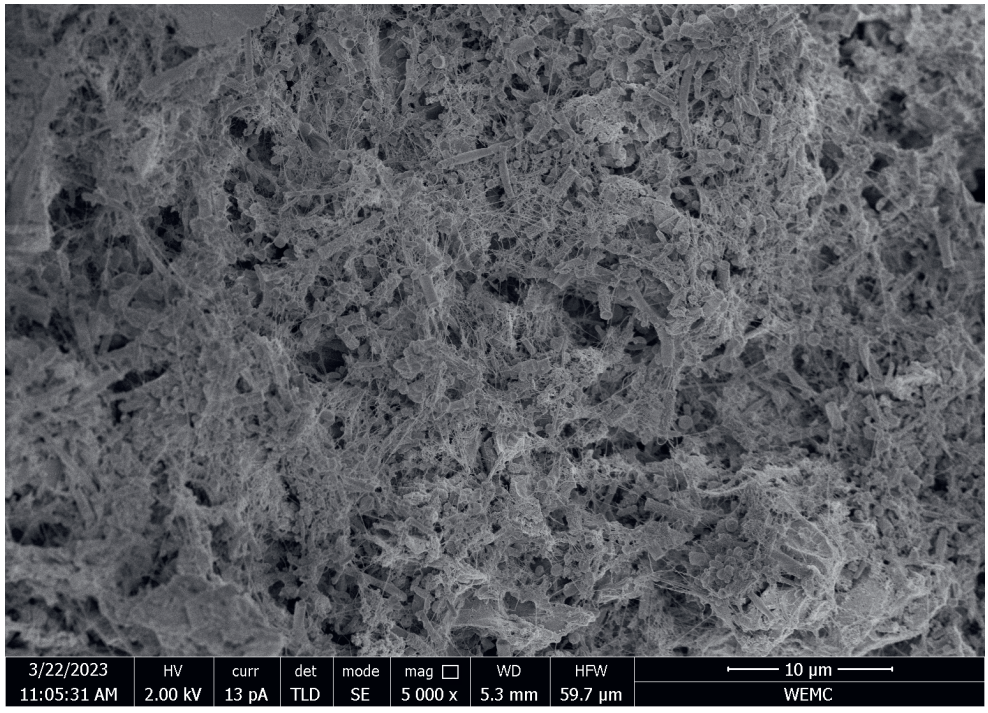

Figure 11: SEM picture taken of granular activated carbon collected from B1.

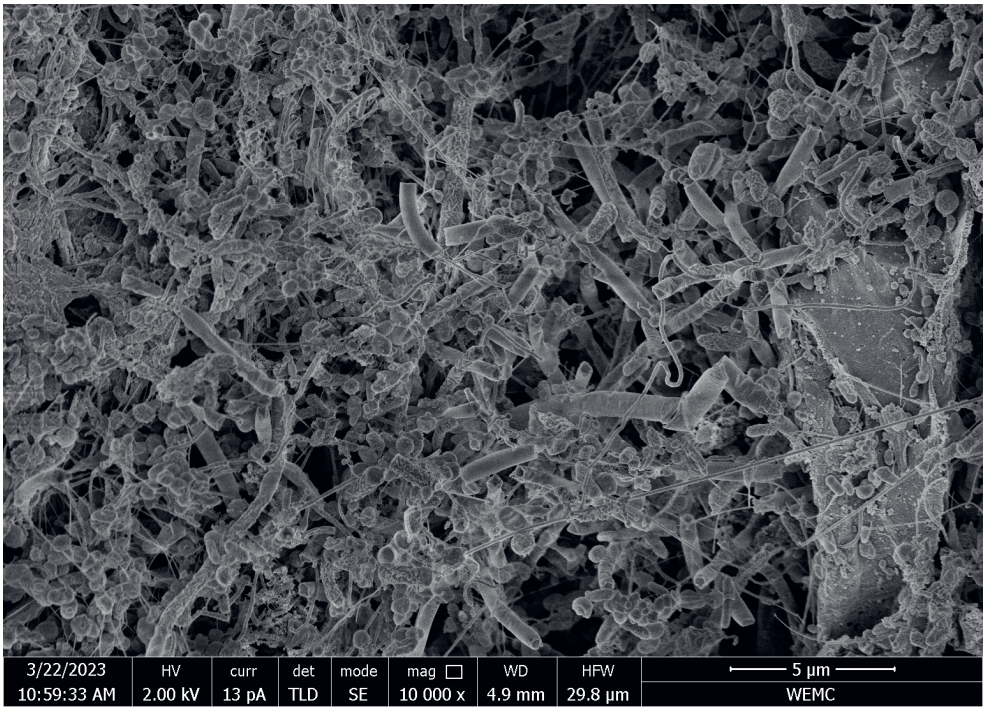

Figure 12: SEM picture taken of granular activated carbon collected from B1.

Supplementary Information Chapter 4

Operational and performance details of scale up methane producing BES

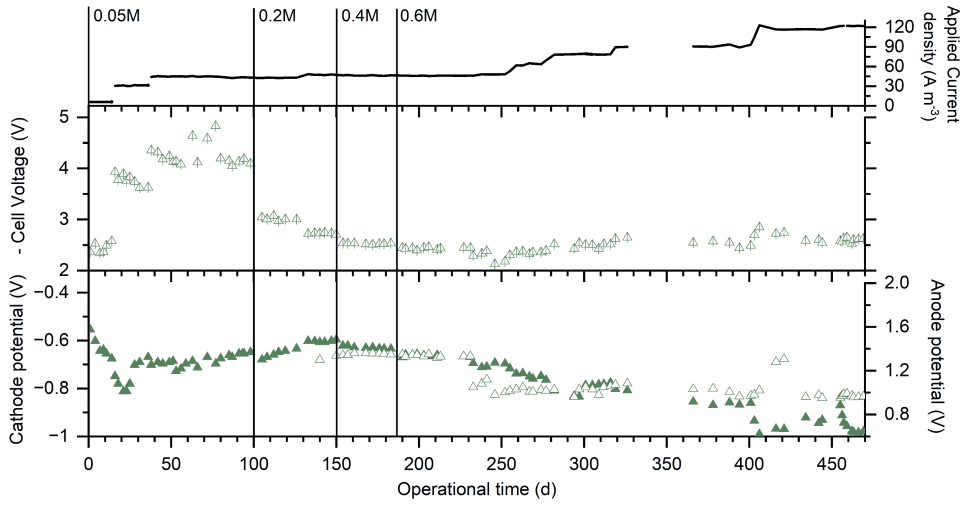

Figure 13: Plot of cell voltage (middle), cathode potential (full triangles, bottom) and anode potential (empty triangles, bottom), throughout the operational time of B1. The control strategy, applied current density, is also plotted for reference (top). Vertical lines represent the change in electrolyte.

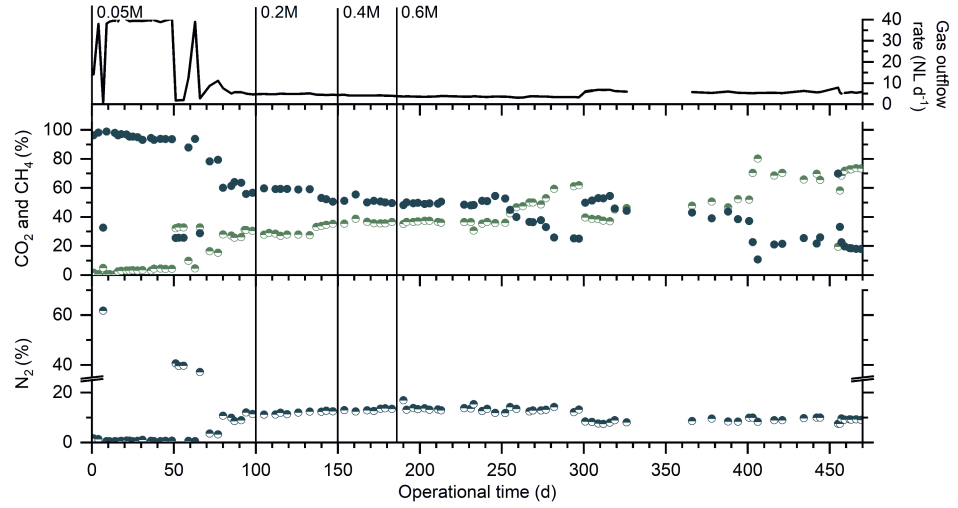

Figure 14: Plot of the composition of the outflow gas from the headspace of the bubble column, including CO_2 (in V%) (dark full circles, middle), CH_4 (in V%) (green half circles, middle), and N_2 (in V%) (dark half circles, bottom). The flow rate of the gas outflow is plotted at the top. Vertical lines represent the change in electrolyte.

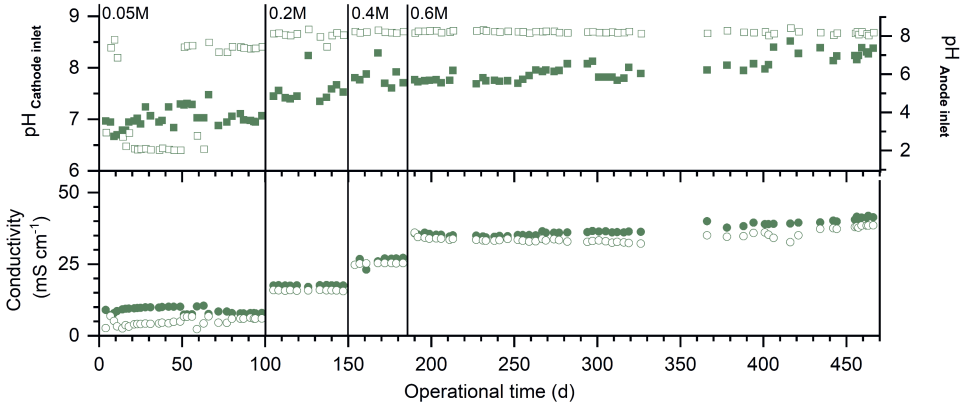

Figure 15: Plot of the pH (top) and conductivity (bottom) of the electrolyte at the inlet of the cathode (green full squares and circles, respectively), and at the inlet of the anode (empty squares and circles, respectively). Vertical lines represent the change in electrolyte.

Supplementary Information Chapter 5

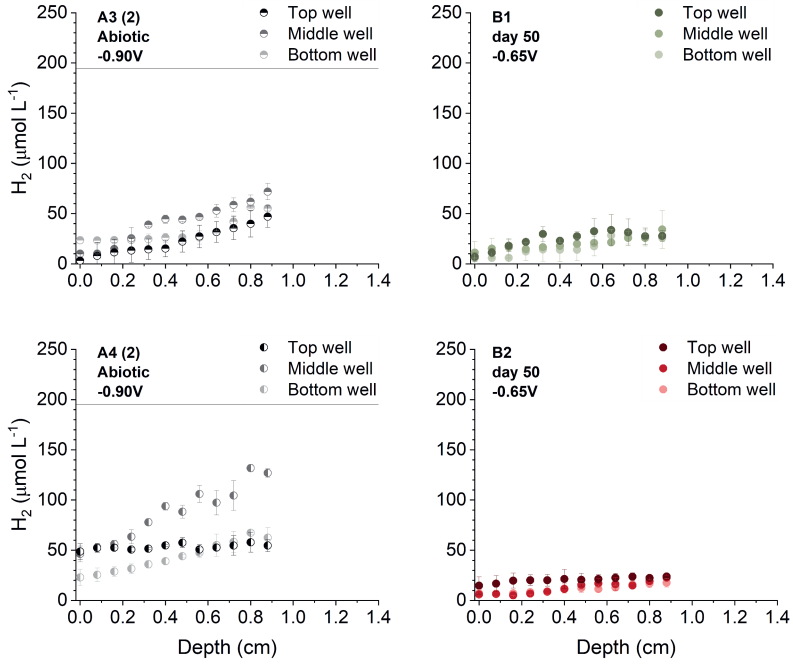

Figure 16: Local H_2 profiles (in μmol L^{-1}) throughout the depth of the granular activated carbon (GAC) bed (in cm). Depth 0 cm corresponds to the current collector and depth 1.4 cm corresponds to the membrane. On the left, a second run of profiles of two abiotic reactors, A3 and A4 (black, half full circle) with cathode potential -0.90 V. On the right, two biotic reactors, B1 (green, top) and B2 (red, bottom), at day 50 after inoculation and at cathode potential -0.65 V. Data was collected at three different heights, bottom, middle and top, and is represented from lighter to darker colour.

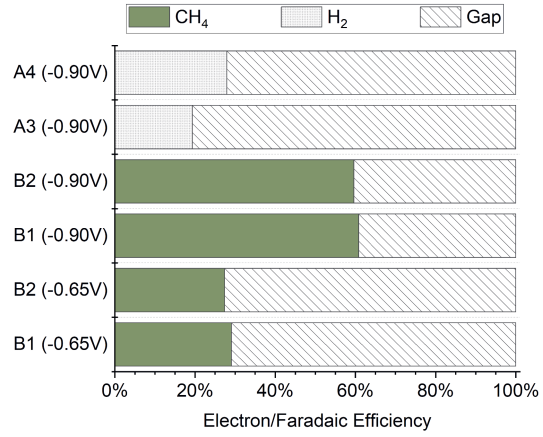

Figure 17: Electron distribution (in %, normalised to total electron supply) based on H_2 and CH_4 concentration found in the outlet gas of two inoculated reactors, B1 and B2 at resulting cathode potential of -0.90V (middle two) and -0.65V (bottom two), and of two abiotic reactors (top two), A3 and A4, with resulting cathode potential of -0.90V.

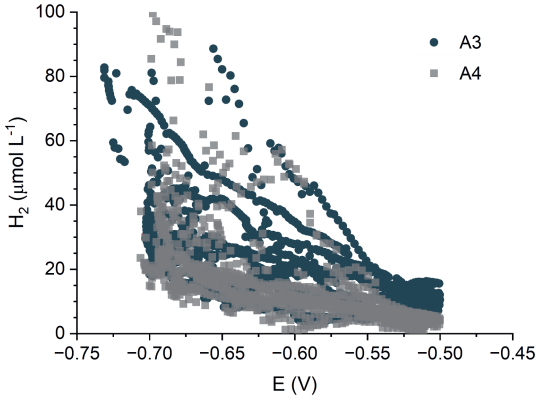

Figure 18: H_2 (in μmol L^{-1}) at depth 0.7 cm (middle well) in relation to observed cathode potential (in V vs Ag/AgCl) as a result of charge/discharge test done for A3 and A4 by alternating between +30 mA and −50 mA.

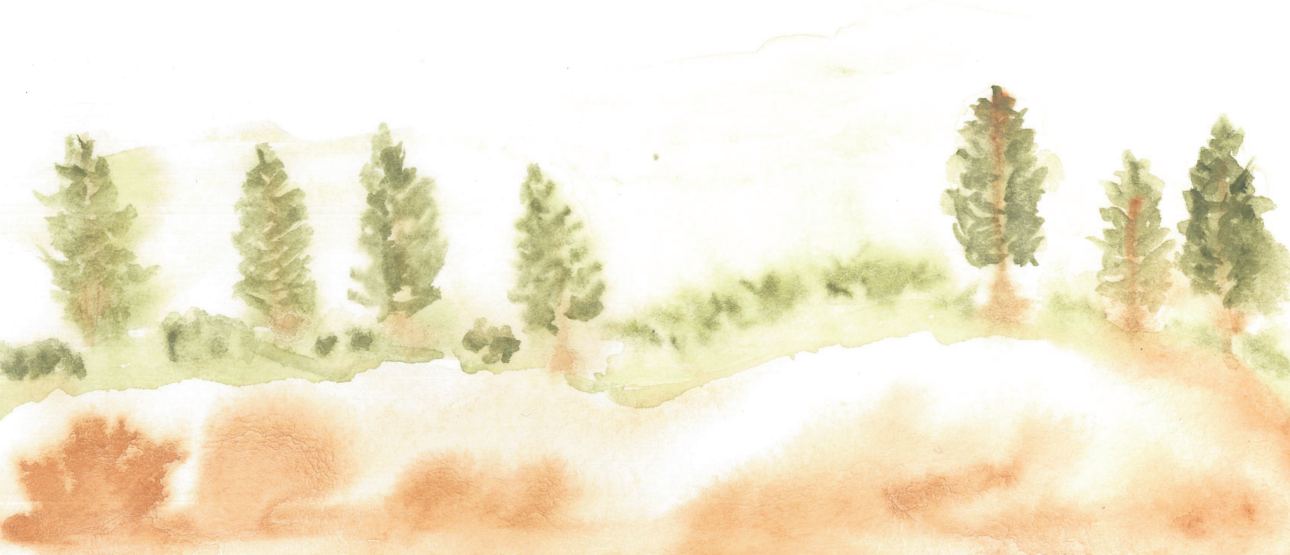

Acknowledgements

Although a PhD is a personal track, it is not a lonely one. Not every contribution to this thesis has been mentioned yet. Here is a shout-out to all those "unsung heroes" who whether directly or sneakily lent a hand, a word or any other gesture in this quest. "Spoiler alert"! The words that will follow are just small droplets in a larger pool of shared moments. Please keep this in mind and that actions are more valuable than words. Nevertheless, you will see I received much support and without it and those behind it this thesis would have ceased to exist.

To my super(vision) team, thank you. To my Promotor, **Annemiek**, it truly has been a lovely journey and in many regards thanks to you. I am thankful for the knowledge you have shared with me, knowledge which goes far beyond science, including working with others, reacting to failures and dealing with the responsibility and freedom that "your own project" entails. However, I am most thankful for the compassion and comprehension you have consistently gifted me. To my Co-promotor, **Sanne**, we started off this journey as friends, fellow PhDers, with me at the starting line and you with the whole route mapped out and already cruising towards the finish line. With your passion for science and determined spirit, it was only a matter of time until I was eager to learn from you. I am very thankful for the friendship and support early on and for the guidance later on. To **Jan** and your creative mindset and boundless energy, I am grateful for the confidence you showed in me during the selection process for this project but most importantly working with you was a true joy. I am deeply thankful to you for fueling further my love for learning with your love of exploration. To **Dandan**, a "Force of Nature" when it comes to research. You were the first person to introduce me to methane producing bioelectrochemical systems and with patience you shared your expertise with me. Your attention to detail and outstanding research inspired me to be a better researcher.

To be supervised or to supervise? No pun intended. I could not have made it without my hard working thesis students, **Esther**, **Aris**, **Nikos**, **Valentijn**, **Jasper**, and **Merijn**. Thank you for your invaluable scientific contributions to my thesis and the overall project but, above all that, I am grateful to you for letting me step into the role of a supervisor and for bearing my faults. I deeply value the time I have fostered with every single of you and I sincerely hope that you are all doing well in your current endeavors.

To Paqell B.V., it was your investment that made this research possible. I wish it brings to the company, as much as it has given to me. To **Joost**, **Gijs**, **Jan Henk**, **Sandra**, **Cora**, **Arthur**, **Willem** and **Uli** thank you for the collaborations and willingness to share your expertise, as well as the nice moments and conversations at company gatherings. A special thanks to **Monica** and **Mark**, whose smiles always brightened my day. Last but not least to **Rieks**, as you were my first thesis supervisor and (somehow) you were pleased to continue working together. I am deeply grateful for your support towards the technical challenges and, most importantly, on a more personal level.

To the Guardians of the Lab, because I think "Lab Team" is too modest a name (also, since Guardians of the Galaxy is one of my favourite movies). To all of you, thank you for keeping a simultaneously professional and fun environment in the laboratories. To **Jean**, **Katja**, **Beatriz**, **Julian**, **Ilse**, **Thomas** and (more recently) **Nick** for happily supporting us and keeping the lab running sparkly and smoothly. Specifically to **Livio**, **Pieter** and **Lucian**, who ensured that my gas chromatography endeavors did not go unassisted (and "Oh boy!" was I dependant on gas chromatography), thank you for developing methods, assisting in problem solving and (above all) for remaining patient through my detailed analysis when checking the performance of the equipment. To **Vinnie**, **Michiel** and **Bert** without whom the many hours I spent in the ModuTech could not have been so enjoyable. From you I learnt many technical skills that I had no idea I could do and I am truly grateful for this knowledge, hands-on experience and camaraderie (mainly, in the form of lively coffee break chats).

To the Secreteriat, **Liesbeth**, **Petra**, **Wies**, **Marjolein** and **Adriana** for "holding the fort" at ETE and doing it with such a lively presence. Administrative issues are an important "pillar" that most of the times remains invisible to the eye. Nevertheless, it must not be forgotten and for your support I am truly appreciative.

To my colleagues but most importantly my recent friends. To **Sha**, since we have supported each other throughout a great part of our PhD trajectories, I am eternally indebted to you (and **Yu**) for our friendship and for the talks, coffee breaks, advice and travels (and energizing Nintendo games and amazing cooking). To **Margo**, because sharing similar struggles brought us close together but it did not stop us from also sharing happy occasions. To **Xiaofang** for having my back especially in my most stressful period, when closing in on the finish line (and for those 2-week straight gym sessions). To **Anran** and **Yue** for having the most infectious smiles, for always carrying kind words at the tip of their tongue and for being the best hosts and sharing with me and Miguel their daily life, culture and family. To **Milan**, who above all taught me about perseverance, and to **Jin Yong**, who along with Milan and Sha made the sweetest (and accidental) dive one could assist, while canoeing. To **Yme**, who always had a joke or sound-proof business plan to crack. To **Chang** for always sharing nice treats and tea and for teaching me Chinese card games along with Yue and Jin Yong. To **Silvana** for the numerous breaks from work and for

her compassionate understanding. To **Dilan** for the exchange of kindhearted (post-it) notes and travel souvenirs. To **Selin** and **Jorn** for always offering a help, a word, a laugh, a party. To those already mentioned above and the remaining "Lions in the Jungle" **João**, **Hooman**, **Paulien**, **Yi** and **Tim** for inviting me to your homes (and coming to my home) for refreshing and fun social gatherings. To the remaining Chinese community at ETE **Zhaolu**, **Yujun**, **Weishen**, **Bochi**, **Shuhao**, **Fang Ding** and others, whom together with those mentioned above shared with ETE their culture, language and cuisine, and in this way created unique moments with which ETE was/is better off. To **Marko**, **Elizabeth**, **Rikke** and **Halimat**, who create a warm and supportive atmosphere at ETE and were always ready to lend a helping hand. To **Pim** for always honoring a bet. To the remaining colleagues, students, and staff at ETE it is hard to acknowledge all those, who have encouraged and boosted my time at ETE but thank you all for contributing and being responsible for a nice and welcoming work environment. I am certain that, like me, each one of you holds fond memories of one another.

Friends are those whom we meet along the way, whom we take with us along new ways and who remain (in any form), when we go our separate ways.

To my paranymphs Sara and Jos. **Sara** you were one of the first people I met when I started my MSc back in 2018. I always considered myself to be a big eater and you always considered yourself to feel too warm but we swapped characteristics soon after meeting each other. This is how I always introduce our friendship, since for some stupid reason I find this funny. However, the truth (and most romantic version) is that after meeting you our friendship grew strong very quickly and ever since then you have been one of my biggest supporters, a go-to shoulder to cry on or a go-to partner in dance moves. We have shared countless memories with our friends group, and I hope many more are to come. I am very grateful for the time you have invested in my well-being and I hope to repay you, whenever needed. **Jos**, though you were one of the last people I met during my PhD journey, you played a crucial role in helping me complete it (it is true!). Your lively personality and readiness to listen have been a source of great encouragement. Well, this and the fun times we had on the beach volleyball field together of course. It takes a rare and kind soul to help someone navigate their own barriers of perfectionism and, for that, I am forever grateful.

To those friends who made it enjoyable - for the most part - to be in what has been my second home. To my **AID families** and **83-crew** for helping me settle in and for sharing joyful and tribal-like moments. A very special and heartfelt "thank you" to **Luísa**, **Bia**, **Pedro**, **Raúl**, **Lucas**, **Rui**, **Catarina**, **Chico**, **Maria**, **Ricardo**, **Nici**, **Primo**, **Claudia**, and **Richard**, among other Portuguese friends, whom I met in Wageningen. I doubt you know how much I relied on our friendship but the only way I can think of trying to explain it is with a quote of Carl Sagan, now picture it, "*for small creatures such as we the vastness is bearable only through love*".

To my volleyball teammates, **WaHo** and those who I played beach volleyball with in better weather, for sharing with me my favourite sport. Volleyball has always been my comfort(-ing) zone. A special thanks to **Remon** and **Ivo** for always believing in me both inside and outside of the court and for making sure I was aware of it.

To my "forever" friends back home, who made it impossible not to go back to Portugal once in a while. To **Araújo**, **Vaz**, **Lucite**, **Bruna**, **Patri**, **Ana** and **Joana** being away from you for so long was challenging but your unwavering support bridged the distance. Even while abroad, we shared many cherished moments together for which I am eternally grateful. Those memories fueled my motivation to keep moving forward.

Family is hardly ever a choice but it is always a cherishable gift. To my whole family, I love you.

To my family back home, I love you. To my parents, my fire and my water, **Mãe**, **Dad**, you have raised me to be the best version of myself not through discipline but through commitment, livelihood and love. I am grateful for the freedom you gave me, when I needed it the most and, above all, I am eternally grateful for every single moment we have shared and those which are still to come. To my siblings, starting with my sister **Monica** for always being an example I could (and should) follow, so much so, that I did not think twice in enlisting for a BSc in Biochemistry and possibly facing future unemployment. To my brother **Pedro** for teaching me the power of resilience and acceptance. To my brother **Nuno** for conveying brains and stability. To my niece and nephews **Gabriela**, **João Pedro** and **Pedro Miguel**, for allowing me to be the "cool aunt" and for rejuvenating my spirits, whenever I was feeling down. To **Zé**, **Joana** and their loved ones for indulging me and the family in our craziness (and for being part of it). To our pets **Lep**, **Soya**, **Oli**, **Dino**, **Targaryen**, **Kiko**, **Spotty**, **Fred** and those who have been because life is nothing without our best friends, the ones whom love us more than what we can ever love them. To **Lia**, **Zé**, **Salomé**, **Francisco**, **Rita** and those loved ones connected by blood, I am truly grateful to have you in my heart. To my "international" family **Mark**, **Sascha**, **Michael**, **Becca**, **Nicholas**, **Robin**, **Hariet**, **Carole**, **Julian**, **Laurence**, **Dom**, **Kevin**, **Jez**, **Josie**, **Felicity**, **Edouard** and their loved ones, especially for the fun family gatherings. I truly believe, we can only grow as big and wise as the family we have in our mind and hearts.

To **Miguel**, my rock, who knows best the path I have taken these past years. It was not always an easy path. However, with you, because of you and by loving you I could endure the worst. There is this quote I recently heard at the movies with you: "*Sometimes the people we save, save us right back*". I can only hope that some day I can be your rock. Thank you, my Love.

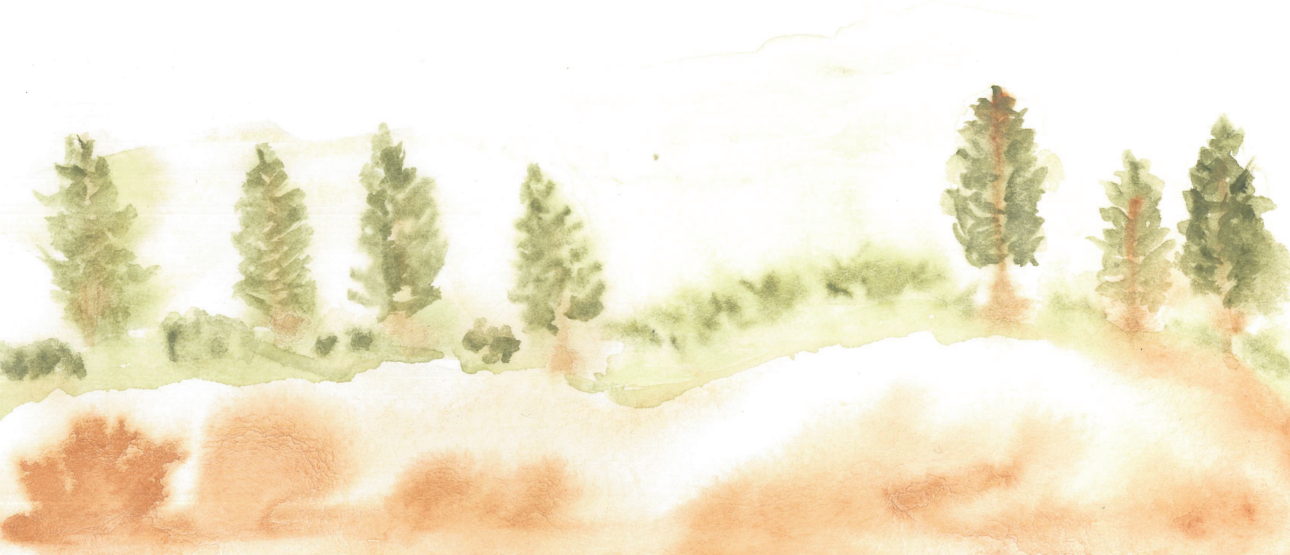

About the author

Ana Micaela Brandão Ferreira Lavender was conceived during an academic conference in Santiago de Compostela, Spain in November 1995 (we bet you did not expect that start), and was born on (the same) St. Tiago's Day, 25th of July 1996 in Famalicão Hospital, Portugal. She was and still is no saint but definitely is a vibrant and fulsome character to whom we frequently recited the little poem below, wise words by Henry Wadsworth Longfellow, to show her that in life it is possible to choose to exhibit good or bad conduct that reflects itself towards others in a way of being happy or miserable. Of course, as parents for us the good far outweighs the bad.

"There was a little girl, who had a little curl,

Right in the middle of her forehead.

When she was good, she was very, very good,

But when she was bad, she was horrid."

Her primary education was undertaken in a bilingual Portuguese-English school and she attended two secondary schools in Braga. At the end of her first secondary school, Francisco Sanches, she was one of a small group of students, who were awarded diplomas for achieving a perfect average of 5 out of 5 in her final year examinations in July 2011 (or 2012, who can even recall that far back?). At the end of her second secondary school, Carlos Amarante, she began her undergraduate studies in 2014 at the University of Minho, Braga, Portugal, where she studied Biochemistry. During her final year at this university, she was selected to undertake an Erasmus Exchange at the University of Wageningen and during this period she became interested in studying for a Masters Degree in Environmental Sciences at this same university, which she was selected to attend and she duly completed her course there in June 2020. Towards the end of this course, she was invited to continue researching in the scientific area of her former thesis, which had been carried out in the Department of Environmental Technology at Wageningen University. This research position is now awarded with this book. The reason why she decided to follow this path is yet unknown to most, even to her, but maybe it is somewhat related to the starting point of this section about her (and her life).

There are two main hobbies in which Micaela partakes, volleyball and travelling. The former we can no longer indulge, after not one, not two, not three but four surgeries. However, it remains her main coping mechanism. The latter hobby is paradoxical, since she does not like flying, all that much. Nevertheless, Micaela has travelled a lot in her life starting with a visit to Oaxaca, Mexico, when she was six-months old, where her father attended an international conference. Her first birthday was celebrated in Kassel, Germany during a two-week Erasmus Media Education project meeting co-ordinated by her father (wait, bragging does not end here) and her second birthday took place in Glasgow, Scotland during a conference of the International Association of Mass Communication Research (also!) organised by her father. From there, her travelling endeavours continued, she has visited Cape Town, Austin and other places in Texas, Arizona, Japan, São Tomé e Príncipe among many other places. Her twenty first birthday was held in Prague, Chequia during a short European tour by car with us to celebrate her undergraduate graduation. I wonder how many more birthdays she's celebrated abroad compared to those at home? More recently, in February 2024, she took a month long visit to China with her partner, in which her love for travelling and culture was extended.

Now we live in the present and we wonder "*what the future may hold*", but there is no point of dwelling too much about the future, likewise Paulo Coelho has written: "*the secret is here in the present. If you pay attention to the present, you can improve upon it. And, if you improve on the present, what comes later will also be better.*"

— Her proud parents,

Cristina Brandão Lavender

Antony Michael Lavender

"A rock pile ceases to be a rock pile the moment a single man contemplates it, bearing within him the image of a cathedral."

— Antoine de Saint-Exupery, The Little Prince

Netherlands Research School for the
Socio-Economic and Natural Sciences of the Environment

D I P L O M A

for specialised PhD training

The Netherlands research school for the
Socio-Economic and Natural Sciences of the Environment
(SENSE) declares that

Ana Micaela Brandão Ferreira Lavender

born on 25 July 1996, Vila Nova de Famalicão, Portugal

has successfully fulfilled all requirements of the
educational PhD programme of SENSE.

Wageningen, 27 September 2024

SENSE coordinator PhD education

Dr Ir Peter Vermeulen

The SENSE Director

Dr Jampel Dell'Angelo

The SENSE Research School declares that **Ana Micaela Brandão Ferreira Lavender** has successfully fulfilled all requirements of the educational PhD programme of SENSE with a work load of 34.1 EC, including the following activities:

SENSE PhD Courses

- Environmental research in context (2020)
- Research in context activity: 'Part of organisation EU-ISMET 2023'

Other PhD and Advanced MSc Courses

- Computational Methods in Water Technology, Wageningen University (2020)
- Project and Time Management, Wageningen Graduate Schools (2021)
- Communication Styles, HOW company (2021)
- Supervising BSc and MSc thesis students, Wageningen University (2023)
- Intensive writing week, Wageningen Graduate Schools (2023)
- Introduction to LaTeX, Wageningen Graduate Schools (2023)

External training at a foreign research institute

- Strength Talent finder course, AP Consulting (2022)

Management and Didactic Skills Training

- Head of PhD event committee of the chair group (2022-2024)
- Head of Lab Research PhD committee of the chair group (2023)
- Supervising two BSc student with thesis (2021-2023)
- Supervising two BSc student with thesis (2022 & 2024)
- Assisting practicals of the BSc course 'Renewable Energy Technologies' (2020-2022)
- Assisting practicals of the MSc course 'Environmental Electrochemical Engineering' (2023)

Oral Presentations

- *Reduced overpotential of methane-producing biocathodes: Effect of current and electrode storage capacity*. CHISA, 22-25 August 2022, Prague, Czech Republic
- *Power-to-methane in a Bioelectrochemical System* PhD trip visiting several universities and companies: GEUS, DTU, Biofos, Recolab, KTH & Uppsala University, 01-09 May 2023

This research received funding from Shell Global Solutions International B.V. and Paqell B.V.

Financial support by Wageningen University for printing this thesis is gratefully acknowledged.

Cover and chapter break design by Cristina Brandão Lavender

Printed by ProefschriftMaken on recycled paper